AD NUMBER
AD844988
LIMITATION CHANGES

TO:

Approved for public release; distribution is unlimited.

FROM:

Distribution authorized to U.S. Gov't. agencies and their contractors; Critical Technology; DEC 1968. Other requests shall be referred to Office of Naval Research, Code 421, Washington, DC 20360. This document contains export-controlled technical data.

AUTHORITY
onr notice 27 jul 1971

RESEARCH STUDY OF A
CO₂ LASER RADAR TRANSMITTER

FINAL TECHNICAL REPORT

December 1968

Prepared by

Perry A. Miles

Raytheon Research Division

Waltham, Massachusetts 02154

STATEMENT #2 UNCLASSIFIED

This document is subject to special export controls and each
transmittal to foreign governments or foreign nationals may be
made only with prior approval of _____ONR/code 421

Wash DC 20360

RESEARCH STUDY OF A CO_2 LASER RADAR TRANSMITTER

Final Technical Report

1 November 1966 through 15 August 1968

Prepared by

Perry A. Miles

Raytheon Research Division

Waltham, Massachusetts 02154

ARPA Order No. 306

Project No NR 015-714

Contract No. N00014-67-C0264

ABSTRACT

A prototype high power laser radar transmitter at 10.6μ wavelength has been developed for installation at Lincoln Laboratory's Millstone Hill radar site. This report summarizes the three phases of its development: 1) Exploratory work on the properties of dc- and pulse-excited CO_2 laser amplifiers and their use in producing trains of high power optical pulses, 2) Design of a 1 kW average (10 kW peak) power transmitter, and 3) Operational tests of the transmitter. In this device the signal from a stable oscillator is amplified to a level beyond 200W, formed into a train of 10μsec pulses by mechanical modulation, and then re-amplified to the 10 kW level. All amplifiers are dc-excited. Subjects treated include gain limitations set by spurious oscillation, pulse-to-pulse amplitude stability, oscillator-amplifier interaction, and output beam profile. Brief proposals are made for future development of the laser radar program.

TABLE OF CONTENTS

TABLE OF CONTENTS (Cont'd)

Page

LIST OF FIGURES

LIST OF FIGURES (Cont'd)

LIST OF FIGURES (Cont'd)

BLANK PAGE

I. INTRODUCTION

By mid-1966, the capability of CO_2 gas lasers to produce infrared power at levels beyond 1 kW and at efficiencies in excess of 10 percent was well recognized and was soon to be accomplished at Raytheon. The question arose as to the potential value of an infrared radar system using such high power lasers in which these devices could serve as coherent sources. Heterodyne detection of the return signal scattered from moving targets would then permit Doppler velocity analysis and signal processing similar to that used in conventional microwave radar systems.

A two-fold investigation of this question was begun, on the one hand to consider the operational requirements of an infrared radar system, and on the other to carry out experiments aimed at producing a prototype radar transmitter which could be used in full-scale field tests.

This report describes the work undertaken at Raytheon's Research Division that resulted in the design and construction of a transmitter capable of generating power in excess of 1 kW. The program contained three distinct phases, each of which took approximately seven months to complete. The first was an investigation into the physical behavior of CO_2-N_2-He discharges when used to amplify pulsed infrared radiation. The second phase involved the design and construction of a source with the potential for an output of 1 kW in a high-frequency pulse train. The final testing of this device and its use, together with a heterodyne detection system, led to improvements in its detailed design and operation prior to its installation at the optical radar facility of Lincoln Laboratory in Westford, Massachusetts.

Recognizing the limited time available, our approach to the project was to anticipate the final transmitter design and perform experiments on components of this design, pushing to high powers as quickly as possible.

1

In this way, operational problems which arose would be relevant in the actual engineering design, while investigation of the processes which would finally determine the gain, saturation, and optical properties of the gaseous discharges could take place in a geometrical form very similar to that of the finished transmitter.

Our initial radar study indicated that coherent signal processing of backscattered radiation could be used over periods of between 10 and 100 μsec, depending on the assumed nature of the target. As a consequence, it was necessary to build a device with output pulses on the order of 10 μsec. Furthermore, the recognition of Doppler frequency shifts due to target movement required that the frequency of the return signal should be compared with that of the emitted pulse. The most straightforward way to maintain a constant frequency in the output train seemed to be the use of a low-power oscillator whose output could be passed through a sequence of amplifiers wherein a pulse train could be formed by electrical or mechanical means or by pulsed amplification.

The most appropriate angular divergence of the output beam depends on the detailed mechanization of the entire radar system, since it depends critically on the target tracking information already available, the mode of target acquisition chosen, the quality of the propagation path from source to target, and on the signal-to-noise ratio to be expected in a typical experiment. The return signal will be maximized, of course, if all the available transmitter power is incident on the target in an area corresponding to the minimum optical resolution element as viewed for the receiver optics. The ultimate flexibility in our control of the output beam will require that the minimum beam angle be set only by the emitting aperture, i.e., that there should be a known (and hopefully a spherical) phase wave front at the transmitter exit plane. Again, the most straightforward way to achieve this condition appears to be to use a single transverse mode oscillator with multiple irises throughout the amplifier to minimize the effects of wall reflections.

We first studied the amplification of 10 μsec infrared pulses in various configurations of discharge tubes, relating the results to a model of the various excitation and decay rates of nitrogen and CO_2 molecular species. As a result of this work, we decided that our objective of a 1 kW transmitter could be accomplished with the least difficulty by using a sequence of dc-excited amplifiers.

The molecular dynamics of the amplifying medium require that for efficient energy extraction from a dc-excited discharge, pulse repetition rates of several thousand per second must be used. From the point of view of radar signal processing at low signal-to-noise ratios, it would be more advantageous to have the 1 kW of average power distributed as individual 10 joule pulses at a repetition rate of 100 pps than have 0.1 joule pulses at a rate of 10,000 pps.

We believe that future developments of these transmitters will have to stress the generation of high-power pulses in a space much smaller than our present design if they are to be accepted as practical radar sources. Nevertheless, the present design is capable of allowing field tests of a new form of optical radar with a potential angular resolution three orders of magnitude greater than conventional microwave systems.

II. TECHNICAL BACKGROUND

A. Molecular Level Populations and Dynamics

At the beginning of this project, a considerable fund of information on the physical processes which dominate the excitation and energy processes in CO_2-N_2-He discharges was available from the work of M. Weber and T. Deutsch[1] and from the high-power oscillator work of D. Whitehouse,[2] all of this laboratory. This work has provided us with measurements both of excited-state lifetimes of CO_2 levels in collision with their neighbors CO_2, N_2, and He, and of the resultant gain, gain profiles, and energy storage capabilities of discharges as functions of temperature, tube diameter, current density, and gas mix.

The problem of producing a compact and efficient power amplifier is essentially a matter of identifying the energy source upon which a specific input signal can draw, and controlling the excitation and decay processes which relate directly to that energy source. From this standpoint, it becomes clear that in CO_2-N_2-He discharges, the dominant energy source depends on the time scale chosen for the input signal.

The 10.6μ CO_2 emission comes from a population inversion established between rotational sublevels of the (00^01) vibrational level as compared to the corresponding rotational sublevels of the (10^00) vibrational level (Fig. 1). This inversion is produced by collisional transfer of energy from vibrationally excited N_2 or CO molecules formed in an electrical discharge which may be operated with dc, ac, or pulsed currents. Due to the near equality of the energies of CO_2 molecules in (00n) vibration states with those for excited nitrogen, this transfer is more likely than is usual in most vibration-vibration transfers, and takes (on the average) some 500 classical collisions. For pressures of N_2 and CO_2 each at 1 torr, this transfer time is of the order of 100 μsec.

4

Etc
J values
13

Upper
laser
levels
11
9
7
5
3
1

P(10)   P(12)

00°1

Laser transition 960 cm^{-1}
$\lambda \simeq 10.6 \mu$

Etc

Lower
laser
levels
14

12

10
8
6
4
2
0

10°0

02°0
02^{2}0

01'0

00°0 —— CO$_2$ Ground state
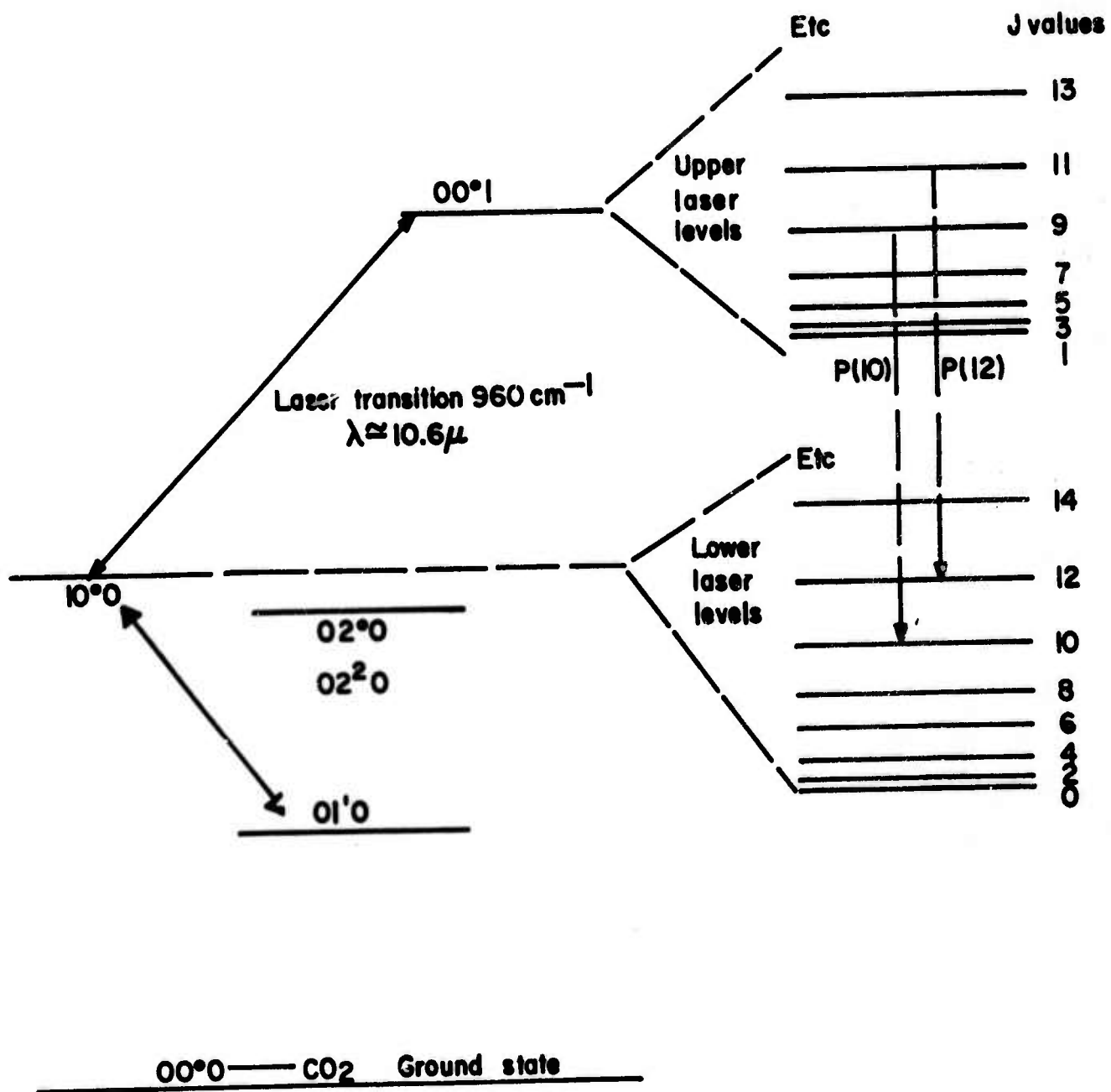
Fig. 1   Vibrational-Rotational Energy Levels of CO_2 Involved in Laser Emission

5

A second requirement for population inversion to exist has to do with the distribution of population among the rotational sublevels of the CO_2 vibration levels. The close spacing of these levels (for 1 to 50 cm^{-1}) makes energy transfer between them and kinetic states of the molecules a more probable process than vibration-vibration transfer. Thus the rotational levels tend to come quickly into thermal equilibrium with the kinetic temperature of the ambient gas. This process is further accelerated by the introduction of helium gas into the discharge, and takes $\simeq 0.1$ μsec in typical gas mixtures containing several torr of helium. As the rotational temperature decreases, the gain in the dominant line of the emission band increases, resulting in more efficient energy extraction. The introduction of helium is also of use in ensuring a rapid relaxation of the 010 and 020 states to which the laser thermal level relaxes by near-resonant collisions with CO_2 molecules in the ground state.[3]

A high inversion in dc-excited discharges requires, therefore, an efficient excitation of nitrogen molecules in a medium with as low a gas kinetic temperature as possible. The dynamics of this system are represented in Fig. 2, albeit in a simplified form. The time constants are approximate, and are relevant to a typical gas mixture of 1 torr CO_2, 1 torr N_2 and 4 torr He. In this figure, the discharge dynamics, having to do with the degree of ionization of CO_2, N_2, CO, O_2 and their constituent atomic ions and the related electron energy distribution, will depend on the gas mixture, pressure, and tube diameter. They will result in excited nitrogen molecules which can come into equilibrium with CO_2 upper vibration levels at a rate governed by a time constant of the order of 100 P_{N_2} μsec where P_{N_2} is the partial pressure of nitrogen in torr. Vibrational transfer among the (00n) vibrational levels can be expected to be of the order of 10 μsec. This fast vibration-vibration interchange is possible because of the near-resonant nature of the transfer, the vibrational levels being essentially equally spaced. We can expect that the population of the metastable nitrogen vibration levels will come into equilibrium with the electrons in
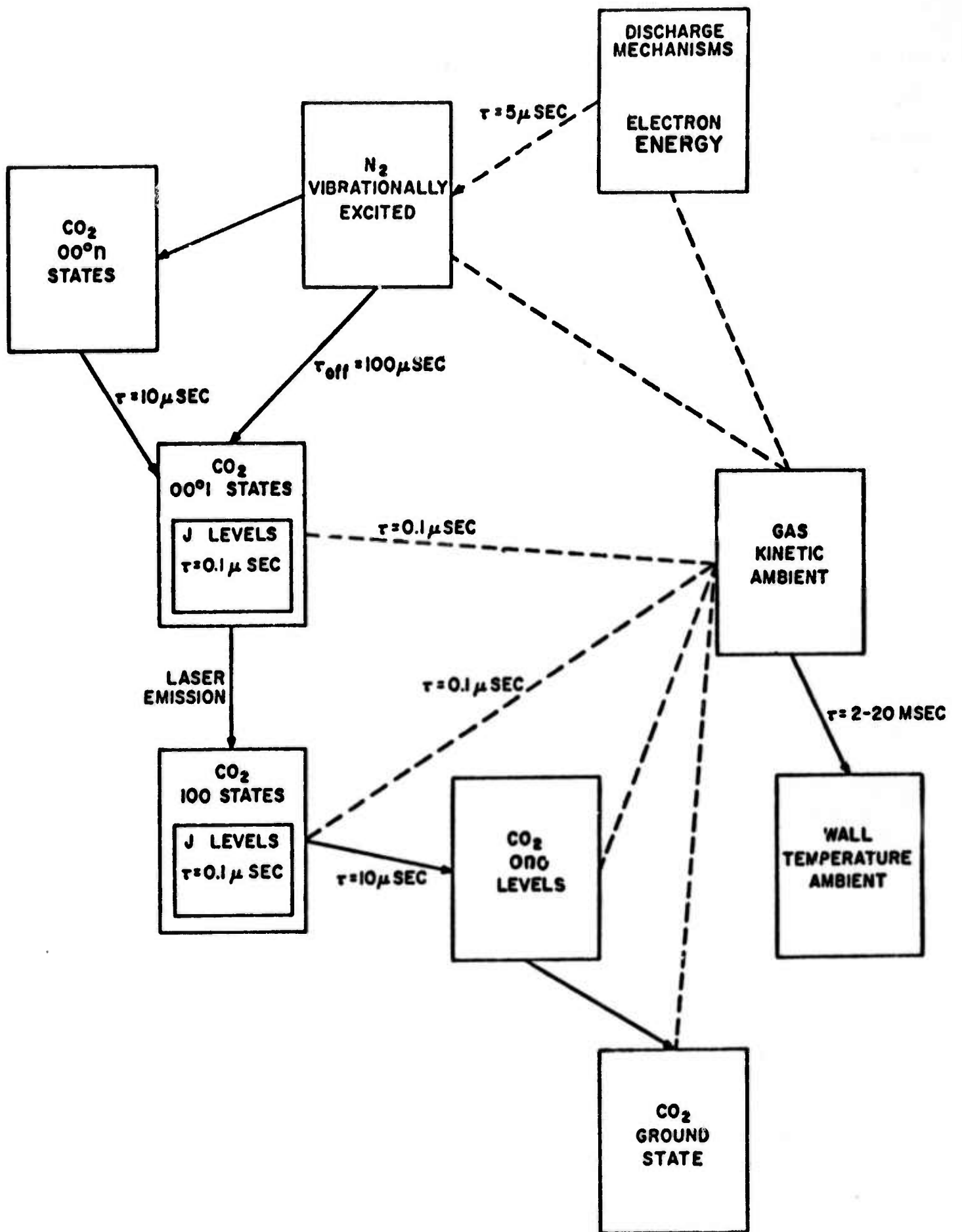
Fig. 2   Molecular Level Dynamics in the CO_2 Laser (schematic)

the discharge and will have an equivalent temperature of some 5000 - 6000° K.
The corresponding CO_2 vibrational modes should also come to thermal equilibrium within each mode line. Direct measurements of the 001 and 100 populations in an amplifying discharge[4] have given equivalent temperatures of 1600° K and 800° K respectively.

Finally, the gas kinetic temperature will relax back to the tube wall temperature at a rate governed by the heat diffusion from the axis to the walls, and by excited molecular migrations, both governed by the degree of macroscopic fluid flow and gas mixing going on in the tube. These rates will depend on tube diameter and flow rate, and typically give time constants of between 2 and 20 msec for tube diameters between 2 and 5 cm. While the dominant excitation of the CO_2 comes from transfer from the excited nitrogen molecules, some direct electronic excitation of all CO_2 levels will take place. In particular, the direct excitation of the 010, 020 and 100 levels will tend to reduce the optical gain at high dc current densities.

B. Energy Storage and Gain Characteristics

In considering the extraction of energy from an excited system of CO_2 and N_2 molecules, we have to take into account the sequence of transfer processes that are going on, illustrated in the previous section. The aspects of the pulse wave train which are relevant in this connection are the pulse length and pulse repetition rate, as well as the pulse height.

As to the individual pulse lengths, there are clearly four time regimes. A pulse input of duration less than 10^{-7} sec can draw on the population inversion of a single pair of rotational levels which exists before the pulse is applied. There will be insufficient time for any transfer to take place from nearby rotational levels. At a maximum, such a pulse could extract energy equivalent to one-half of that initial inversion, after which the level populations would be equal (under special conditions, this limit could be exceeded and approach unity, but such conditions are unlikely in

the present amplifier). Whether the factor of one-half is reached depends also on the type of spectral line-broadening present. For a homogeneously (e. g. , collision) broadened line, the input radiation may be considered to interact with all excited molecules at all times. For an inhomogeneously broadened line, e. g. , for Doppler broadening, the radiation interacts only with those molecules whose characteristic frequencies lie within the larger of the intervals $\Delta \nu = 1/2 \pi T_{coll}$, $\Delta \nu = \mu E/h$, or $\Delta \nu = 1/2 \pi T_{sp}$, where T_{coll} is the collision lifetime, T_{sp}, the radiative life, μ is the dipole moment associated with the molecular transition, E is the electric field strength associated with the applied radiation, and h is Planck's constant.

In the present context, the total linewidth is typically 80 Mc wide, made up of approximately 50 Mc to 60 Mc from Doppler broadening, the rest from collision broadening. Thus we expect an essentially homogeneously broadened response, taking into account both the actual collision width and the fact that individual molecules will change their position under the Doppler envelope in a time of the order of 10^{-7} sec.

Input pulses with lengths between 0. 1 and 10 μsec can affect all rotational levels of the (001) vibrational state, while the population of this state should be replenished from others of the (00n) series in a time less than 10 μsec. These pulses last long enough for population transfer between CO_2 vibrational levels to take place, but with little chance for transfer from the main energy reservoir, the excited nitrogen molecules. Such pulses, then, can draw on a greater excited-state population than those less than 0. 1 μsec, indicating an upper limit of repetition rate of 10, 000 pps. As we will see later, our experiments confirm this prediction. Pulses between 10 and 100 μsec duration fall into an intermediate category, while pulses longer than 100 μsec can draw on the full energy storage in the excited

9

nitrogen molecules, and upon the continual replenishment of these levels from the electron bath itself. The behavior of the amplifier subjected to such long pulses should tend progressively to that for the amplification of a cw signal.

In discussing the gain characteristics of $CO_2:N_2:$He discharges, it must be borne in mind that there will be an interplay of many elements of the system. Experimentally, we find that the small-signal gain co-efficient α in dc-excited tubes depends on gas mixture, current density, gas flow rate, wall temperature, and tube diameter as well as the distances for the axes of the discharge at which the measurement is made (Fig. 3). As the current increases, the radial gain profile saturates and then decreases along the axis, while the off-axis gain keeps increasing before saturating at a higher current level. Further, the highest value of gain obtainable in a tube of given diameter d tends to vary inversely with d (Fig. 4). Finally, the gain will depend on the level of the input signal and will tend to saturate as the incoming power depletes the excited state population. This effect bears directly on the efficiency of power extraction in an amplifier chain and deserves explicit consideration.

If we use a one-dimensional model of an amplifying medium with constant gain and saturation parameter excited by a uniform plane wave and assume that the exponential gain coefficient α for a wave of intensity I W/cm^2 can be written as

$$\alpha = \frac{\alpha_o}{1 + \dfrac{I}{I_{sat}}} \quad ,$$

it follows that the linear gain $G = P_{out}/P_{in}$ of an amplifying length L is given by

$$\ln G + \beta(G - 1) = \alpha_o L \quad ,$$

10
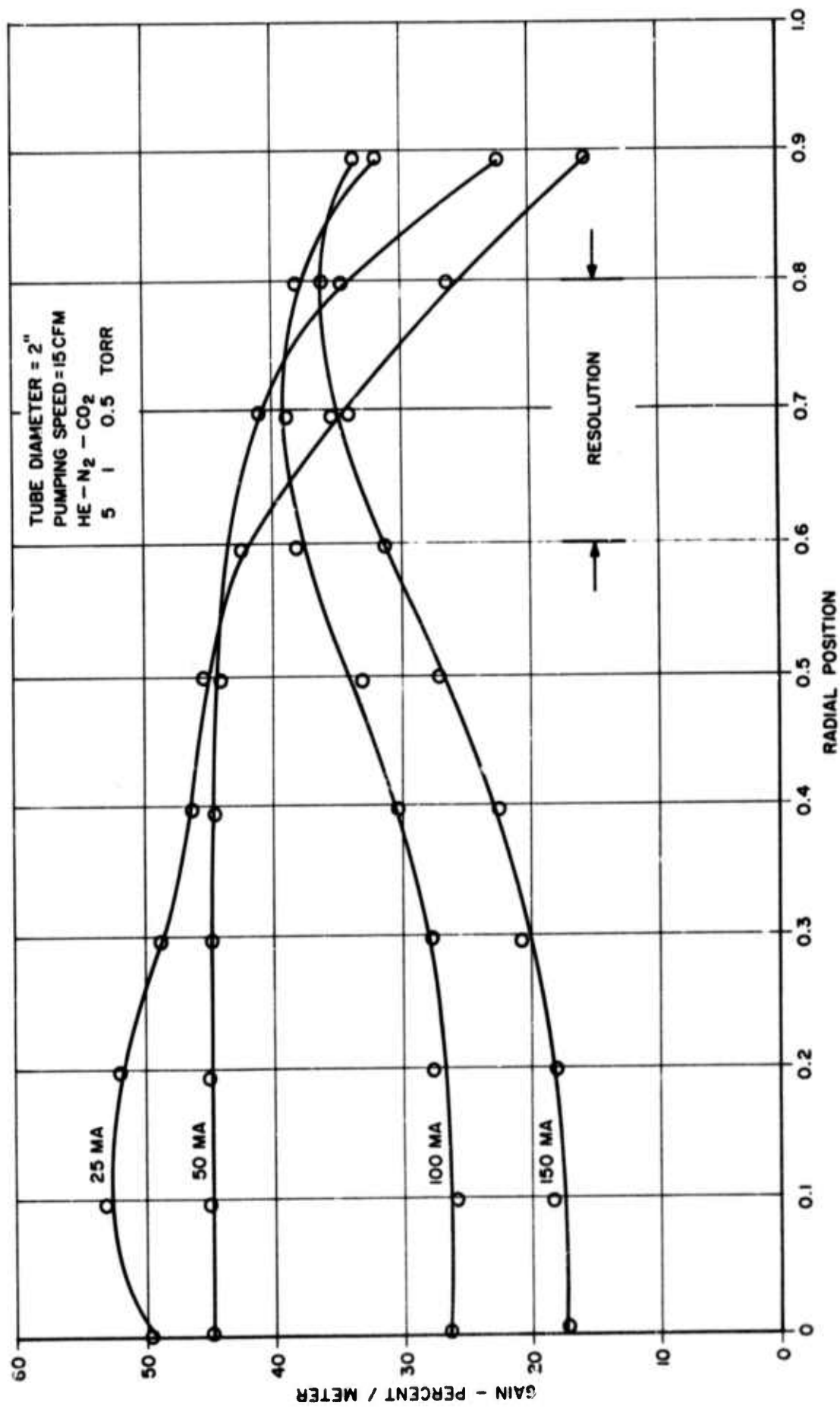
Fig. 3   Radial Profile of Single-Pass Gain of a 1-meter long, 2-in. Diameter Laser Tube with 15 CFM Pump for Various Currents

11
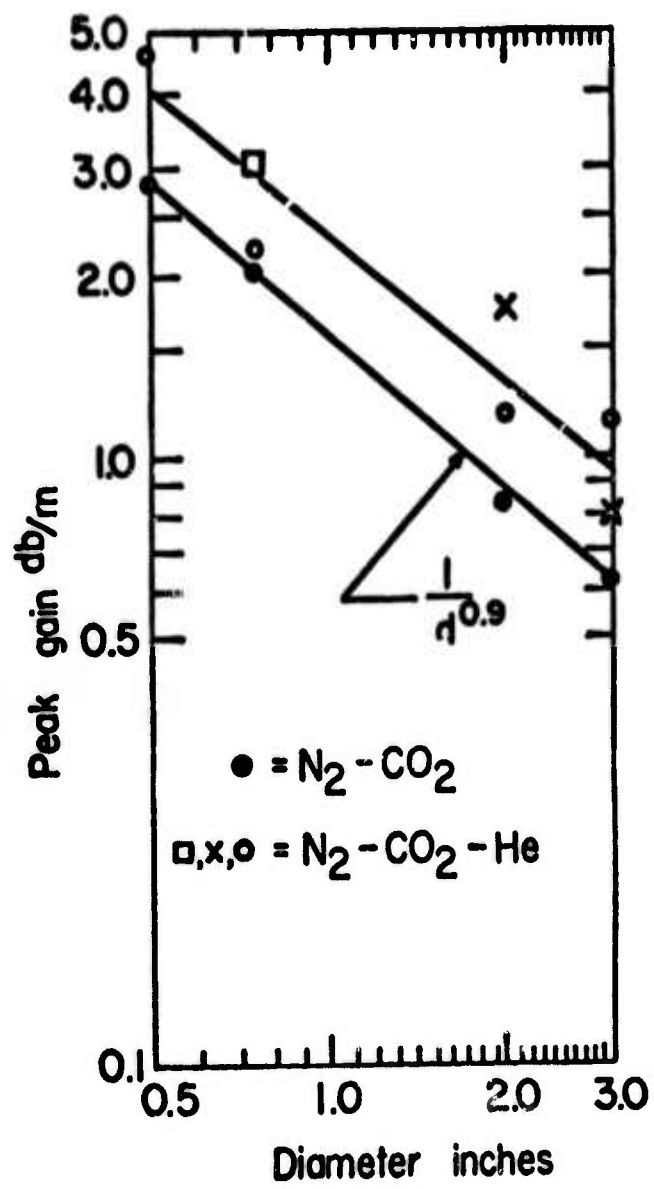
Fig. 4   Peak Gain vs Tube Diameter for N_2-CO_2 and N_2-CO_2-He Mixes

where $\beta = I_{input}/I_{sat}$. The relationship is presented graphically in Fig. 5. If the same conditions hold for a length of discharge L to operated as an oscillator in a resonator whose loss is dominated by the output coupling, the output flux intensity is simply $I_{output} = I_{sat} a_o L$.

Thus for an oscillator of cross-sectional area A and power output P watts

$$I_{sat} = \frac{P_{out}}{a_o LA}$$.

Typical values of these parameters for a 5-cm-diameter amplifier are $P_{out}/L = 75$ W/m, $a_o = 0.3$ m^{-1}, $A \simeq 19$ cm^2 from which $I_{sat} = 13$ W/cm^2. Similarly, for a 2-cm-diameter tube, $P_{out}/L = 50$ W/m, $a_o = 0.7$ m^{-1}, $A \approx 3$ cm^2 to give $I_{sat} = 24$ W/cm^2.

The analysis of the saturation of an amplifier subjected to a pulsed, as distinct from a cw, input signal is more complicated because the gain now depends on space and time. Thus the leading edge of any input pulse enters an undisturbed, high-gain medium. By contrast, later stages of the pulse experience low gain. It is more meaningful in this case to discuss the efficiency with which an input pulse of a defined size can extract the available stored energy.

The relationship between low signal gain and available stored energy again depends on the pulse lengths involved. The instantaneous population inversion which is established between two specific rotation sublevels of the 001 and 100 vibrational states is proportional to the infrared amplification constant a. From the analysis and data from Djeu et al.[5], a typical flowing gas laser with a gain coefficient of 0.01 cm^{-1} ($\simeq 4.3$ dB/m) on the P18 line runs at a total inversion of 1.8×10^{15}/cc measured as the population difference between the 001 and 100 levels. For their experiment, the partial pressures of CO_2, N_2 and He were 0.65 torr, 1.40 torr and 2.9 torr respectively. These pressures are comparable to our own. The total available energy from this inversion ($\Delta n = 1.6 \times 10^{17} a$) is given by

$$\Delta W = 1/2 h\nu \cdot \Delta \eta.$$

$a_0L=4.6$

$a_0L=3.0$

$a_0L=2.5$

$a_0L=2.1$

$a_0L=1.7$

$a_0L=1.3$

$a_0L=0.9$

$a_0L=0.5$

Curves derived from
$$\ln G + \frac{I_{in}}{I_{sat}}(G-I) = a_0 L$$
where $G = \dfrac{I_{out}}{I_{in}}$

$$\left[a = \frac{a_0}{1 + \dfrac{I}{I_{sat}}} \right]$$

$G-1$

$\dfrac{I_{in}}{I_{sat}}$
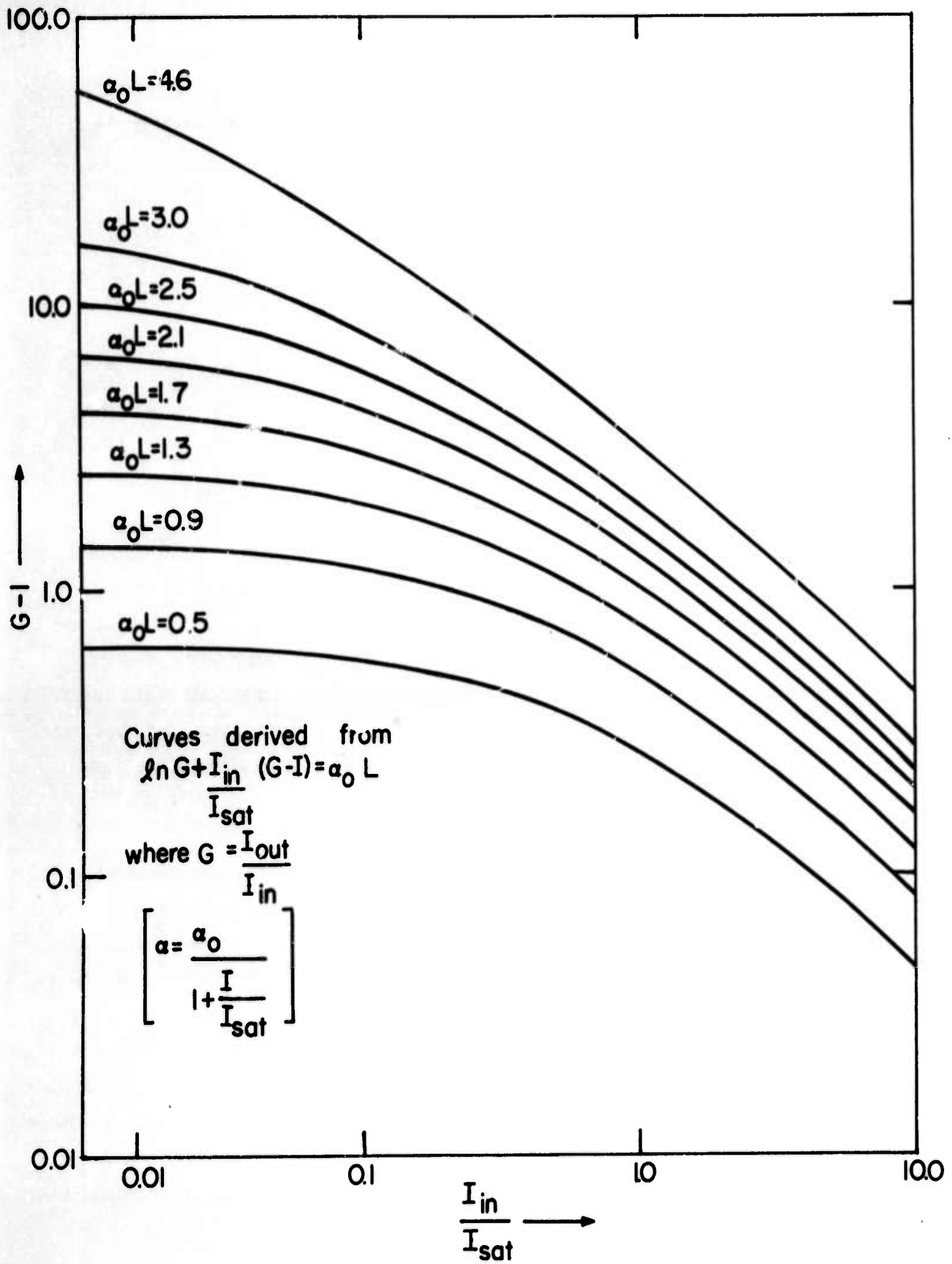
Fig. 5   Plots of ln (G-1) vs Input Power for Various Values of $a_0 L$

14

With this preface, let us consider the energy storage accessible to a 10 μsec input pulse, passed through a dc-excited tube of two-inch diameter with a typical low-signal gain of 1.2 dB/meter ($\alpha = 0.003$ cm^{-1}). From this data, the inverted state density is 5×10^{14}/cc, and at a photon energy of 1.7×10^{-20} J/photon, the stored energy is W $= 4.2 \times 10^{-3}$ J/liter of discharge. On this basis some 420 mJ would be available from the full set of rotational levels in a 50-meter length of two-inch discharge. This number could be added to by transfer from other vibrational states. On the other hand, if only one of the set of 001 rotational states were involved, only 20 mJ would be available as a lower limit for the pulse output.

A second estimate of the available energy can be derived by considering the power output from a two-inch tube operated as an oscillator. Such a tube delivers 75 W per meter (at a gas flow rate of approximately 2.5 meters/sec).

Thus in any 100 μsec interval, an energy of $75 \times 10^{-4} \times \frac{1}{1.8}$ J/liter is delivered. We can draw the inference that 3.7 mJ/liter would be accessible to a 100 μsec pulse. In terms of length, a 50-meter discharge would have approximately 370 mJ accessible to a 100 μsec pulse.

The fraction of this energy available to a 10 μsec pulse would depend on the relative populations of excited CO_2 to excited N_2. The ratio of these populations will be the ratio of gas pressures, modified by a factor depending on the relative number of available rotational-vibrational states in the same energy range. The ratio is of the order $N_2/CO_2 = 4:3$ for equal pressures of N_2 and CO_2. As a result we expect approximately 1.6 mJ/liter to be available to a 10 μsec pulse under dc excitation (or 160 mJ/pulse for a 50-meter, two-inch tube). These two estimates set upper and lower limits to the energy available per 10 μsec pulse; i.e., 50 meters of dc-excited tube should give between 20 and 160 mJ per pulse when driven as a saturated amplifier.

15

C. Energy Conversion Efficiency in Oscillators and Amplifiers

The efficiency with which energy from the primary power source is converted into useful output radiation depends in part on the excitation and collision processes occurring in the electrical discharge, in part on geometrical factors which determine the fraction of the total excited volume accessible to the radiation field of the device, on the efficiency with which radiant energy is coupled out from the active region, and finally on the temporal aspects of the excitation and emission processes. The most complicated of these determinants are the multiple ionization, collision, and excitation effects which go on to establish the inversion between the emitting molecular levels. These depend on gas mixture, current density, temperature, and gas flow rate. Despite the complexity of the details, we can state over-all experimental results for oscillators.

Experiments have been performed in which at least 80 percent of the available energy generated as a molecular inversion has been extracted in the output beam. Under these conditions, and using laser mirrors which maintain a radiation field filling the active region of the discharge, efficiencies of 15 - 20 percent have been achieved. That is, 15 - 20 percent of the energy dissipated in the discharge itself has been converted to an output beam which, although belonging to a single P line, usually contains a number of separate modes. Under these conditions, some 75 watts per meter of discharge is obtainable. The number depends on the gas flow rate, and at higher flow rates, 100 W/meter has been quoted. In annular type discharge tubes, output figures of 200 W/meter have been quoted.

On the other hand, the need to produce a single-mode output forces a restriction of the radiation field to a size smaller than that of the actual active discharge region. As a result, we can expect the output efficiency to decrease, roughly by a factor of two. While this figure may be improved by more sophisticated designs of discharge tubes, we will consider our own transmitter designs to be based on a 10 percent efficiency for power extraction in a single mode.

16

The efficiency with which one extracts energy from a single-mode amplifier will depend on the level at which it is driven. In the limit of large input signals where the amplifier becomes nonlinear and is driven into saturation, its efficiency should approach the cw oscillator figure, namely 20 percent multimode, 10 percent single mode. As will be seen in the next section, our experiments indicate that strong saturation takes place when the input intensity is of the order of 60 W/cm^2. For an efficient amplifier, then, one should arrange to reach this level of radiation density as soon as possible.

In an amplifier where the input is a sequence of pulses, with a duty cycle of one-tenth or less, the power extraction problem is more complex, as indicated previously. If we are concerned with extraction of energy in 10 μsec pulses, the repetition rate of these pulses should be increased until the pulse spacing is of the order of the time for energy transfer from the reservoir of excited N_2 to the upper laser level, a time which we estimated to be of the order of 100 μsec in the normal gas mix. For repetition rates greatly in excess of 10,000 pps, the output efficiency should again be comparable to that of a saturated amplifier driven by a cw signal.

The output power depends on an integration of the low-signal gain across the tube cross section, and this will be a maximum for current values greater than for optimum gain measured on axis. In choosing amplifier cross sections for our present program, we wish to obtain the highest gain in initial amplification stages, the largest total power in later stages, and overall, an output intensity distribution either: a) as uniform as possible across the output plane, or b) as close to gaussian as possible. Choice a) maximizes the use of the amplifier tube cross section, and at the same time minimizes the angle of the central lobe of the transmitter pattern (at the expense of introducing a side-lobe structure) whereas choice b) eliminates the transmitter side-lobes at the expense of less efficient use of the tube cross section. In either case it seems that in the preamplifying section constant gain off-axis would be helpful to preserve the input intensity distribution. In the power amplifier sections, either a uniform gain or one peaked up off-axis is called for. These conditions are closer to those appropriate to maximum power output than to those chosen for maximum axial gain.

17

III. INITIAL EXPERIMENTAL PHASE

A. Gain and Saturation Measurements in dc-Excited Amplifiers

The first seven months of this project were devoted to meas-
urements of the amplification characteristics of dc- and pulse-excited
amplifiers. The exact chronological order of the various measurements
was rather involved and depended on the availability of the various amplifier
components and power supplies. The detailed form of the equipment used in
these experiments also underwent a variety of changes. Its general form is
indicated in Fig. 6. The primary signal is derived from an oscillator emit-
ting between 15 and 35 W single mode, whose output was focused either by
mirrors or NaCl lenses to permit a focal plane shutter to form the pulse
train signal. After recollimation, the beam passed through two 3-meter
lengths of 2 cm i.d. amplifier and, at times, a further section of 20 meters
of a 5 cm i.d. amplifier. The small-bore amplifier could be excited with
ac, dc, or pulsed current; the large-bore amplifier was always driven from
a dc supply. NaCl windows have been used throughout this system.

The mirrors on the oscillator were usually a 10-meter radius,
gold-coated silica reflector set in opposition to a one-quarter inch thick
germanium optical flat, mounted in a water-cooled holder. The open
structure of the oscillator allowed the introduction of irises to produce a
single-mode output. Due to air currents in the open sections, however,
the output tended to fluctuate with time. In the later stages of the program,
a much improved oscillator was used that had internal optics, polarizer
and irises. The gain experiments in this first phase, however, were all
carried out using the oscillator with external optics. The mirror surfaces
exposed to high powers in the latter stages of the amplifier were made of
stainless steel or sapphire, both gold plated.

Signals were detected using a gold-doped germanium photoconductor,
operated at 77°K. Average powers were measured using an anodized

18
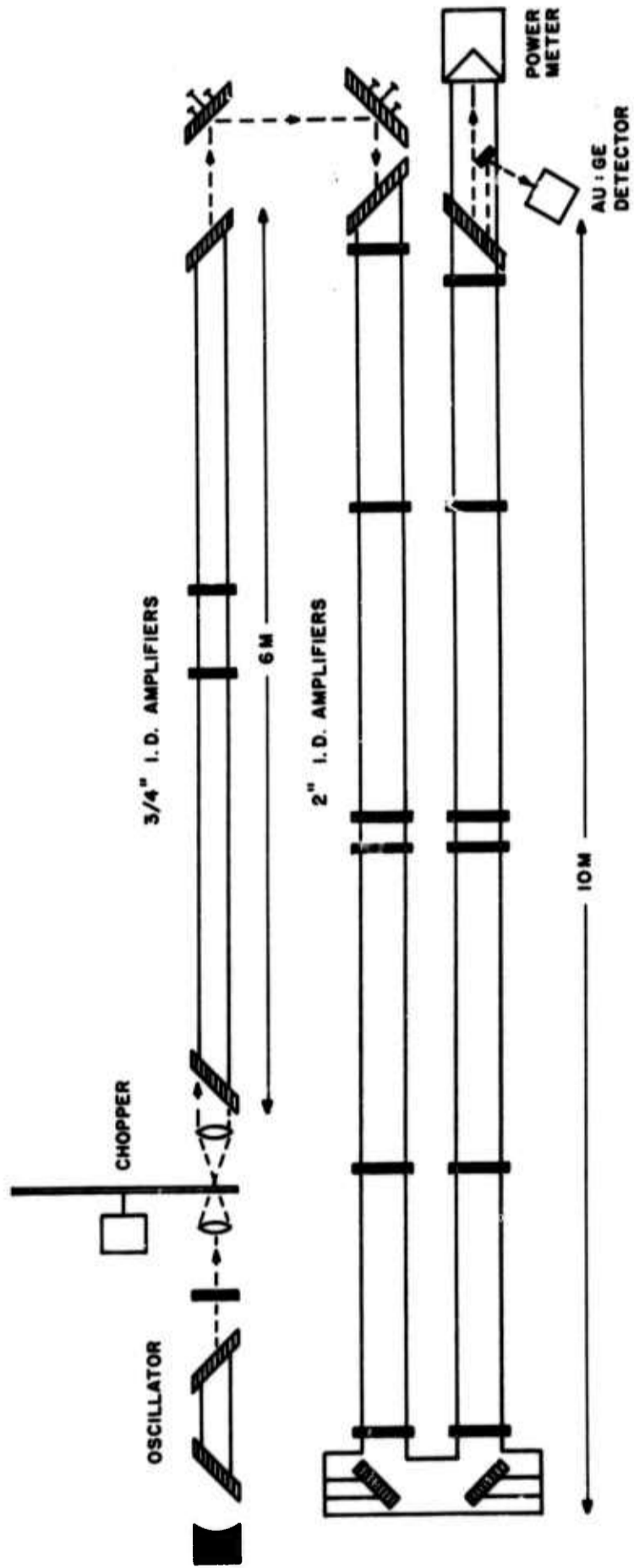
Fig. 6 Experimental Arrangement for High Power Amplification Measurements

19

aluminum, conical absorber cooled by a known flow of water. Measurements of the increase of water temperature, usually of the order of several degrees, gave a direct calorimetric determination.

For the purpose of clarity, we will divide the discussion into the following categories: cw amplification, amplification of a cw signal by current-pulsed amplifier, and of pulse trains by dc- and pulse-excited amplifiers. We will first treat the cw case. In its simplest form, a beam of uniform intensity would be amplified by a medium with uniform gain and saturation parameter. By contrast, our measurements have been taken on a more complicated system, where a roughly gaussian beam has been amplified by a medium where there is likely to be a strong radial dependence of gain. In Section II we indicated that the relationship between gain G and input $\beta = I_{input}/I_{sat}$ for a uniform case is expected to be of the form

$$\ln G + \beta(G - 1) = \alpha_o L \quad .$$

In the analysis of experimental data, it is useful to plot $\ln G$ vs. $P_{in}(G - 1)$. This should give a straight line plot with intercept $\alpha_o L$ at $P_{in} = 0$ and a slope of $-1/P_{sat}$.

We carried out such experiments on cw gain in dc-excited amplifier tubes of i. d. $= 2$ cms (3/4 in.). Figure 7 shows the results of two sets of experiments, one with a convergent beam, the second with a uniform beam. From both sets of data, we obtain $d^{\alpha_o L} = e^{2.2} = 10^{0.95}$ for a length of three meters ($\alpha_o = 0.73$ nepers $= 3.2$ dB/m). The uniform cross section beam gave an effective saturation power of 13 W, an average saturation intensity of 28 W/cm^2. The corresponding intensity at the center of the beam was ≈ 56 W/cm^2. A similar experiment has been performed by
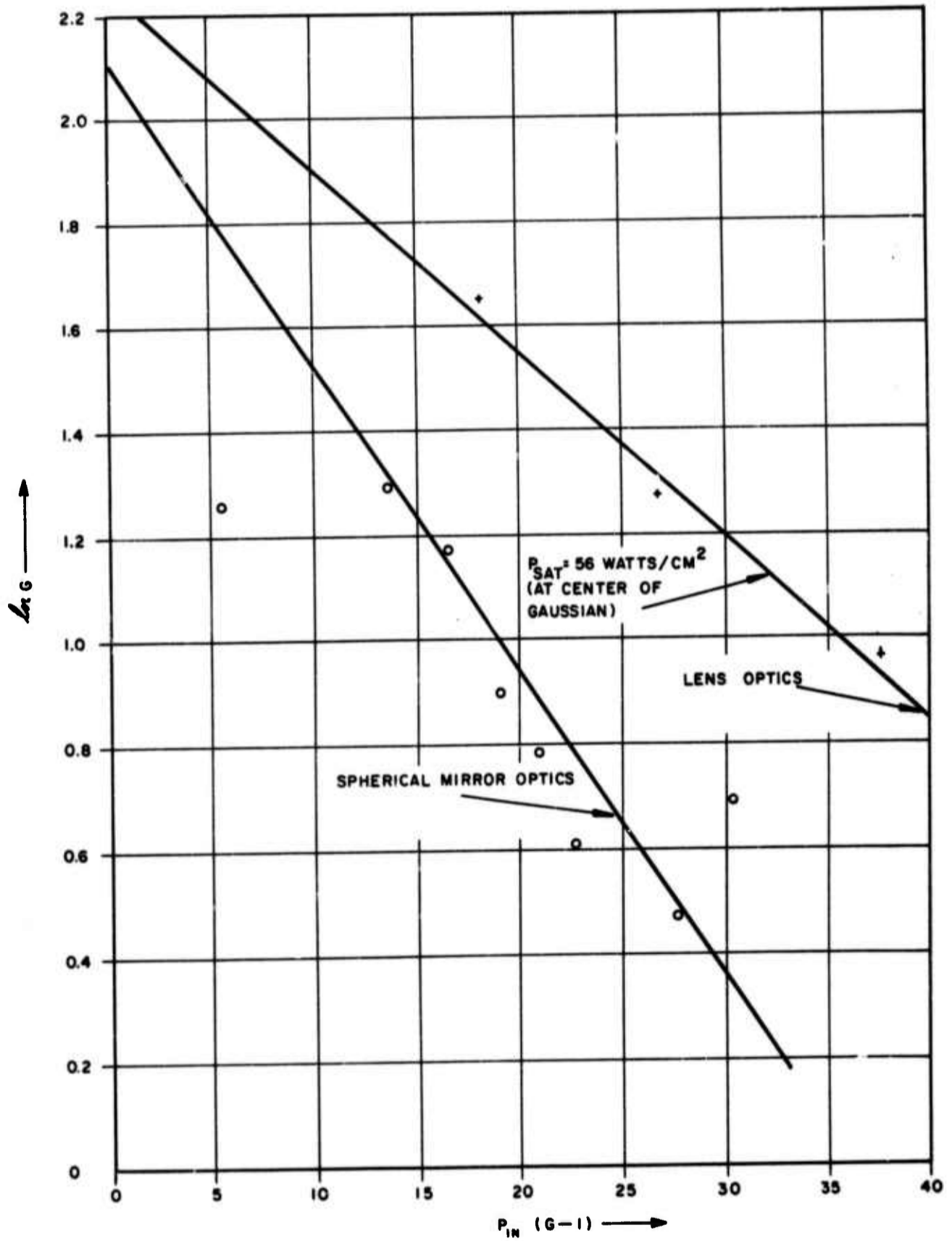
Fig. 7 Experimental Data for a 3-Meter Amplifier
Plotted as ln G vs. P_{in} (G-1)

21

Kogelnik and Bridges[6] who also obtain a gain of 3.2 dB/meter for a 2 cm tube. They quote a central intensity of 100 W/cm for I_{sat}, but on reanalyzing their data in the manner indicated above, we obtain a value of 65 W/cm^2 (Fig. 8).

These results must be compared to the value of 24 W/cm^2 which we made on the basis of the saturated power output per unit – length of such a discharge. It will be seen that the average saturation intensity derived for the amplification measurements agreed well with our estimate, and gave some substance to our use of similar estimates for the amplifiers of other diameters.

B. Optical Pulse Amplification in dc-Excited Amplifiers

Figure 9 shows an early result of the amplification of 20 μsec pulses in the small bore (2 cm i.d.) amplifiers excited by a 60 cps current. The multiple traces indicate the variation of pulse profile with time during the current cycle. Figure 10 gives a better sense of this variation. The original flat-topped pulse becomes progressively distorted by depletion of the molecular inversion by the leading edge of the pulse. In dc-excited discharges, the saturation behavior is the same, although the peak gain observed is somewhat lower in the dc case as compared to the peak gain for ac excitation. For a steady input signal of 15 W, ratio of peak gain was approximately 2 to 1. In early experiments of this type, we found that input intensities of the order of 200 W/cm^2 were required to reduce the gain of a 3-meter length of such a tube by a factor of 2 from the low-signal value. It is clear that the effective saturation parameter for short pulses is considerably larger than the corresponding cw case.

An alternate way to present the data is to plot the observed gain level as a function of time after turning on a long pulse input signal. Figure 11 shows the result of such an experiment, contrasting the pulsed results with data taken using a cw input of identical geometric form.

22
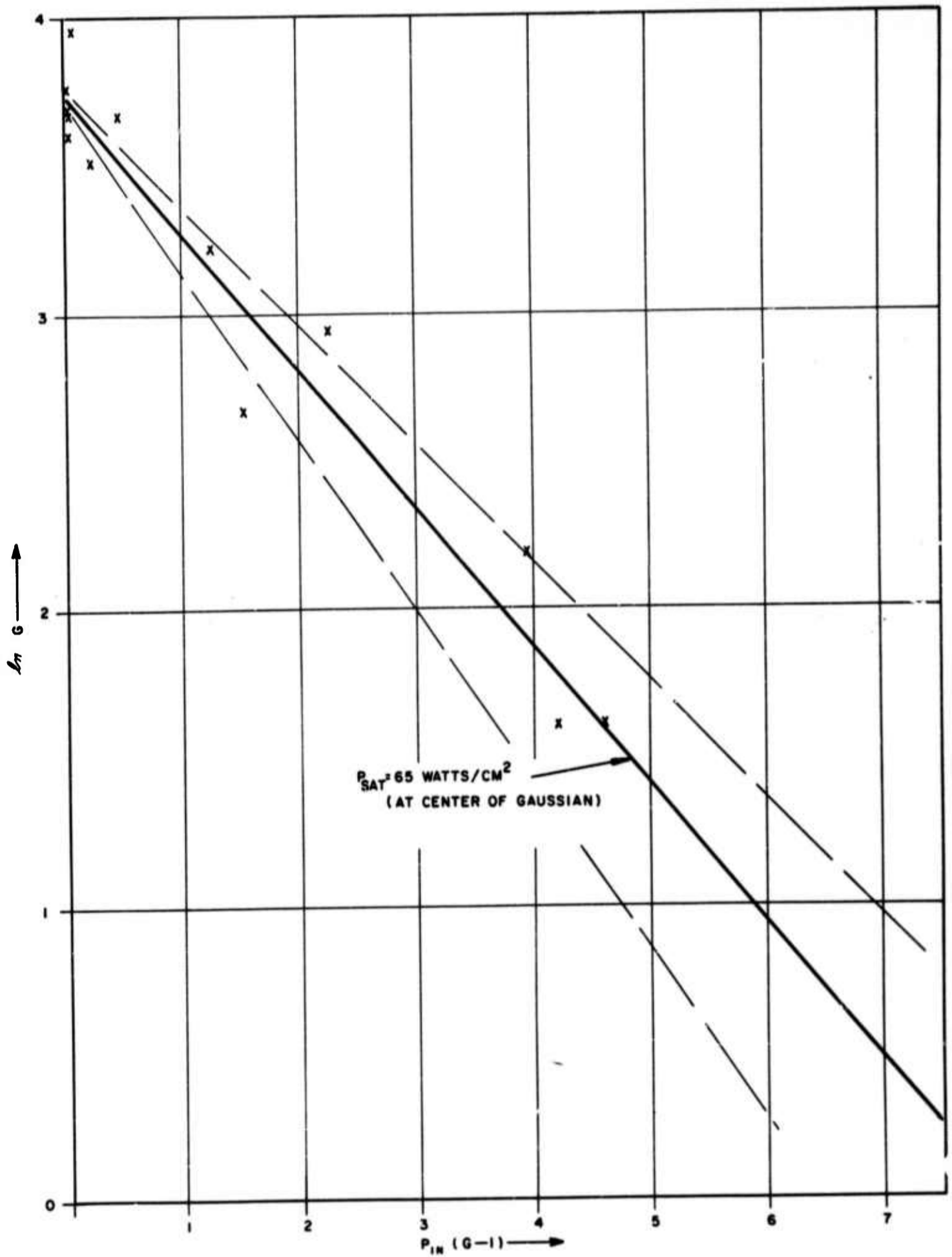
Fig. 8 Experimental Data from Kogelnik and Bridges[6] for a 5-Meter Amplifier Plotted as $\ln G$ vs. P_{in} (G-1)

23
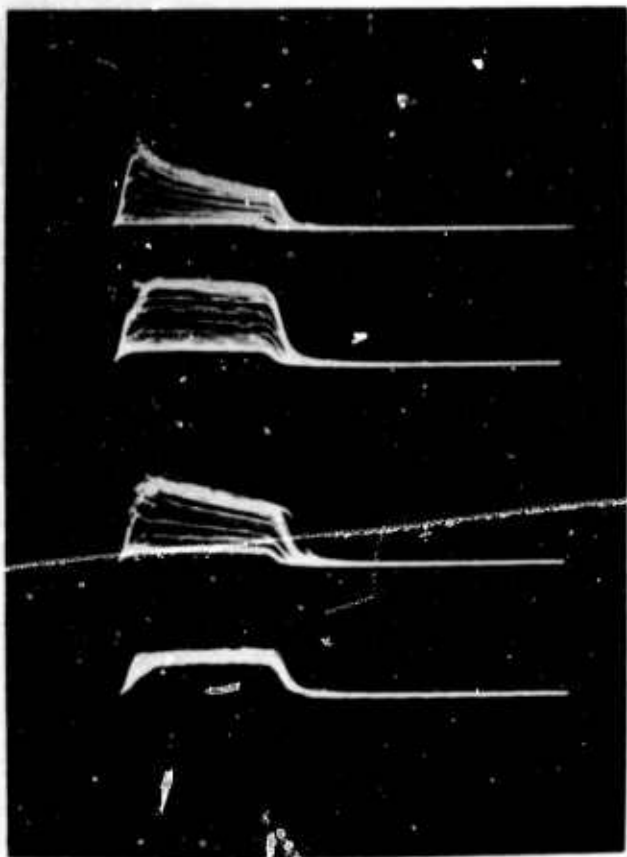
(a) Output pulse after amplification
sequentially by Amplifiers A and B

(b) Output pulse from Amplifier B
in which there was uniform propagation

(c) Output pulse from Amplifier A in which
severe beam constriction took place

(d) Input pulse (Length 20 μsec)

Fig. 9   Pulse Distortion Produced on Amplification
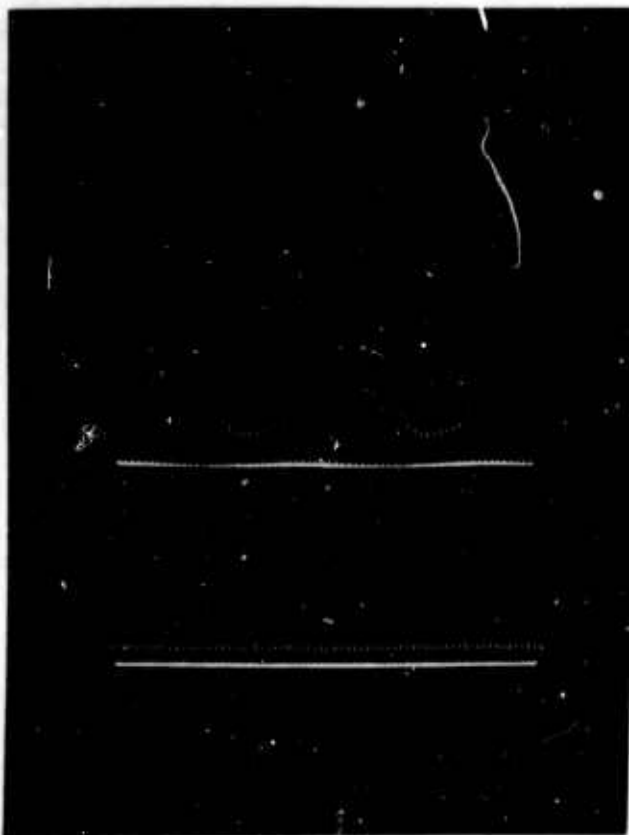
(a) Amplifier output

(b) Input – a train of 20 μsec pulses

Fig. 10   Time-Dependent Amplification in a Discharge Excited
by 60 cps Current

24

100

$t = 8\,\mu sec$

$t = 120\,\mu sec$

$t = \rightarrow \infty$ (C.W. EXP)

$(G-1)$ →

1

0

0.01   0.1   1   10

P_{IN}/P_{EXP}
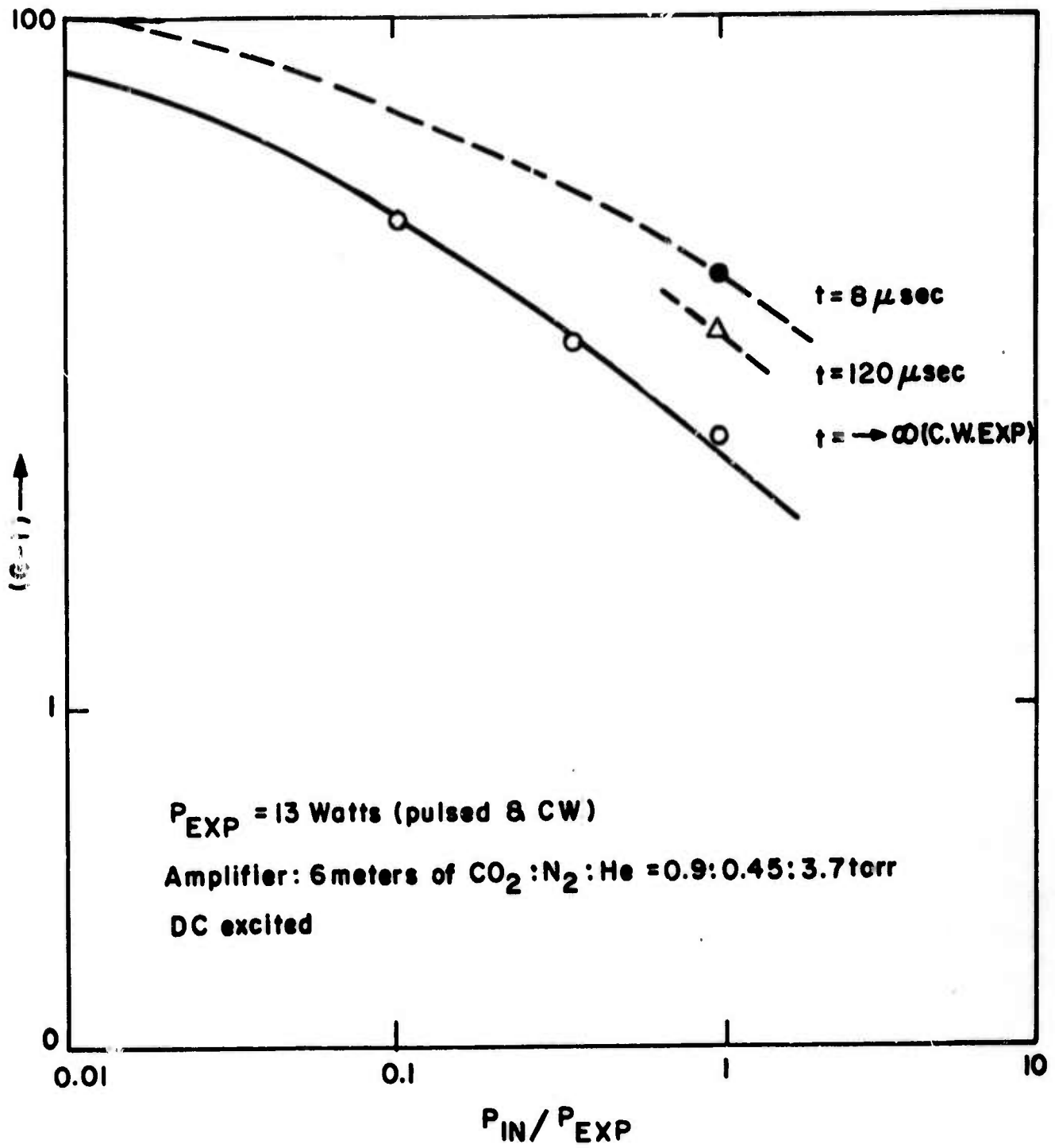
Fig. 11   Large Signal Gain Observed as a Function of
Time for a Single Input Pulse

Drawing the dashed curve appropriate for the cw analysis through the 8 μsec point is admittedly done on shaky grounds, but it indicates a displacement of some 7 times to higher powers and would then give 7 × 28 or approximately 200 W/cm^2 for a spatial average saturation power density.

The detailed analysis of data of this type must take into account both the spatial and temporal varieties of the driving signal. We did not have time to attempt this analysis. Instead we simply used the elemental data to form the basis of a design for an experimental high power amplifier.

It was clear that as a design parameter, an input power density of this order (200 W/cm^2) was required to efficiently extract the energy stored in the excited CO_2 molecules. The efficient extraction of energy for the reservoir of excited N_2 molecules now required a repetitive application of the 10 μsec pulses. We have taken data on the complete system of three-quarter and two-inch diameter amplifiers shown in Fig. 6. Due to the limitation of our recollimating optics at the time of the experiment, the full cross section of the large bore amplifiers was not used. As a result, we estimated that only one-half of the available volume of excited gas molecules was influenced by the injected signal. The data is shown in Fig. 12. For the 10 μsec pulses, the initial slope is 25 mJ/pulse with a progressive falling away from the line with increasing repetition rate. If we interpret this data on the basis of a model with single time constant τ connecting the N_2 and CO_2 states, τ is the reciprocal of the frequency at which the curve drops away from the initial straight line by 1/e. In our case $\tau = 100$ μsec. In this experiment we used a standard gas mix of 0.5 torr CO_2, 0.9 torr N_2, and 3.7 torr He in the small bore section. At these pressures, and a gas temperature of, say, 500° K, a time of 100 μsec would imply that approximately 200 collisions are required per quantum transfer.

As a practical matter, we were able, in the first high-power amplifier, to obtain 200 W of average power at the 12 kc repetition rate,

26
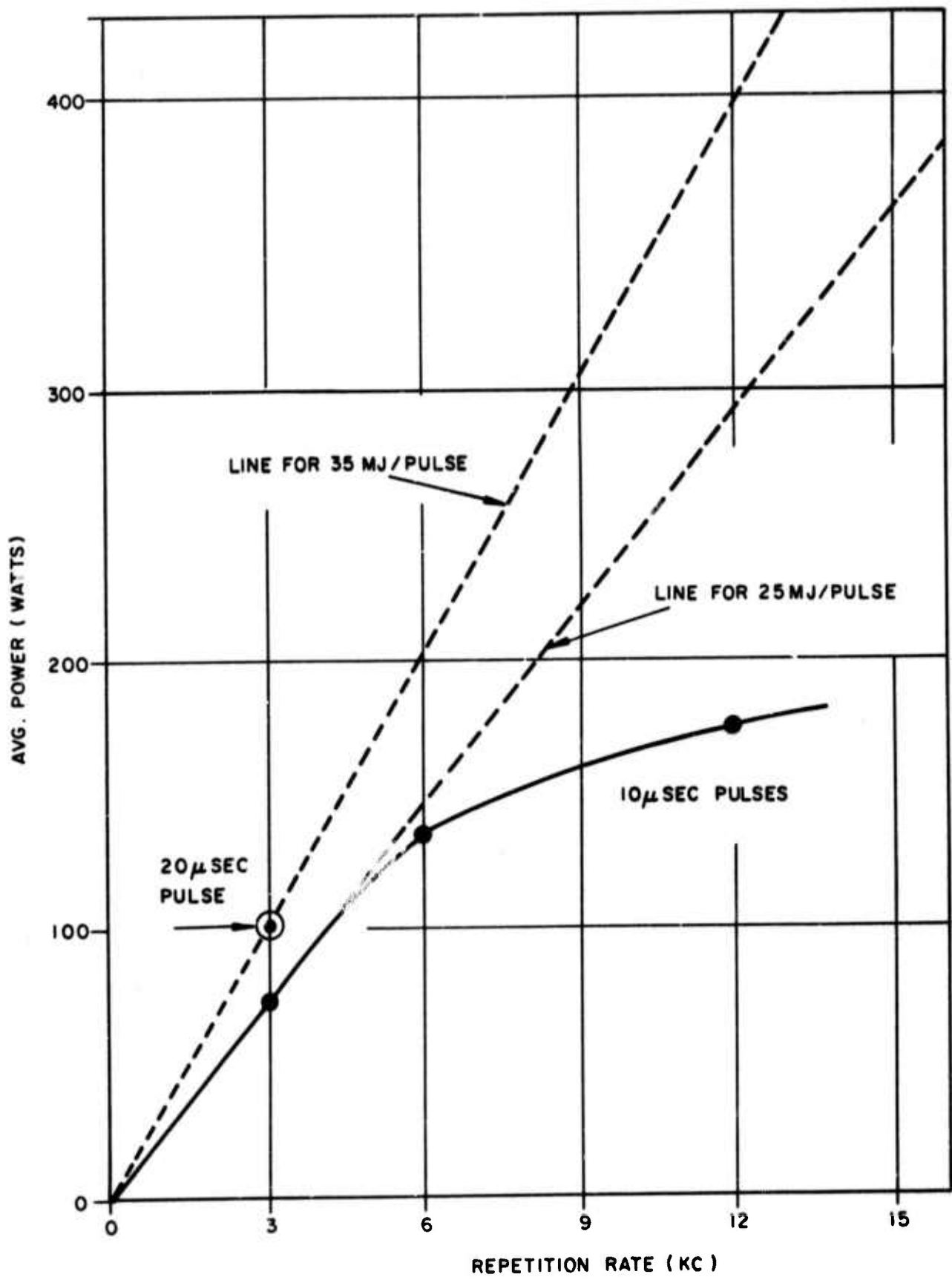
Fig. 12   First-Phase Experimental Results on Pulse Amplification

a level which would correspond to an initial slope of 28 mJ/pulse. This implies that if the same excitation had been applied to the total active volume, some 56 mJ/pulse would be achieved. At a repetition rate of 12 kc, the output per pulse will have dropped to some 60 percent of the low rate value, namely to 33 mJ/pulse. This figure is to be compared to the estimate of 65 mJ/pulse derived from earlier analysis in this report of the cw emission properties of oscillators. The present results suggested that the large-bore amplifier should be driven more vigorously and, in fact, the experimental output peak intensity was only 150 W/cm^2 while the input was approximately 100 W/cm^2.

C. Optical Pulse Formation and Amplification in Pulse-Excited Amplifiers

At the beginning of our experimental program, it appeared that electrically pulsed amplifiers would be well suited to our purpose. The published work of Frapard et al.[7] had indicated a considerable increase in output power level of a pulsed oscillator as compared to the same device operated in a cw mode. Our experiments verified this work, but soon revealed a serious deficiency. While the output power level in a single pulse was enhanced, it proved impossible to repeat the process at a rate sufficient to maintain a high average power from the device. In fact, the highest average power was less than the corresponding cw power by a factor between 2 and 3. In these first experiments, we studied the output formed by passing a uniform train of pulses with peak height approximately 15 W through pulse-excited discharges in small-bore amplifiers. Figure 13a shows typical traces obtained in this type of experiment. In this particular case a current pulse of 120 μsec duration was applied to the mix normally used for dc-excited tubes, namely 0.5 torr CO_2, 1 torr N_2, 3.7 torr He.

28
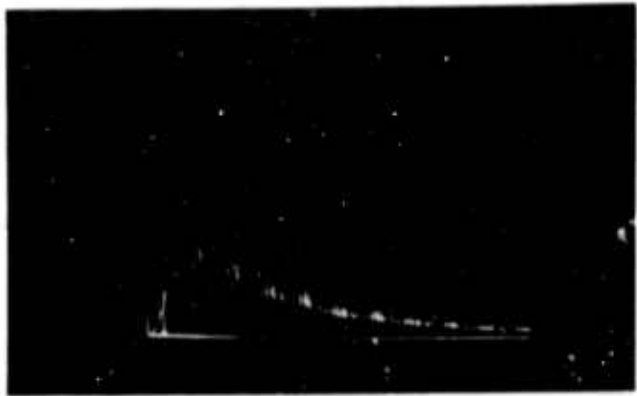
Trace a) Gain profile measured with 10 μsec pulses during and after the application of a 120 μsec current pulse . (Time scale: 1 division = 200 μsec)
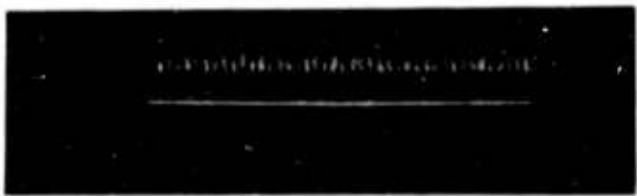
Trace b) A similar measurement using dc excitation

Fig. 13   Optical Gain Enhancement Under Pulse Excitation
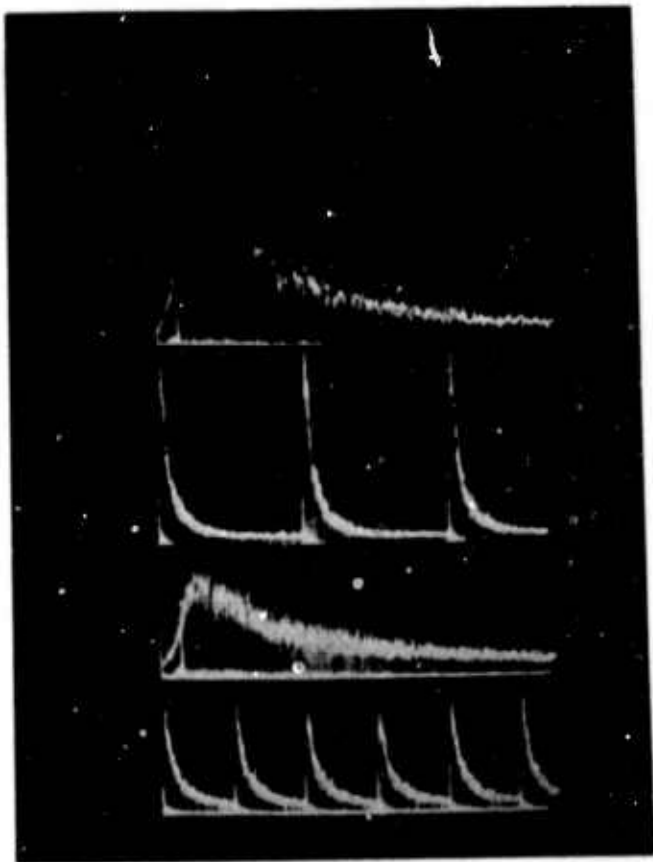
Trace a) Gain profile using 120 μsec current pulses rep rate of 100 pps (Time scale: 1 division = 200 μsec)

Trace b) As for a) but with reduced time scale

Trace c) As for a) with 300 pps

Trace d) As for b) with 300 pps

Fig. 14   Deterioration of Gain in Pulse Excited Amplifiers

29

The photograph shows the superposition of many traces, each of which has separations of 330 μsec between the 10 μsec measuring pulses. In this particular instance, we see that the pulse gain profile continues to rise after the termination of the 120 μsec current pulse, passes a maximum some 200 μsec later, and slowly decreases over the next millisecond.

By using 15 μsec current pulses, we produced a situation wherein most of the increase of gain with time occurred after the current pulse. This buildup in the normal gas mix is governed by the N_2 - CO_2 energy transfer. The observed curves are again consistent with a 100 μsec transfer time.

We found also that the pulse gain measured at its maximum value after the application of the current pulse was increased by a factor of 2 over that measured in the same mixture using dc excitation (Fig. 13b). By increasing the length of the exciting current pulse to approximately 250 μsec, we achieved a gain enhancement of three times the dc value. In interpreting this factor, it should be noted that the output pulse profiles indicated that partial saturation was occurring in the pulse amplification. Thus the small signal gain may have been increased by an even greater factor. This data implies that for a period of some 200 μsec, it is possible to at least triple the energy storage in levels accessible to a 10 μsec pulse, a result which at first sight is very attractive from the point of view of producing a compact pulse amplifier. However, if we have to provide high average powers by using high repetition rates, we would be required to pulse excite at a correspondingly high rate. Unfortunately, the gain enhancement achieved with each current pulse decreases as the pulse excitation repetition rate increases. Figure 14 shows the corresponding profiles for repetition rates of 200 pps and 300 pps. The obvious drop-off in gain indicates that a process with an effective decay time of some 2 - 3 milliseconds comes into play in a 2 cm i. d. tube. Following a comparison of this data with

that obtained by our companion contractor T. R. G. , Inc. at the first quarterly review, it appeared likely that the time constant was associated with the temperature of the gas mix, and depended on both the nature of this mix and on the tube diameter, becoming longer as the tube diameter increased.

Subsequent gain experiments on a 5 cm diameter tube (Fig. 15) confirmed this interpretation indicating a recovery time of just over 5 millisec. We were also able to compare these results with measurements taken by Van Lerberghe et al.[8] on the pulse recovery on double pulsed oscillators. Their work (Fig. 16) showed a recovery time which depends on both gas composition and tube diameter.

In using the latter data, we have chosen those measurements with maximum helium content in which case the gas dynamics in the two experiments will be properly comparable. Figure 17 shows the general agreement between the two sets of data. The observed recovery times of several milliseconds are consistent with the time for thermal diffusion to the walls at the gas pressures and tube sizes used in our experiments. On the other hand, the data are not consistent with a simple diffusion model in which the gas conditions are assumed to be identical for all tube sizes. In the latter case, we would expect the recovery time to depend quadratically on tube diameter. Whether the recovery mechanism has to do simply with a thermal relaxation, or whether there are other important diffusion effects at work such as the diffusion of excited molecular species having to do with the relaxation of the 0n0 levels of the CO_2, or the elimination of ionization which may determine the efficiency of excitation in the next pulse, is not clear from our limited experience.

The key to the use of pulse-excited amplifiers will be the overcoming of this recovery process, whether by the use of small bore tubes, additional surfaces for gas-surface collisions, or by brute force removal of the gas at high velocities.

31

GAIN VARIATION OBSERVED IN A PULSE EXCITED
AMPLIFIER TUBE DIAM 5 cms, LENGTH 8ft

Gas pressures	He	CO_2	N_2
●	1.8	0.6	1.0 torr
○	1.8	1.8	1.0 torr

Pulse gain (G)

Pulse repetition rate (pps)
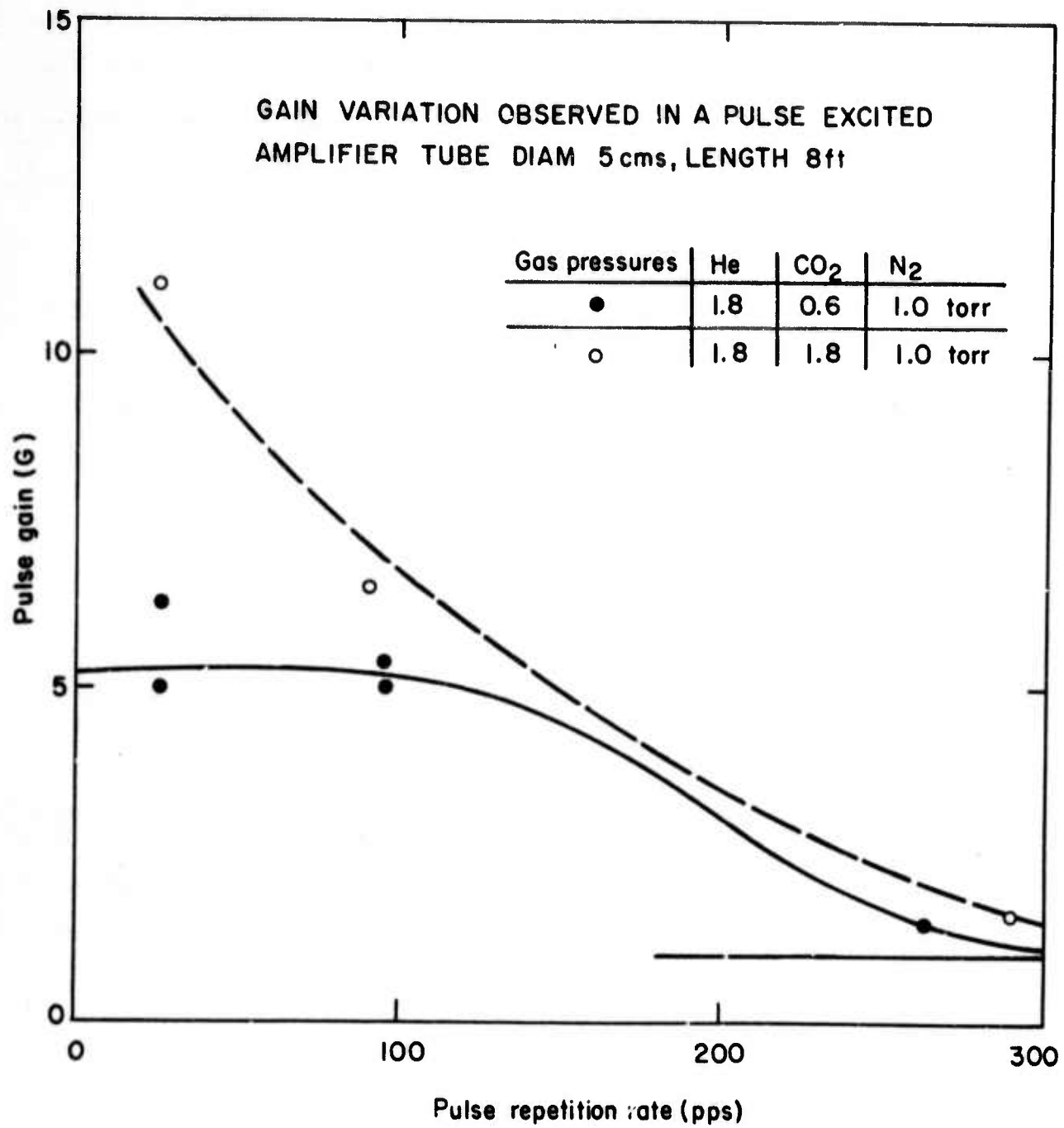
Fig. 15   Dependence of Small-Signal Gain on the Repetition Rate in a Pulse

32
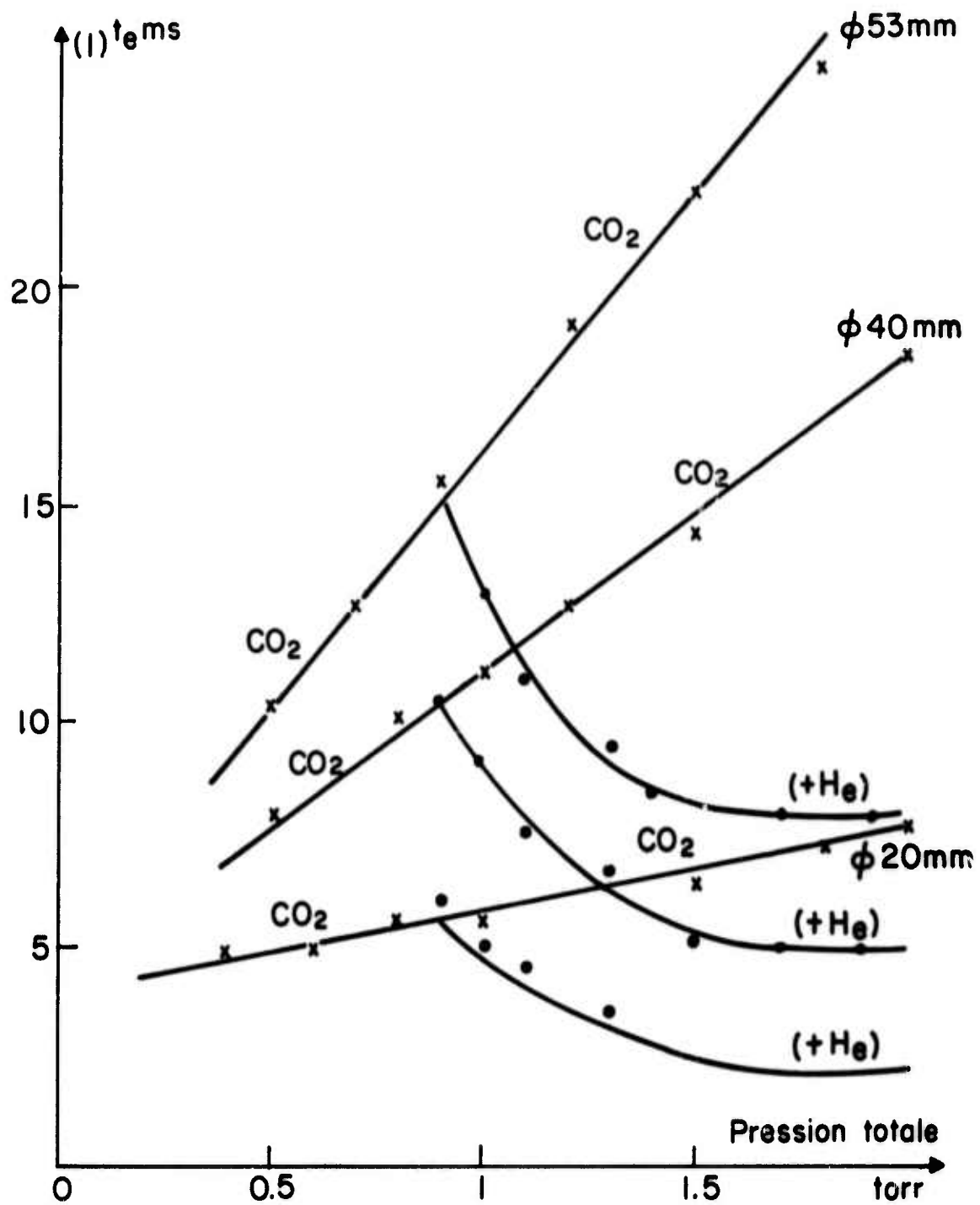
Fig. 16   Dependence of Recovery Time of a Double Pulse Oscillator on
Tube Diameter and on Total Gas Pressure for Pure CO_2 and
CO_2:He Mixes (after Van Lerberghe et al. [8])

33

τ Recovery (msec)

Diameter (cm)

	CO_2	N_2	He
●	0.6	1.0	3.0
▲	0.95	0	1.0
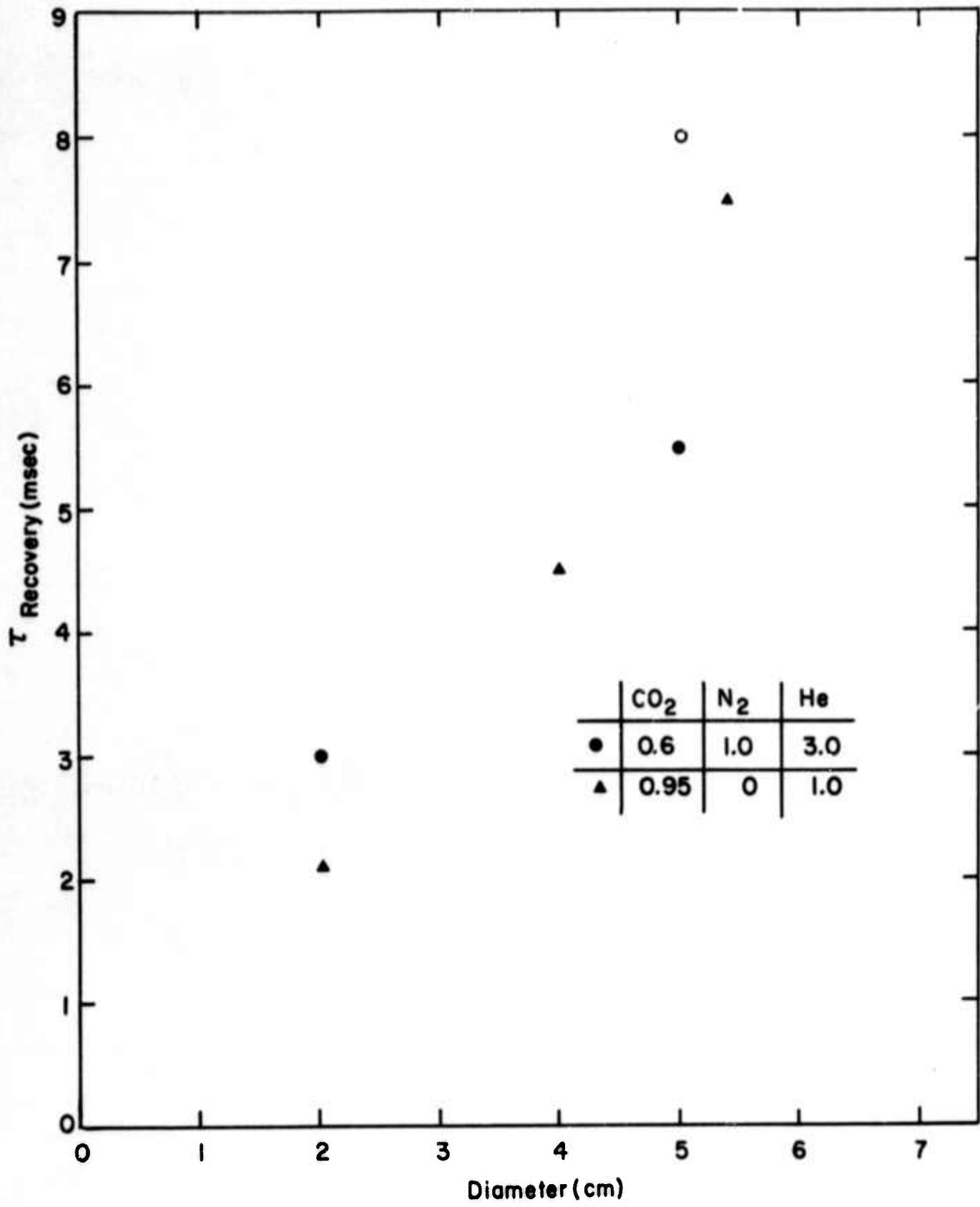
Fig. 17   Dependence of Recovery Time on Tube Diameter (composite data)

34

In our development of a 1 kW transmitter, however, these experiments suggested that pulse excitation was less efficient from the standpoint of the over-all size of the amplifier. Furthermore, other problems appear associated with the intrinsic high gain present in pulse-excited amplifiers in the absence of strong optical driving signals. This leads to spurious oscillations of the amplifier chain.

In a second set of experiments, we studied the pulse formation that occurs when a cw signal, present at all times in the system, is amplified during and after the application of a current pulse to the second section of the amplifying chain. Figure 18 indicates the type of pulse profile that results in such cases. The profile depends on the gas mix. Its decay time is shortest for pure CO_2 and increases significantly with the addition of nitrogen to the discharge. The profile becomes sharper as the gain is increased by raising the pulse current. The shortest pulse (≈ 70 μsec on base) was observed in pure CO_2, but the energy per pulse was much less than for the case of CO_2, N_2, He mixes.

D. Spurious Oscillations in High Gain Amplifiers

One of the major problems in handling high gain optical amplifiers, as in rf amplifiers, is the suppression of spurious oscillations which draw the power into unwanted output beams. An over-all power gain of 100 was contemplated in the production of 1 kW output power. With a duty cycle of one-tenth, this corresponds to an average gain of 1000 during each pulse and a corresponding small signal gain of at least 10^4.

In our first phase experiments, we detected self oscillations of the amplifier at a single-pass gain of 10^4 using 20 meters of two-inch diameter, and six meters of three-quarter inch diameter tube with a NaCl slab on one end, giving $\simeq 10$ percent Fresnel reflection, and a NaCl flat set at Brewster's angle at the other end. The effective double pass gain was $10^4 \times 1/10 \times 10^4$, or 10^7. Reduction of the single-pass gain by

Trace a) CO_2, Ne, He gas mix

Trace b) CO_2, He

Trace c) Pure CO_2

Fig. 18 Pulse Emission Profiles Generated when a cw Signal Is Passed
Through a Pulse Excited Amplifier
(Time scale: 1 division = 200 μsec)

a factor of 5 suppressed this effect. Apparently, there was sufficient surface backscatter from the NaCl Brewster window to cause oscillation at an effective total gain of approximately 10^6. That is, the Brewster window has an effective reflectivity of 10^{-6}. The oscillations appear as a steady output in the absence of any signal from the oscillator. With the chopper blade removed, the output rose to as much as 200 W, in a spatial pattern showing the circular fringes characteristic of reflections from the tube walls. With the chopper in place, the oscillations appeared as noisy spikes of the order of 2 μsec on base, with a delay of 1 - 3 μsec after the opening of the chopper (Fig. 19). The average power of these pulses could be as much as 30 W. In addition to these pulses, a noisy spectrum occurred when the amplifier was operated at maximum gain. This noise was apparently produced by reflections from the chopper blade itself (Fig. 20). The latter noisy oscillations gave average powers of up to 100 W.

When the primary oscillator was turned on, the spatial form of the output changed abruptly, and it became dominated by a pattern similar to that observed in the absence of any amplification. At the same time, the spurious oscillation pulses which had occurred while the chopper was open were completely suppressed by the incoming signal.

From these experiments it became clear that for stable operation of an amplifier one should either drive it into saturation with a cw signal, or isolate sections (each of which has a small-signal gain of less than 10^6) using reflective optics and well-made Brewster (or at least angled) windows. The separation could be achieved either with multiple shutters or by beam division and subsequent amplification in parallel elements. Alternatively, saturable absorbing cells could be used between the various segments of the amplifier, provided that they were inserted at a point where they would be driven by an input pulse large enough to initiate the saturation process.

37

Fig. 19   Spurious Oscillation Pulse in a dc-Excited
Amplifier. (Time scale: 1 division = 1 μsec)
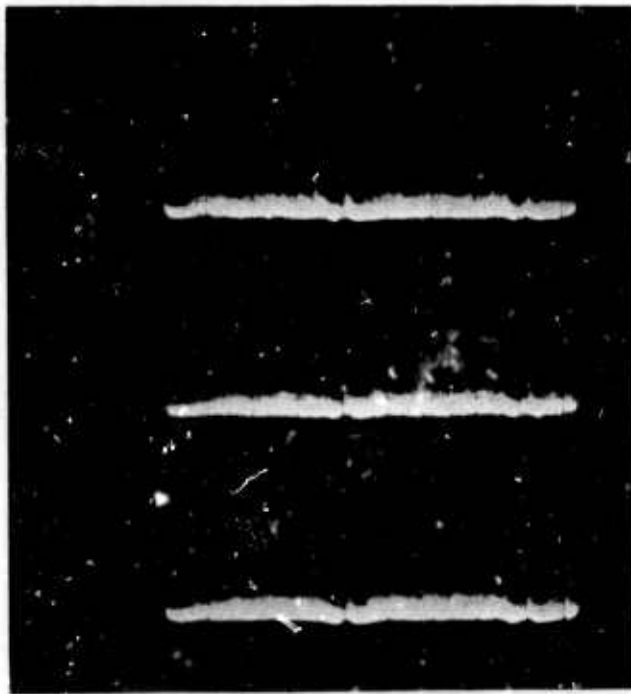
Fig. 20   Self-Oscillation Signal Produced by Reflections
from the Chopper Blade. (Time scale:
1 division = 20 μsec)

The self-oscillation problem complicates the design of a pulse-excited amplifier because of its inherently high gain per unit length. It is clear from the previous section that, if a series of 10 μsec pulses are required, total reliance on pulse forming by the pulsed amplifiers is inadequate (at least for pulse excitation in low-pressure discharges). Isolation of the various amplifier segments during the time that no optical input signal is present is therefore a necessity. Nevertheless, we conceived of a system of double-modulated pulse trains which provide an alternative to the dc- and single-pulse systems. Consider a system of pulses each 10 μsec long, separated by an interval of 160 μsec, which pass into a 50-meter length of two-inch amplifier, pulse excited at 100 pps. Each exciting pulse lasts approximately 500 μsec, somewhat longer than the time required for energy transfer from excited N_2 molecules to the CO_2 upper laser levels. For a period of approximately 1 msec, the train of 10 μsec input pulses can draw on an inversion of ≈ 750 mJ per pulse, repeated up to three times.

In this mode of operation, three pulses, each of approximately 750 mJ/pulse would form a 0.5 msec burst repeated 100 times/sec. In this type of amplifier, we take the fullest advantage of the high energy storage in the pulse-excited mode without as large a loss of average power as occurs when only one 10 μsec pulse is used per excitation pulse. We would expect an average power of 280 W to be obtainable from a 50-meter section of two-inch amplifier. While development of this type of excitation and operation may result in an increase of the usable repetition rate; i.e., beyond 100 pps, it is evident that in order to produce a 1 kW source by this means, a much longer amplifier will be necessary – approximately 200 - 250 meters.

E. Superradiance Effects

A problem related to spurious oscillations is the loss of energy due to amplification of the natural spontaneous emission at 10.6μ. While this is of low intensity and emitted isotropically, it will finally set a limit on the length of amplifier which can be kept excited continuously.

In a discharge with a small-signal gain of 1.5 dB/M, the instantaneous total population of the rotational levels of the 001 vibrational mode is approximately 1.5×10^{15}/cc.

The population of these states produces a spontaneous emission of the order of $\dfrac{1.5 \times 10^{15} \times 1.8 \times 10^{-20}}{4} = 0.7 \times 10^{-5}$ W/cc

As a simple model, consider a straight length (L) of tube 5 cm diameter filled with this medium and calculate the power flux from one end due to the amplification of the spontaneous emission along the tube length. For a long tube of diameter D, the solid angle of importance is $(D/L)^2$. Using the low signal gain formula the power flux at one end is approximately

$$ S_0 \cdot \frac{D^2}{4\pi\alpha} \times \left(\frac{D}{L}\right)^2 (e^{\alpha L} - 1) \quad , $$

where S_0 is the spontaneous emission power per unit volume and α is the gain coefficient. For

$$ S_0 = 0.7 \times 10^{-5} \text{ W/cc} $$
$$ D = 5 $$
$$ \alpha = 0.002 \text{ cm}^{-1} \quad . $$

we find the limiting length, $\overline{L}$, which produces the saturation power of 200 W, to be given by

$$ \frac{e^{\alpha \overline{L}}}{(\alpha 4)^2 e} \simeq \frac{200 \times 4\pi}{0.7 \times 10^{-5} \times (5)^4 \times .002} $$

$$ \simeq 3 \times 10^8 \quad . $$

Thus,

$$ \alpha \overline{L} \simeq 26 $$
$$ e^{\alpha \overline{L}} = 3 \times 10^{11} \quad . $$

40

It follows that severe population depletion will take place for a small signal gain of approximately 115 dB, assuming that low angle reflections from the tube walls are suppressed. On the other hand, if it is assumed that wall reflections at angles less than 10^{-2} radian are loss free, and are not suppressed by the use of apertures, the effective solid angle for amplification increases by three orders of magnitude, and the limiting gain would be reduced to approximately 80 dB. However, considering the likelihood of the onset of spurious oscillations at gains of 10^6, we do not believe that population depletion by superradiance will be a problem in practice.

F. Refractive and Distortion Effects in Amplifiers

For its present application, it is important that the transmitter have accurate definition and control of the output wavefront. The most obvious effects which could produce distortion of the output beam are:

1. Warping of the various optical elements (particularly mirrors) due to heating produced by absorption of the incident radiation.
2. Refractive effects produced by temperature gradients and molecular dissociation within the discharge.
3. Effects of nonuniform amplifier gain across the tube diameter.

Simple heating effects will cause a time average distortion proportional to the average power level. We have observed such effects in operating a 1200 W oscillator and have devised mirrors which essentially eliminate this form of beam distortion. This is done by making the mirrors from a material with good thermal conductivity (k) and high modulus of rigidity (G), and low thermal expansion (a). Defining a figure of merit kG/a gives the following result for a number of common materials.

41

Material	Figure of Merit
Aluminum	0.08
Brass	0.08
Nickel	0.19
Copper	0.33
Silver	0.17
Stainless	0.026 - 0.044
Fused Silica	0.025
Sapphire (20°C)	0.33

Of these materials, either copper- or gold-plated sapphire is to be preferred for this application. The mirrors used in the first phase 2-inch diameter amplifier were sapphire, while later transmitter designs used copper mirrors and, in some cases, fused silica, gold plated. In either case, approximately 1.5 percent loss occurs at each reflection. The resultant heat (15 W per mirror) must be removed by conduction cooling. In addition, there are likely to be transient distortions set up by pulse heating effects. A rapid expansion occurs at the absorbing surface each time a 10 μsec pulse is reflected. When an absorptive surface was used in amplification experiments, a clearly audible tone could be heard at 3, 6, and 12 kc, even at average power levels of a few watts.

As far as refractive effects are concerned, we studied briefly the nonuniform refractive index of discharges of a 2 cm-diameter amplifier tube, operated under both the normal conditions for a maximum amplification at 10.6 μ and with other gas mixtures. This was done by passing a collimated probing beam (λ = 6328 Å) along the tube axis and also along the tube wall parallel to the axis. We found that a refractive index gradient appears along the tube wall in discharges containing N_2, O_2, CO_2, and mixtures thereof. The introduction of 3 - 4 torr of helium into the discharge reduces the effect by a factor of approximately two. A pure helium discharge shows no observable effect. A

3-mm-diameter beam sent along the tube axis shows an expansion at its edges approximately three times less than the observed displacements for the beam along the wall. These effects are consistent with an axially symmetric negative lens effect with a parabolic dependence on radial position:

$$n(r) = n_o (1 + \gamma r^2) \qquad .$$

Our measurements show that for a discharge in 1 torr of CO_2, the refractive index at the wall is greater than that along the tube axis by an amount of 3×10^{-7}. This is to be compared to the refractive index contribution of 1 torr of CO_2, namely 4×10^{-7}. Whether the cause of this effect is purely a density variation or due to molecular excitation and dissociation is not clear. Assuming that the same refractive effect occurs for 10.6 μ radiation, and that the amplified beam extends over two thirds of the amplifier diameter, a high-gain amplifier mix should show an optical path change of approximately $\lambda/2$ for a 50-meter amplifier.

IV. INTERMEDIATE EXPERIMENTAL PHASE

A. Transmitter Design and Test Results

As a result of our gain and saturation experiments, we decided that the most appropriate design for a 1 kW source would use dc-excited amplifiers and mechanical optical modulation. Before deciding on the final design of this service, we constructed a test model capable of producing several hundred watts of average power. The design, as indicated in Fig. 21, consisted of a 2 m, 1/2 in. i.d. oscillator, a folded 12 m section of 1 in. i.d. buffer amplifier, NaCl modulator optics, and a 20 m section of 2 in. i.d. power amplifier. The discharge tubes were water cooled. The oscillator was run from a 30 kV supply with a 150 KΩ ballast at currents between 30 and 50 mA. The various sections of the amplifiers (four sections in the buffer amplifier and four sections in the power amplifier) were all fed in parallel from a 30 kV supply with multiple ballast resistors. Typical current levels were 60 mA for the individual buffer amplifier sections and 90 mA for the power amplifier sections. A 5 percent voltage ripple at 360 cps produced a 20 percent peak-to-peak current ripple in the amplifier tubes as a result of the negative impedance characteristic of the discharges.

The gas flow to the discharge tubes in the power amplifier entered at each end of the sections and was pumped out at the center by a 100 cfm pump. In the buffer amplifier this flow pattern was reversed with a 15 cfm pump attached to each end of the assembly. Three separate gas flow controls were provided for the oscillator, the buffer amplifier, and the power amplifier respectively. Considerable attention had to be paid to the symmetry of the electrical ballasting, the gas flow pattern, and the water cooling flow pattern, to ensure easy starting of all the discharges in parallel, their stability while changing gas mixture and tube current and their stability over long periods of operation. From the viewpoint of safety, it is desirable to have the end

44
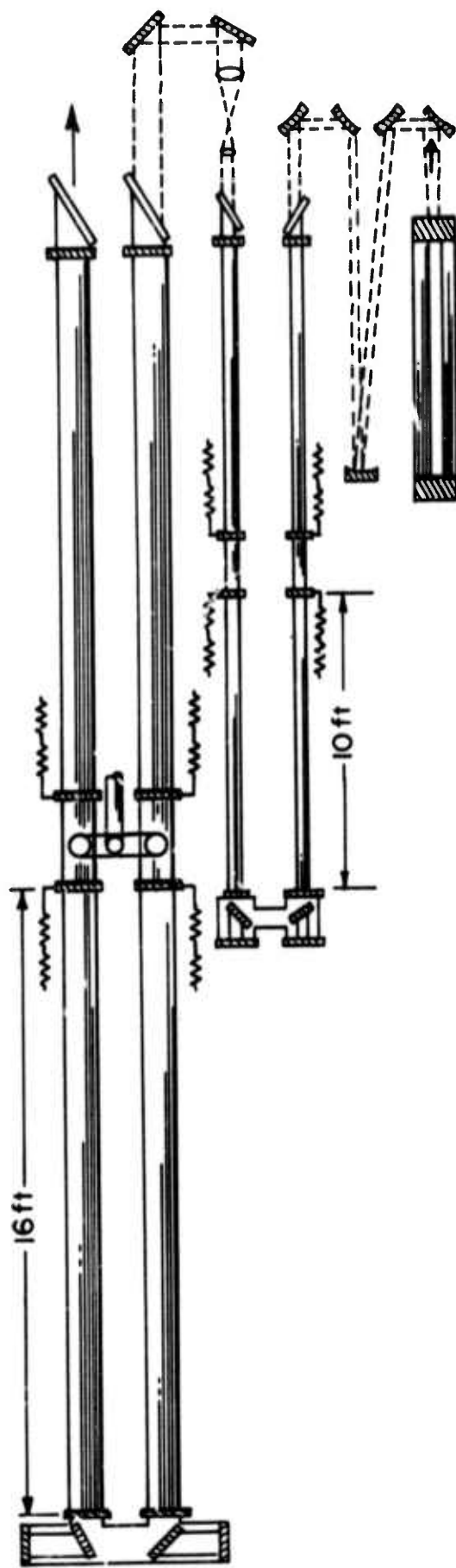
Fig. 21   400 W Breadboard Transmitter (schematic)

16 ft

10 ft

electrodes of all amplifier sections at ground potential. As a consequence, only one ballast can be introduced for each tube. This makes it necessary to introduce an unexcited section of tube between each discharge path. We find that a 10:1 ratio of discharge length to separation length is adequate to ensure a stable discharge pattern.

The optics in the oscillator consisted of a spherical back mirror (radius of curvature four meters) made from gold-coated silica together with an uncoated germanium flat for the output reflector. The latter was set in an aluminum housing and water cooled. The mounts for both mirrors were adjustable in angle; in addition, one end mount could be moved to allow length tuning. The output from this device was over 20 W when run without internal irises. The mode structure was usually in a spatial mode with two lobes. Introduction of an iris at the output end gave a single lobe output, but at cost of a power reduction to some 15 - 17 W. Mode jumping still occurred, but this could be eliminated for a period of the order of one minute by adjusting the resonator length. While this oscillator was adequate to perform the initial experiments on the amplifier, it was obviously not good enough for testing of the final transmitter design.

The beam divergence at the oscillator was approximately 3×10^{-3} radian. In order to recollimate the beam for projection through the buffer amplifier, a single concave spherical mirror (5 m focal length) was used at close to normal incidence. It was set 5 m from the exit window of the oscillator. The amplifier beam, observed as it emerged from the buffer amplifier, filled the full aperture and showed a concentric ring structure characteristic of reflection from the tube walls.

The buffer amplifier had NaCl Brewster windows at each end with the full 12 m folded into two 6 m sections by using a pair of gold-coated silica mirrors set up internally to the amplifier with two-angle controls on each surface. These controls could be operated from outside their housing.

Apart from the size of the structure, and the details of the mirror controls, the design of the power amplifier was little different from the buffer stage amplifier. In this case, however, the turnaround mirrors were made of gold-plated sapphire to minimize thermal distortion of the optics. In fact, no distortion effects due to heating were detected in either amplifier. (One of the silica mirrors, 1/8 in. thick, in the first collimating assembly did distort and was replaced by a gold-plated stainless steel mirror.) The modulator optics consisted of a pair of f/4 NaCl lenses with four- and eight-inch focal lengths. No attempt was made to eliminate the Fresnel reflection from the lens surfaces. As first set up, two gold-plated pyrex mirrors were set one on each side of the focal plane of the system, and approximately two inches from the focal point. This proved to be a mistake: the second mirror surface, which was subjected to pulsed heating, deteriorated by developing spherical bulges in the gold plating, while the first surface finally broke. A more successful arrangement took the beam directly through the modulator before letting it strike the surfaces of the turnaround mirrors.

The most difficult task in the alignment of the entire system proved to be control of the beam as it passed through the buffer amplifier. The process was greatly hampered by our inability to observe the beam directly as it approached the turnaround mirrors. The 1 kW transmitter was designed with this difficulty in mind.

Figures 22 and 23 show two views of the system. Figure 22 shows the back end of both the power amplifier and the buffer amplifier. The mounting and controls of both pairs of turnaround mirrors are partially visible. The vertical mounting of tubes was done to conserve space, but has the disadvantage that dust can collect more easily on the lower mirror in the turnaround assembly. Figure 23 shows the somewhat involved arrangement at the operating end as it was first set up. The output end of the oscillator can be seen at bottom center. The adjustable mirrors form part of the first collimator. The original arrangement of the modulator lenses can be seen clearly at the lower right.
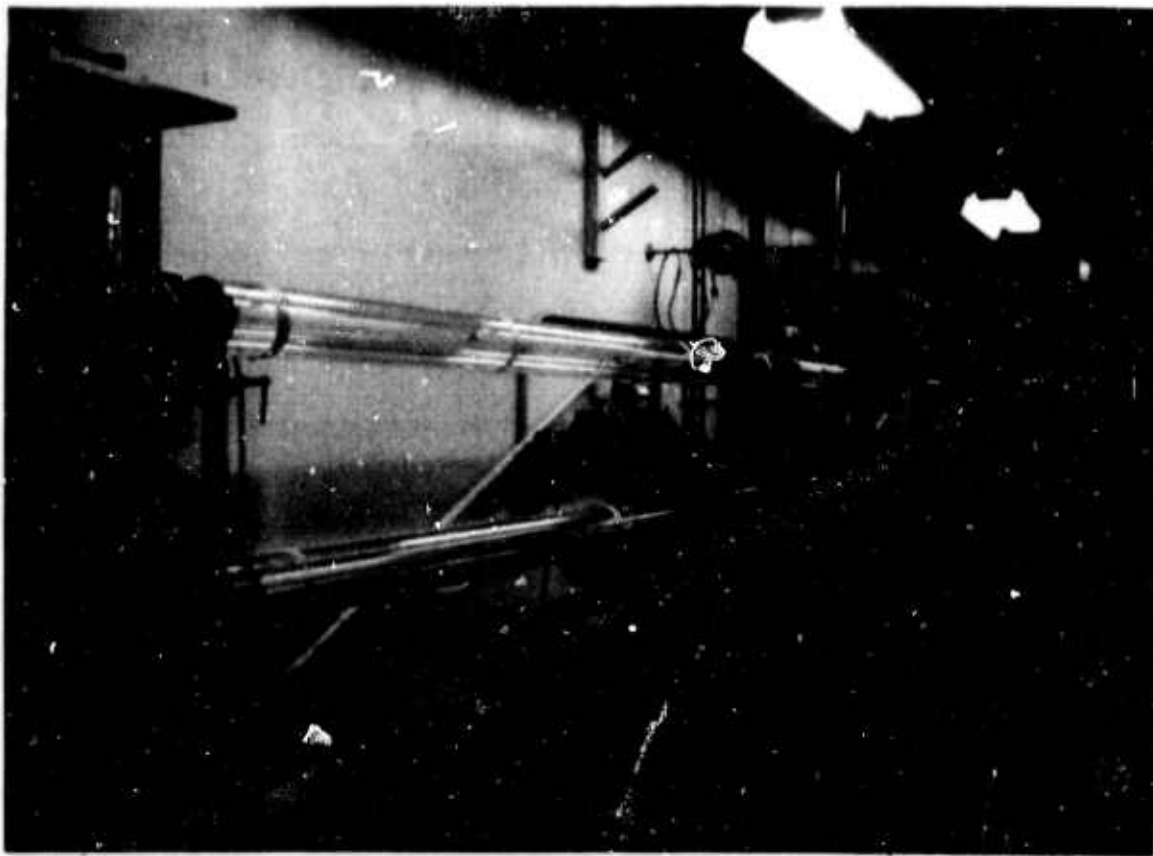
Fig. 22   The 400W Transmitter - Rear View

Fig. 23   Front View of the 400 W Transmitter Showing the Primary
Oscillator, Modulator Optics, and Amplifier Ports

The output for the entire system was measured by a flowing water calorimeter and its temporal behavior was observed with an Au-doped Ge photoconductive detector operating at 77° K.

Figure 24 shows the form of the final output pulse train running at 12,000 pps and an average power near 350 W. In this particular experiment the pulse-to-pulse stability was unusually good. A more typical output (Fig. 25) on a slower sweep scale, shows large low-frequency fluctuations traceable to the oscillator, but augmented by the amplifier. Together with these there appears a higher-frequency variation associated with ripple in the amplifier currents.

The physical form of the output beam showed a fine structure originating in the NaCl Brewster windows together with a larger-scale pattern which followed the form of the output from the buffer amplifier. As the gain of the power amplifier was increased, the form of this pattern remained unchanged, but experienced a general brightening. This encouraged us to believe that actual beam distortion by the amplifier discharge itself would not be a major problem in beam control.

Our earlier experiments on small-signal gain and gain saturation had led us to expect 500 W from this breadboard device. In fact, we obtained only 400 W when the oscillator was running in a mode with a single lobe and 435 W when the oscillator mode had two lobes. These data resulted in an increase in size for the power amplifier section in the design for the 1 kW transmitter.

B. Conclusions

The major conclusions which derived from our experiments on the prototype high-power transmitter were:

50
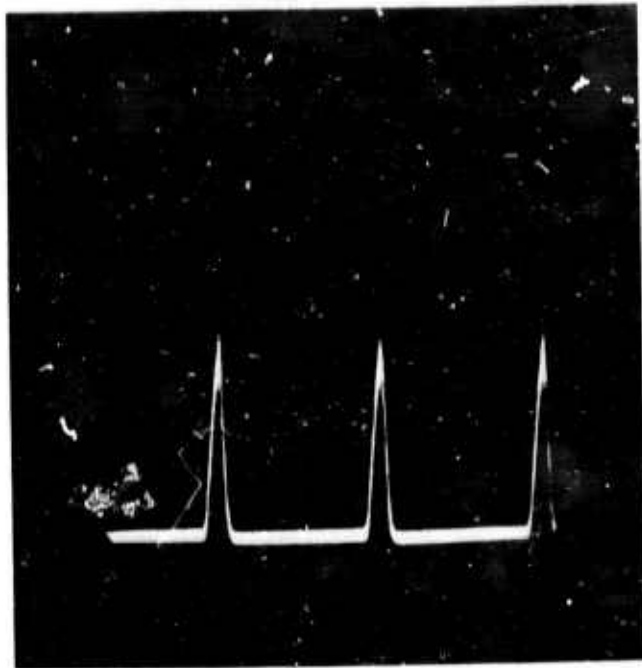
Fig. 24   Transmitter Output Pulse Train with 12,000 pps
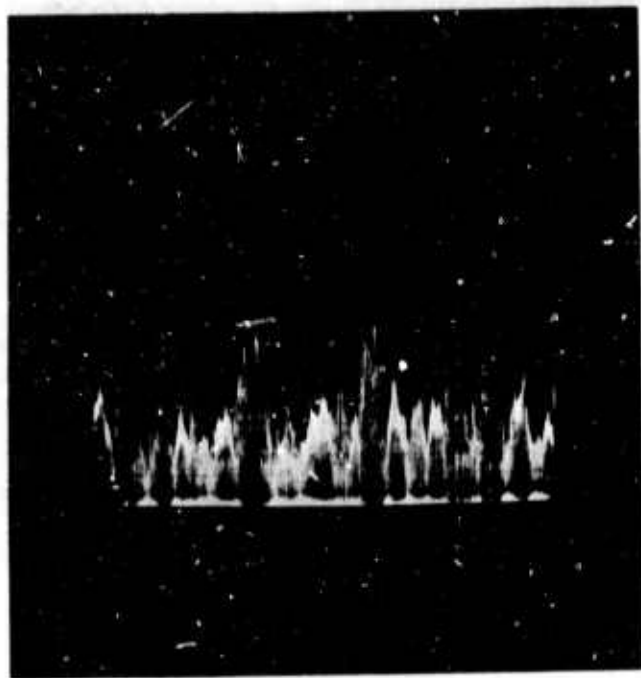
Fig. 25   Low Frequency Modulation of the Output Pulse Train Caused
by Oscillator Instability and by Amplifier Gain Modulation

1. The over-all design concept was workable.
2. A power amplifier of 50 meters of discharge should be used to ensure an output in excess of 1 kW.
3. Attention should be paid to avoiding wall reflections in the small bore high-gain amplifiers.
4. Current stabilization was essential to avoid large output fluctuations.
5. The mechanical modulation technique was usable at focused power levels beyond 200 W, but some fluctuation of the leading and trailing edges of the transmitted pulse was observed. At that time we believed them to be due to simple diffraction effects. Their origin was, in fact, more complicated, and will be discussed in a later section.

V. PROTOTYPE 1 kW TRANSMITTER DESIGN

A. Opto-Mechanical Details

The design and layout of our prototype transmitter is shown in Fig. 26. It is quite similar to the test model on which we performed our high-power measurements. The differences appear in the size, the quality of the optics, and design features to improve the alignment and form of the beam. The 35 W output from the primary oscillator is collimated by a reflective telescope and passes through two stages of amplification before reaching the modulator. Each stage consists of a separate pair of discharge tubes with Brewster angle windows of NaCl at each end. The first stage provides six meters of 1 in. i. d. discharge separated by an unexcited central section of 0.75 m. The second stage gives 12 1/2 of 1 1/2 in. discharge with 0.75 m central section. In both cases the new gas mix enters through the anodes at each end of the amplifier and is pumped out at the center. This design was chosen to do two things:

1. To allow examination of the beam after it has passed through the 1 in. i. d. amplifier.
2. To introduce more flexibility into the structure of the buffer amplifier.

Our analysis indicated that the use of a 1 in. i. d. discharge throughout the entire length of the preamplifier would give approximately 550 W at the modulator, whereas we can expect only 450 W from the present design. It is clear that efficient use of the final power amplifier stage requires as high a power level as possible at the input end. Consequently, the smaller choice of tube diameter would enhance the final output. However, our past difficulties in beam alignment in 1 in. tubes led us to choose a larger-diameter amplifier for the second stage to minimize the effects of wall reflections. In actual fact, the transmitter has rarely been operated with more than 250 W incident on the modulator optics. This input level has proven sufficient to produce an average output power of 1 kW.

6ft 4 in

46ft 9in

Pumping ports

Power amplifiers 2"ID

Second stage
Amplifier 1.5"I D.

First stage
Amplifier 1.0 I.D.

1.0−1.1 kW
Average

Concrete pier

35 W
(cw)

Telescope

Oscillator

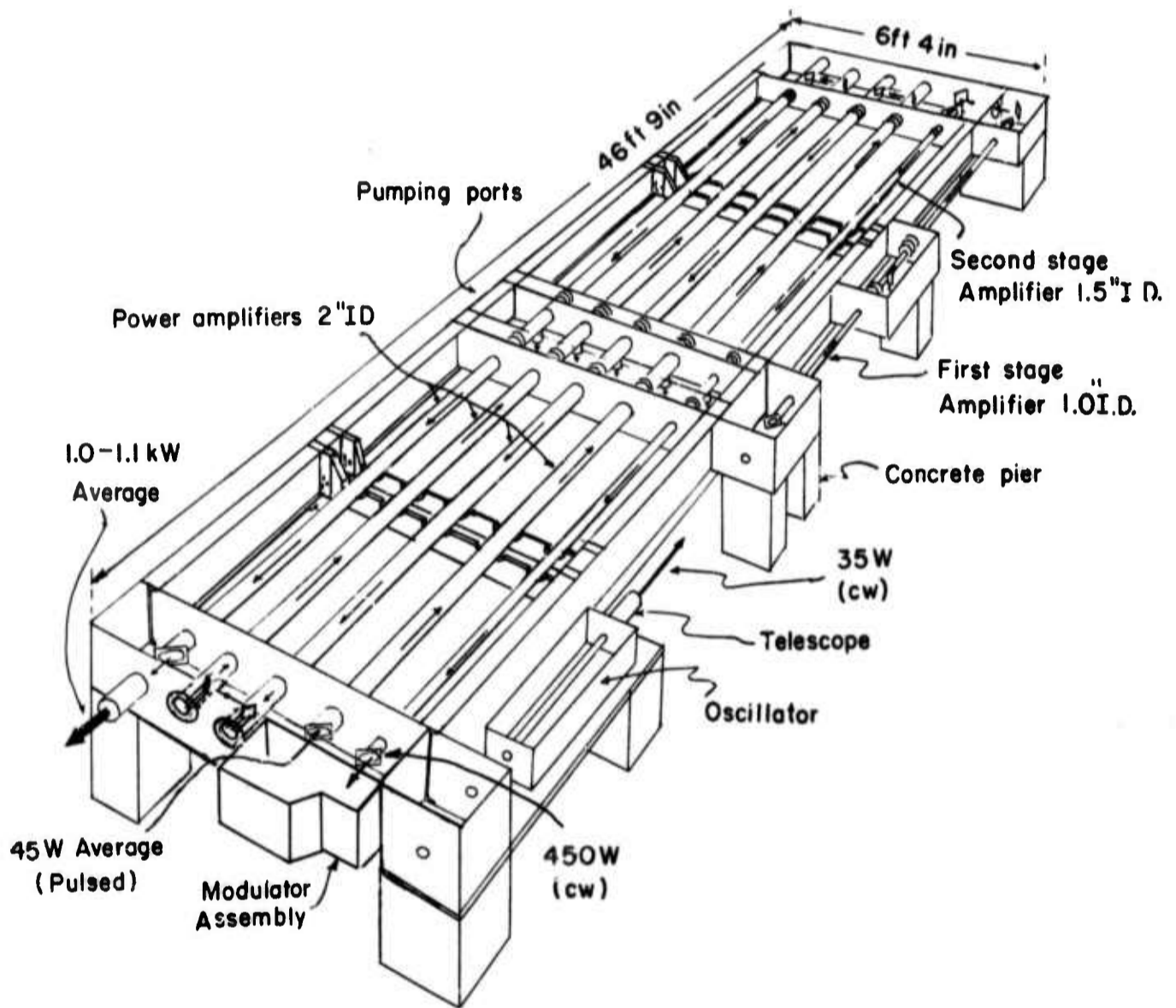45 W Average
(Pulsed)

Modulator
Assembly

450W
(cw)

Fig. 26   Prototype 1 kW Transmitter Design

55

A novel design for the modulator optics introduces on-axis parabolic focussing mirrors in place of the NaCl lens assembly used in our previous experiments. This is done to eliminate a specular reflection from the modulator back into the power amplifier, an effect which increases the possibility for spurious oscillation in this latter amplifier. Figure 27 shows the optical arrangements in more detail. The main design feature is a pair of perforated plane mirrors set at 45° to the optical path and spaced out to allow a chopper blade to pass through the confocal point of the parabolic mirrors. The focal lengths of these latter mirrors, namely 4 in. and 6 in., have been chosen to give a 1.5-fold expansion of the beam as it passes from the second-stage amplifier into the power amplifier. Gold-plated silica mirrors were used for these optics.

In designing the perforated optics, it was necessary to make sure that no radiation falls on the absorbent silica surfaces. In particular, the plane diagonal mirrors have a pair of holes set at 90° to each other (and each one at 45° to the mirror face) to remove as much extraneous wall material as possible. In addition, a gold-plated reflecting cylinder is set in the center of the incoming beam to reflect out to an absorbing sheet that part of the beam which would otherwise fall on the central hole in the diagonal mirrors.

The chopper blade itself is made of 1/16 in. thick polished aluminum with perforations set at 45° to the blade face and arranged around a circle of approximately 6 in. radius. The perforations in the final design were 0.09 in. in width measured along the circumference of the wheel and 0.025 in. long. The incoming radiation is focused down to approximately 0.05 mm at the plane of the blade. The resultant intensity ($\approx 10^7$ W/cm^2) causes destruction of the blade if the latter is held stationary. Even spinning at 7000 rpm, this effect causes slight roughening of the polished surface.
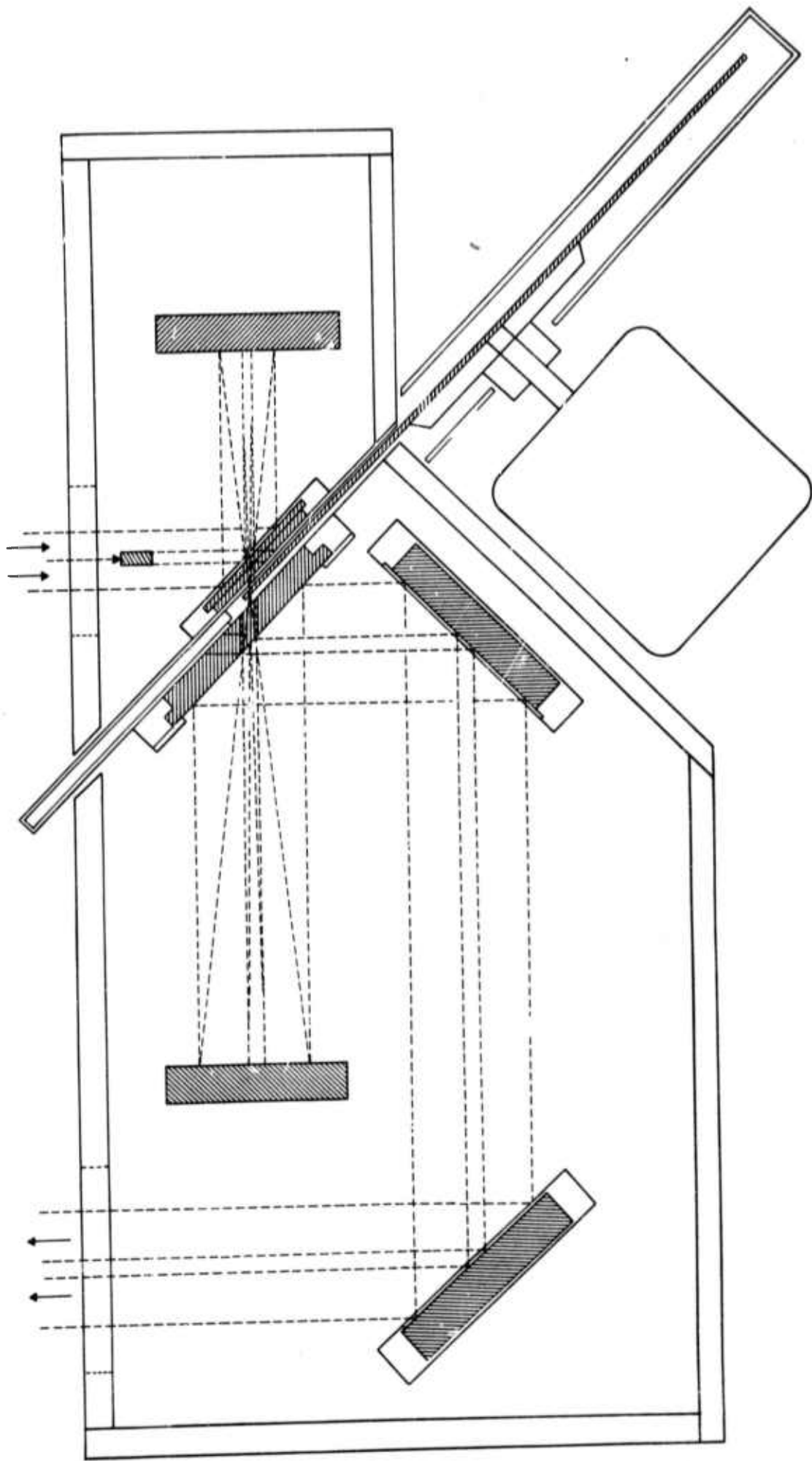
Fig. 27   Reflective Modulator Design

57

The power amplifier itself consists of four runs of 2 in. i. d. tubing with each run having 12 1/2 m of discharge path and a 0. 75 m central unexcited section. The total amplifying length is thus 50 m. The entrance and exit Brewster windows are again of NaCl. This material has been used throughout because of its ready availability and relatively low cost. At the end of each of the four runs, a pair of gold-plated copper mirrors is used to reverse the direction of the beam. One of the mirrors is housed in a preset aluminum mount, while the second member of the pair is set in a mount whose attitude can be controlled by micrometer adjustment from the outside of the amplifier housing. Figure 28 shows one of these mirror pairs.

Our experience with the first high-power transmitter showed the importance of eliminating forward wall reflections and edge back reflectors in the amplifier tubes. Such reflections distorted the output beam and gave rise to spurious oscillations respectively. As a consequence, several absorptive irises were placed in the power amplifier and intermediate amplifier tubes. Made from lava stone, they were strongly absorbent to 10. 6μ radiation and were machined to reflect as little as possible. The nonreflective iris design is depicted in Fig. 29.

The gas feed to the power amplifier is again accomplished by injection at the end anodes of each run, with a balanced flow towards the output pumping port at the center section. A single 300 cfm pump is used to evacuate all amplifier tubes with pneumatically controlled valves housed below the closed end section of the power amplifier. This assembly can be seen partially in Fig. 30. Gas flow velocities are usually 3 m/s at a total pressure of between 5 and 6 torr.

As originally designed, the gas for all amplifier sections was mixed at one control station. While this arrangement was adequate, it proved awkward in sequential starting of all three amplifiers. It was
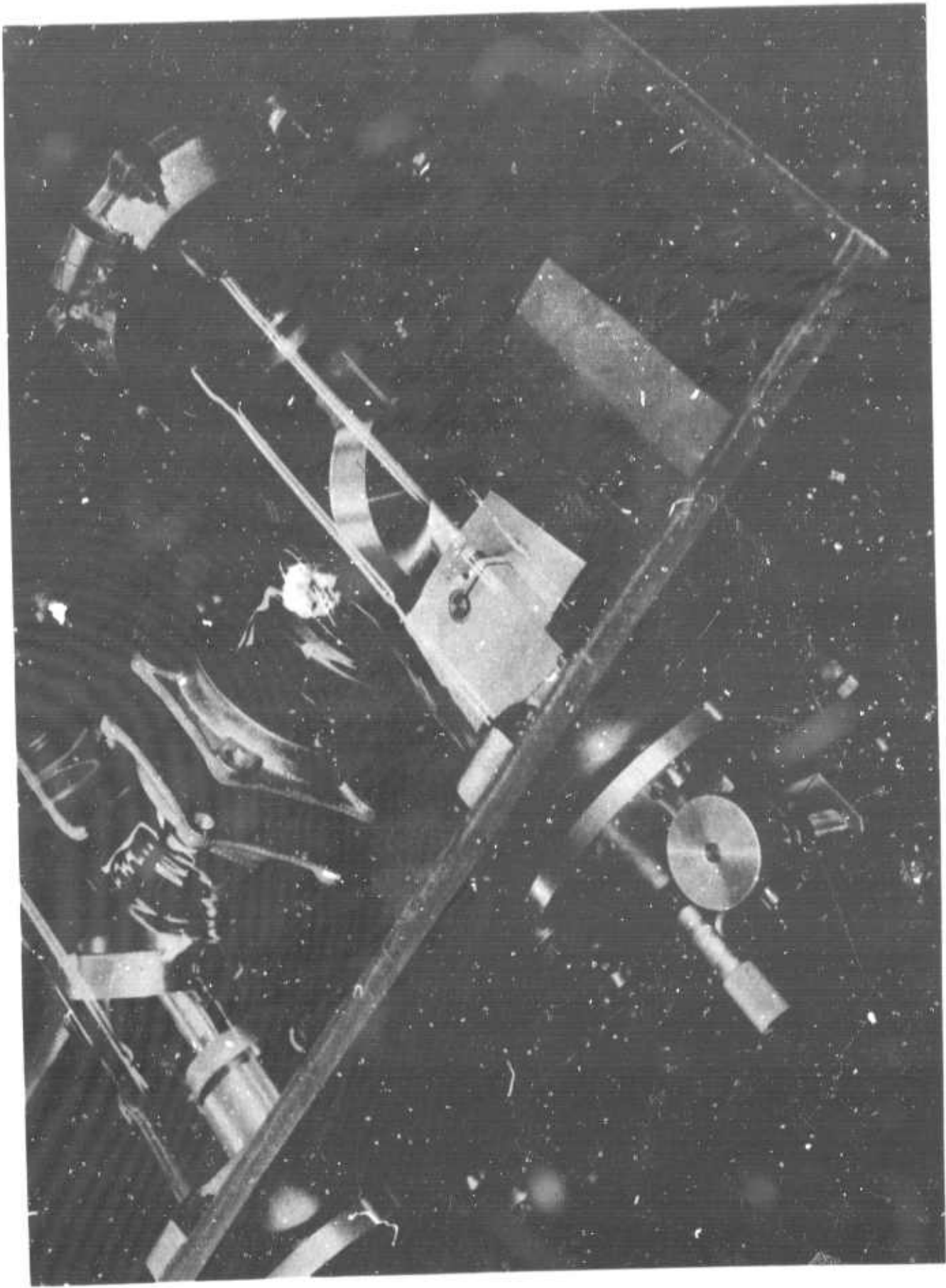
58

Fig. 28   Turnaround Mirror Assembly in the Power Amplifier

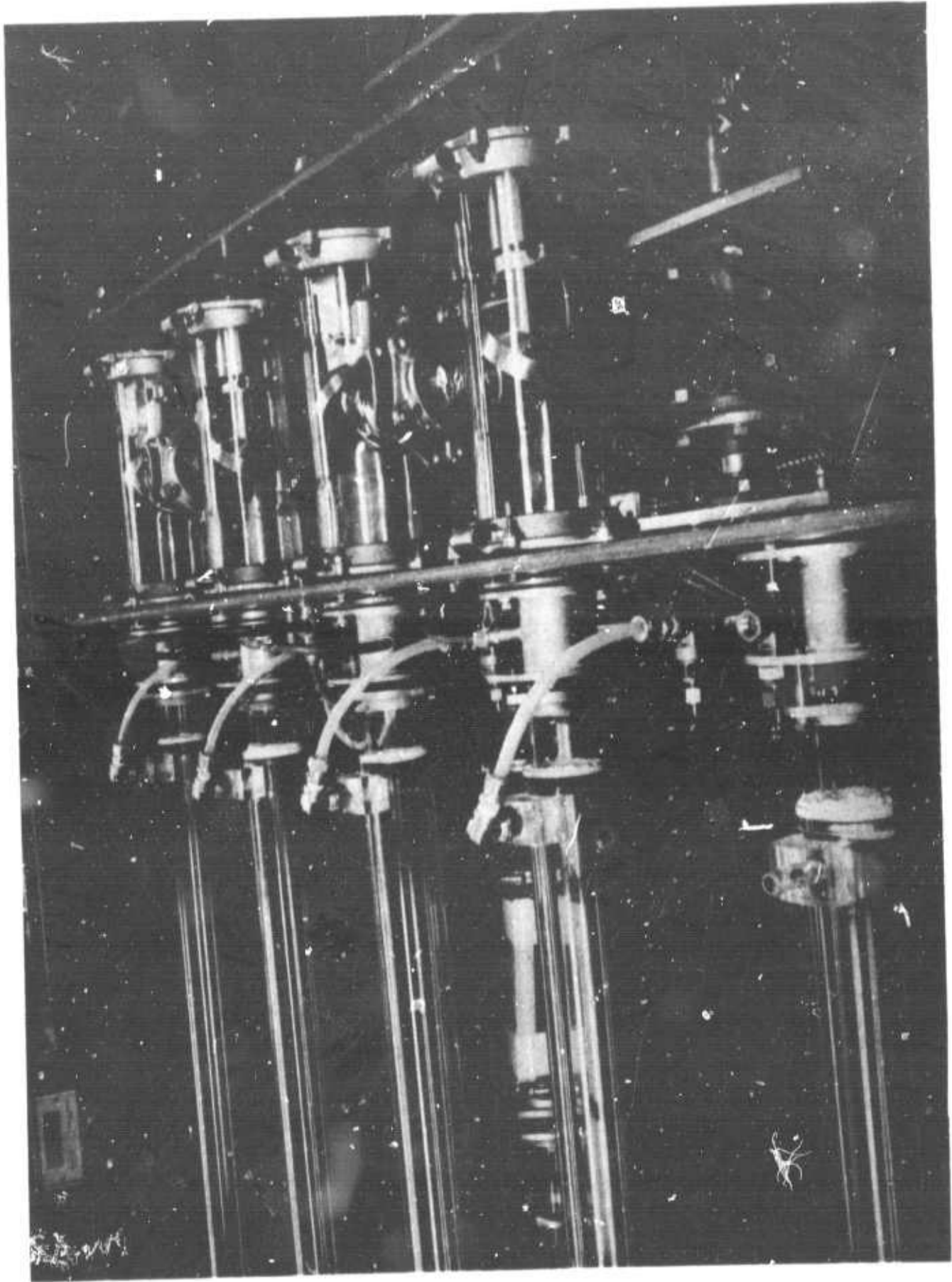Fig. 29   Nonreflective Iris Design (cross section)

60

Fig. 30   View of the Back End Assembly of the Transmitter Showing Mirror
Housing and Vacuum Control Valves

61

replaced by an arrangement with one gas control station for the first and second stage amplifiers and a separate one for the power amplifier. The controls for the power supplies and gas flow are shown in Fig. 31.

The gas flow is controlled by three needle valves together with a set of precision flow tubes to give a visual indication of flow and flow stability. The operating pressure is measured at the pumping manifold and is the same for all three amplifiers. While a marginal increase in efficiency might be achieved by independent control of the pressure for each amplifier, it is unlikely to be worth the added complexity of design.

The entire amplifier assembly is held together in an aluminum and steel frame. It was designed both to provide a stable and dependable mounting for the optics and to be of a form to allow disassembly and transportation of the transmitter with as little difficulty as possible. There are three aluminum boxes, one at each end to house the mirrors and window mounts and one in the center to hold the cathode assembly and exit pumping ports. These boxes are connected by steel H beams in 10-ft. sections spaced out by intermediate cross-frames which provide a cradle support for the amplifier tubes. Figure 32 shows this assembly and gives an overall view of the complete device as it was first built. The primary oscillator appears at the lower right of this view. The entire frame is mounted on molded rubber vibration pads set on twelve concrete piers and set so that the central plane of the optics is 50 in. above the floor level. The space underneath is used to house the high voltage supplies and current stabilization equipment.

In testing the transmitter, we found that the optical beam was displaced by expansion and contraction of the discharge tubes themselves. The total beam displacement amounted to ± 2 millirads. This difficulty was overcome by placing flexible metal bellows in the end electrode assemblies. With this correction the output beam center was stable to within 1 cm, i.e., to an angle of $\pm 10^{-4}$ radian over a period of one hour. Initial alignment of the optics was achieved by replacing the primary transmitter with a He:Ne laser.
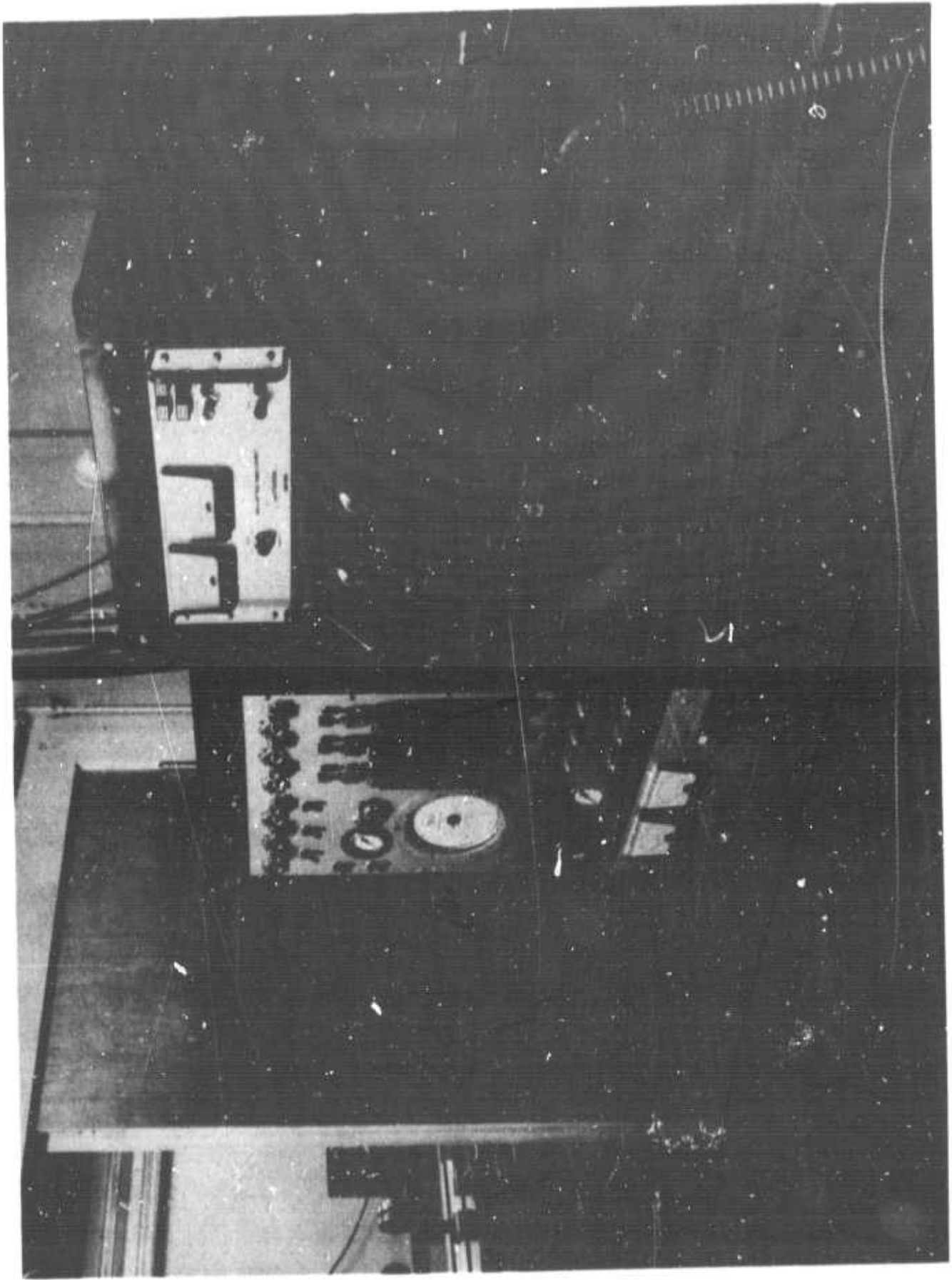
62

Fig. 31 Gas Flow and Power Control Station for the Transmitter

63
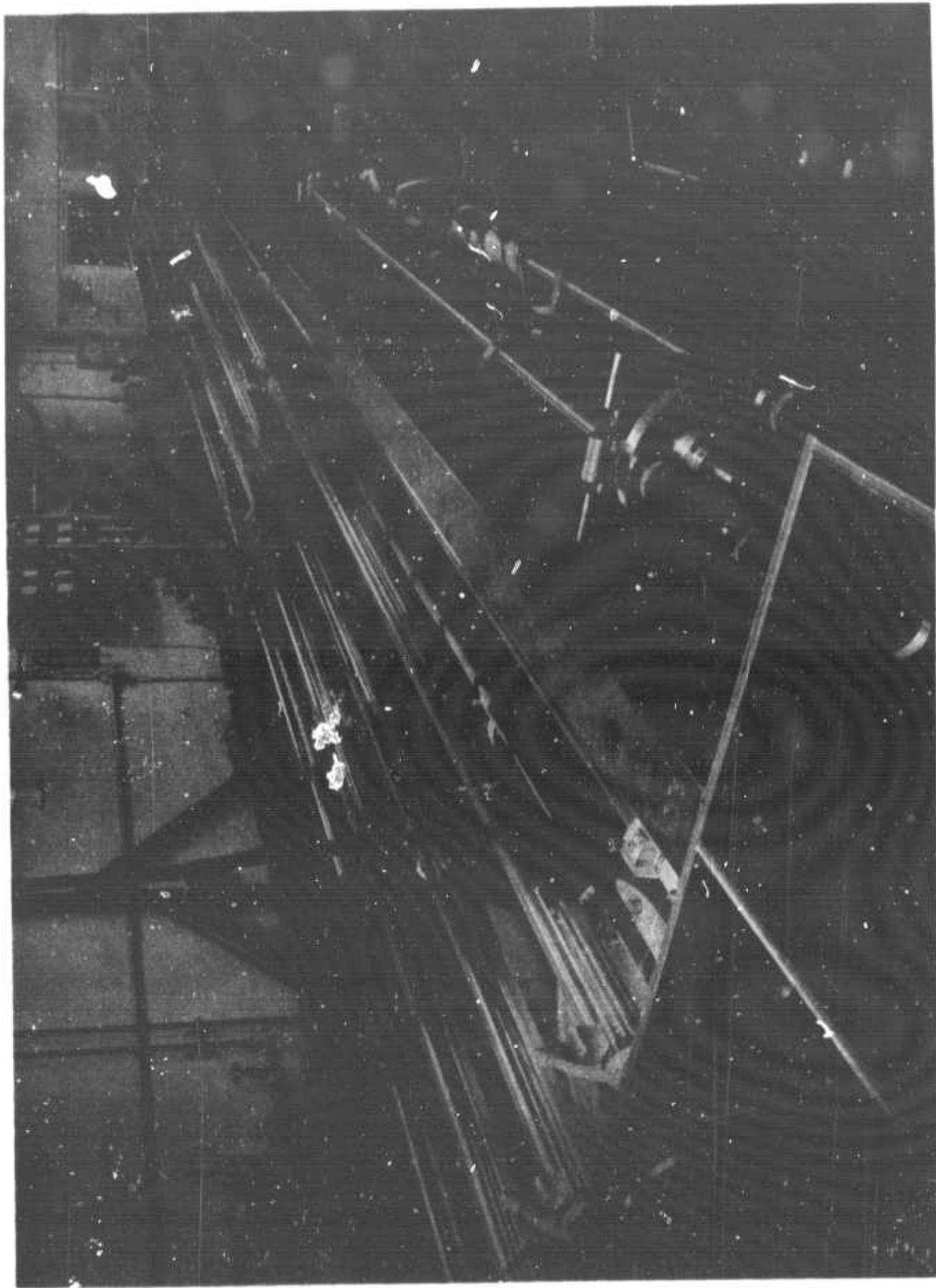
Fig. 32   Over-all View of the 1 kW Transmitter

All discharge tubes are water cooled, with the coolant being fed in a symmetrical fashion to each pair of discharge tubes. The water enters at each extremity (anode) and is exhausted at the center (cathode end). In our first experiments, the water cooling jackets were made of glass, sealed at each end by rubber and cement gaskets. To avoid breakage, they were replaced by plastic tubes when the transmitter was first assembled. After six months of operation, the tubing began to crack and was replaced by aluminum. The end sealing was accomplished by the use of annular vices which force neoprene gaskets against the aluminum and glass tubes.

B. Electrical Details

Two separate power supplies are used to excite the amplifier. A 32 kV, 275 mA supply activates the first and second stage amplifiers, while a larger 32 kV, 750 mA unit provides the current for the main power amplifier. Each supply is a simple three-phase rectifier circuit giving a five percent voltage ripple at 360 cps. In our initial tests on the transmitter we used 120 kΩ resistive ballasts with each amplifier discharge section. The use of two independent power supplies makes for a more flexible use of the equipment.

The optimum currents in the various discharge tubes for maximum power output depends on the gas mix, but is approximately 30 mA for the 1-in. dia. tubes, 50 mA for the 1 1/2-in. tubes and 110 mA for the 2-in. tubes of the power amplifier. In fact, the power amplifier is normally operated at 90 mA. The electrodes are simple brass cylinders with external fins to facilitate cooling.

Under normal operating conditions, each discharge tube in the amplifier array has a negative resistance characteristic with an effective impedance of between -40 kΩ and 60 kΩ. At an operating voltage of 20 kV across the discharge and a 10 kV voltage drop across an accompanying

65

120 kΩ resistive ballast, a 5 percent voltage ripple (1500 V) will result in a current ripple of 20 mA on an average current of 80 mA, i.e., a 20 percent ripple. This ripple is reflected in the amplifier gain coefficient and results in a severe modulation of the output signal. In the 50-meter amplifier, the result is 100 percent modulation. In order to overcome this difficulty, we have built an electronic ballast which can operate with an over-all voltage drop of 4 kV and provide an output current stable to one part in 500 when a voltage variation of 5 percent is applied to the ballast and discharge tube combination. Figure 33 gives a block diagram of this device. Figure 34 shows the complete circuit.

A feedback-stabilized difference amplifier amplifies an error signal produced by comparing the voltage across a sensing resistor with that of an adjustable reference voltage. The output of the amplifier controls the grid voltage of a tetrode in series with the laser and high voltage power supply. The feedback and gain are arranged so that the effective output impedance of the ballast is 10 MΩ.

The electronic ballast has several advantages over conventional resistive ballasts, one of which is the ability to vary discharge current linearly from zero through maximum. Also, the electronic ballast requires generally much less voltage drop for a given current; hence, less power dissipation, smaller power supplies, and lower supply voltages result. The ballast compensates for power supply ripple as well, again decreasing the demands for quality and capacity in the high voltage supply. The frequency response of the ballast (Fig. 35) will substantially reduce any tendency of the discharge current to fluctuate at frequencies below 10,000 cps.
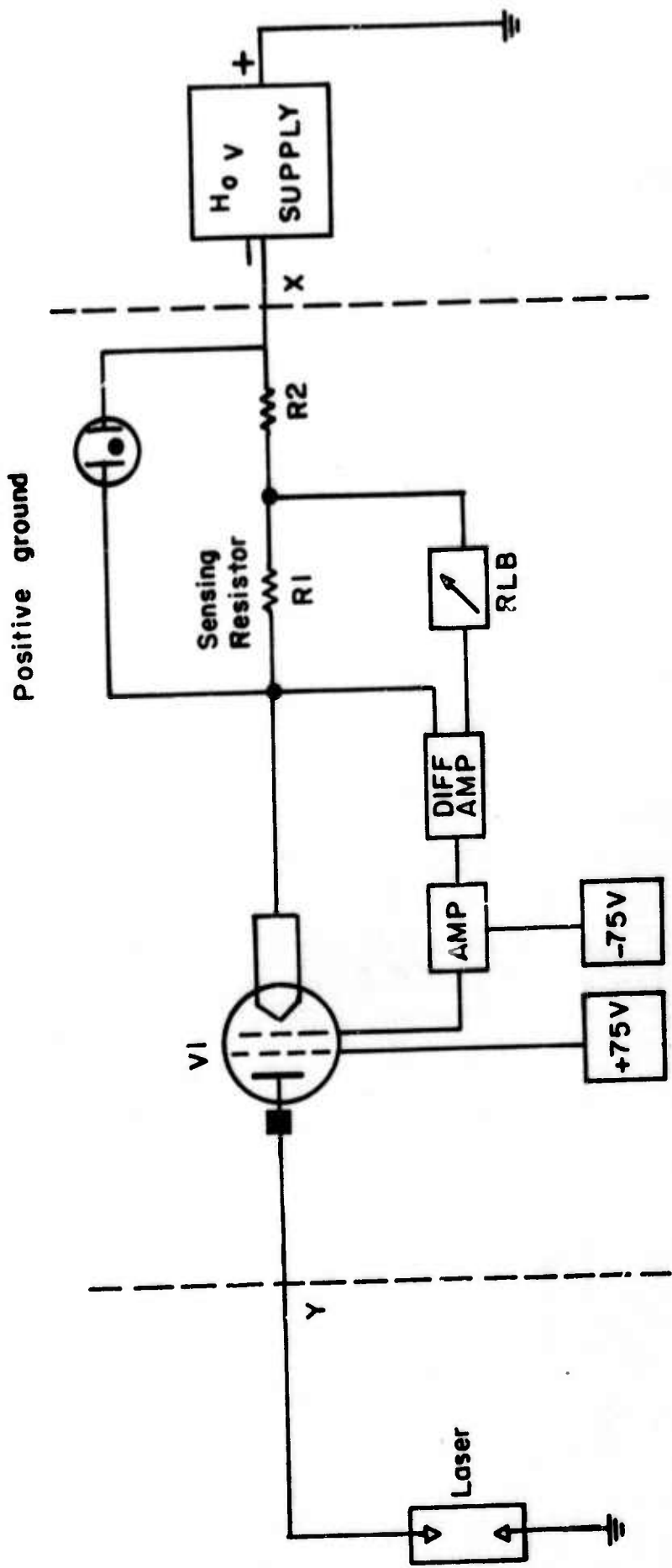
Fig. 33 Schematic Diagram of Electronic Ballast Circuit

67
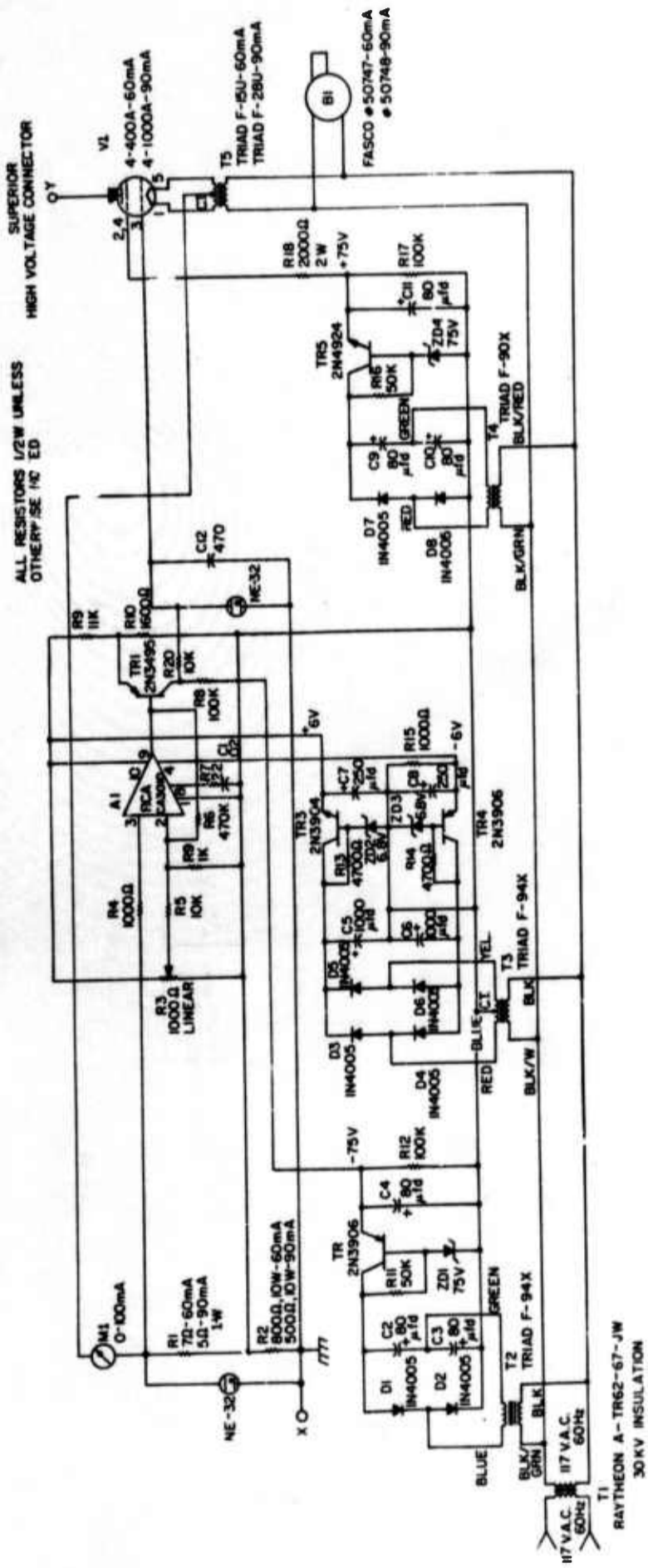
Fig. 34   Electronic Ballast Circuitry

68
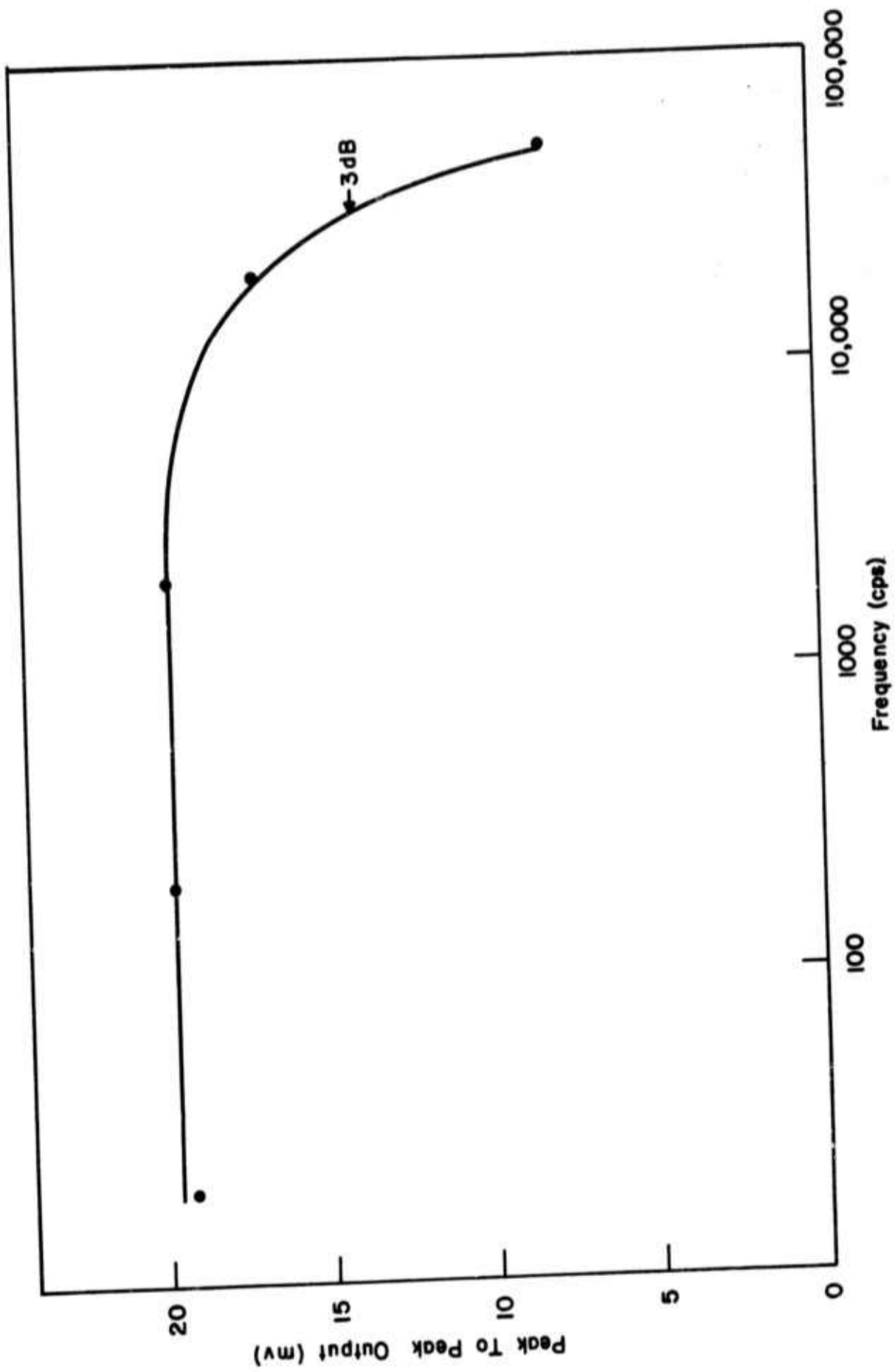
Fig. 35   Frequency Response of 60 mA Electronic Ballast Circuit

69

Meanwhile, the dynamics of the N_2-CO_2 energy transfer process, which is governed by a relaxation time of ≈ 100 µsec, prevents any high frequency fluctuation in the nitrogen excitation ratio from being impressed upon the amplifier gain. The only way in which the gain could be affected at frequencies above 10 kc would be by direct electronic excitation or de-excitation of the CO_2 levels themselves.

The only real difficulty with the electrical system has been electrical breakdown across the insulating bands holding the current stabilizer, and electrical breakdown from the center of each 20-ft discharge tube to a nearby metal support. Both problems were reduced by increased insulation.

VI. TRANSMITTER PERFORMANCE

A. Output Power

The relatively inflexible nature of a mechanical modulator makes awkward the gathering of extensive data at various pulse lengths and repetition rates. As a consequence our data is somewhat skeletal. It is nevertheless adequate to the purpose and shows (Fig. 36) that for a 200 W average power input at the modulator, an output of 1 kW was obtained in 10 μsec pulses at a pulse repetition rate of less than 7000 pps. At 12,000 pps the output power was 1200 W. Used as a complete cw amplifier, with the modulator blade removed, the output was 1390 W. (From past experience with high-power oscillators, we would expect that the whole device operated as a multimode cw oscillator should emit between 2.5 and 3 kW.) The variation of output power with repetition rate, as in our exploratory experiments, is consistent with a 100 μsec transfer time between the emitting CO_2 states and the N_2 energy reservoir. The power output increases by approximately 10 percent if the cw power at the modulator is raised from 200 to 350 W, but the additional output is not worth the added risk to the modulator optics. The output also changes with the temperature of the amplifier tube walls, decreasing by about 0.5 percent /°C rise.

We have found that the simplest way to control the power output has been to vary the nitrogen content of the gas mix. The power output figures mentioned above were obtained at a current of 90 mA in each of the eight power amplifier tubes and at an operating voltage of 23 kV across each section. The input power to the discharge was therefore 16 kW. This represents an output efficiency of nearly 7 percent for the power amplifier operating at a pulse repetition rate of 10,000 pps.
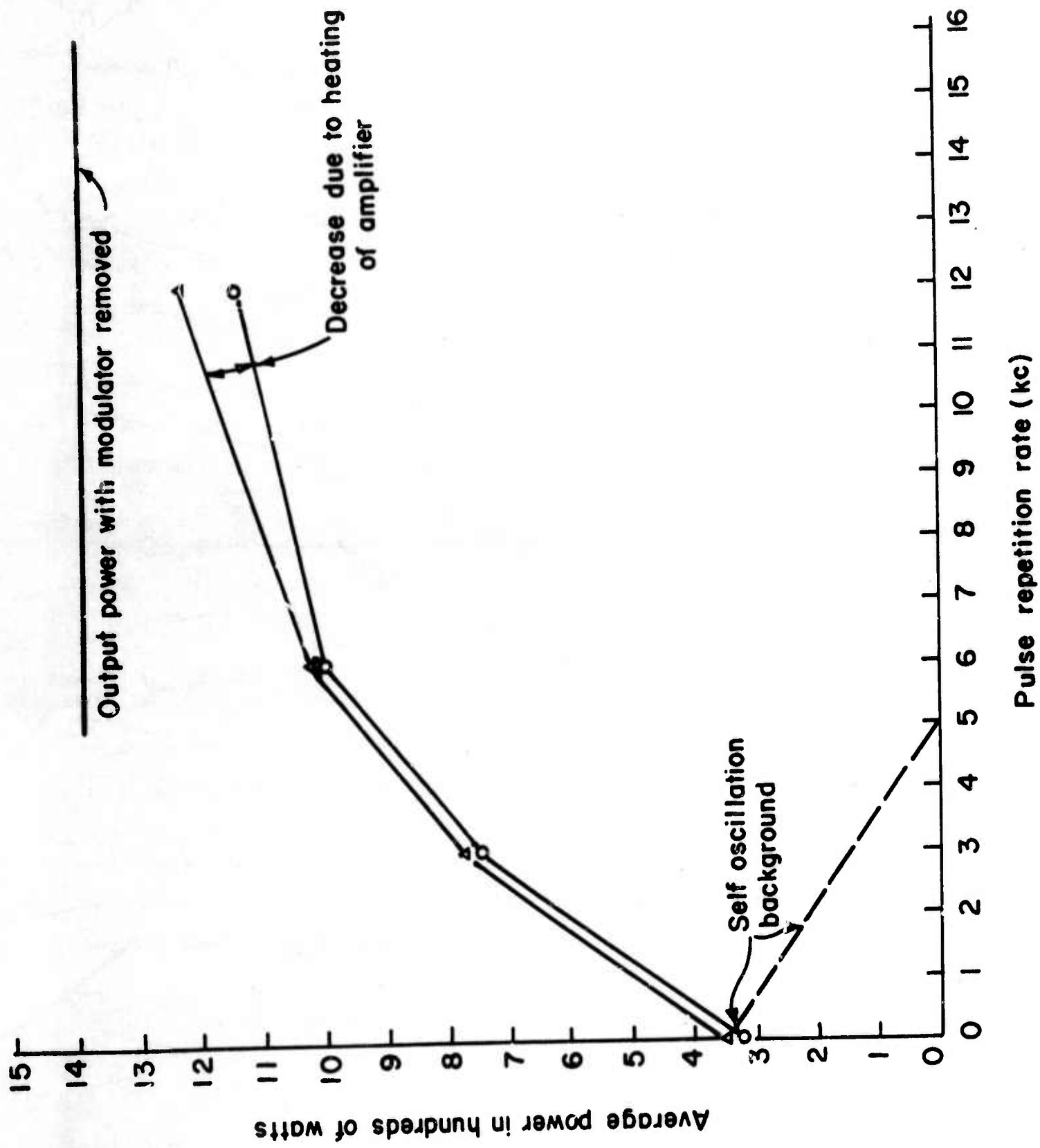
Fig. 36 Power Output of the Transmitter vs Repetition Rate of the 10 μsec Infrared Pulse Train

72

At the same operating point some 3 kW are dissipated in the electronic ballasts. There are three reasons for the reduction of output efficiency below that to be expected from a multimode oscillator of identical dimensions:

1. Use of repetition ratio of 10,000 pps reduced the output below that for cw operation.

2. Injection of a 200 W signal ($\simeq 20\,W/cm^2$) at the input of the power amplifier leaves the first 10 meters of the latter underdriven.

3. The deliberate avoidance of the tube walls by limiting the size of the input beam, and by the use of multiple irises reduced the volume of the discharge which is driven into strong saturation.

In principle each of these limitations could be reduced by increased pulse-repetition rate, increased level of pulse-signal injection and more sophistication in the design of the optical beam and the geometry of the discharge tubes themselves. It was our judgment, however, that a conservative and dependable design was appropriate in this first source, regardless of the over-all efficiency.

The line in Fig. 36 labeled "self-oscillation background" refers to the spurious oscillations in the power amplifier produced by diffuse reflections from the chopper blade during the time that it intercepts the infrared signal coming from the second-state amplifier. This effect is clearly seen in Fig. 37. The bottom trace shows the normal profile of pulses at a repetition rate of 7500 pps. The center trace, on the same voltage scale, shows the development of a background oscillation when the output for the second-stage amplifier is blocked off. (This signal disappears if the chopper blade is removed from the optical path.) The top trace shows the effect of deliberate misalignment of the beam as it passes through the amplifier. A similar effect is achieved by increasing the pulse-to-pulse spacing. From the latter experiment, we estimate that the spurious oscillations are suppressed at a pulse-repetition rate of 5000 pps.
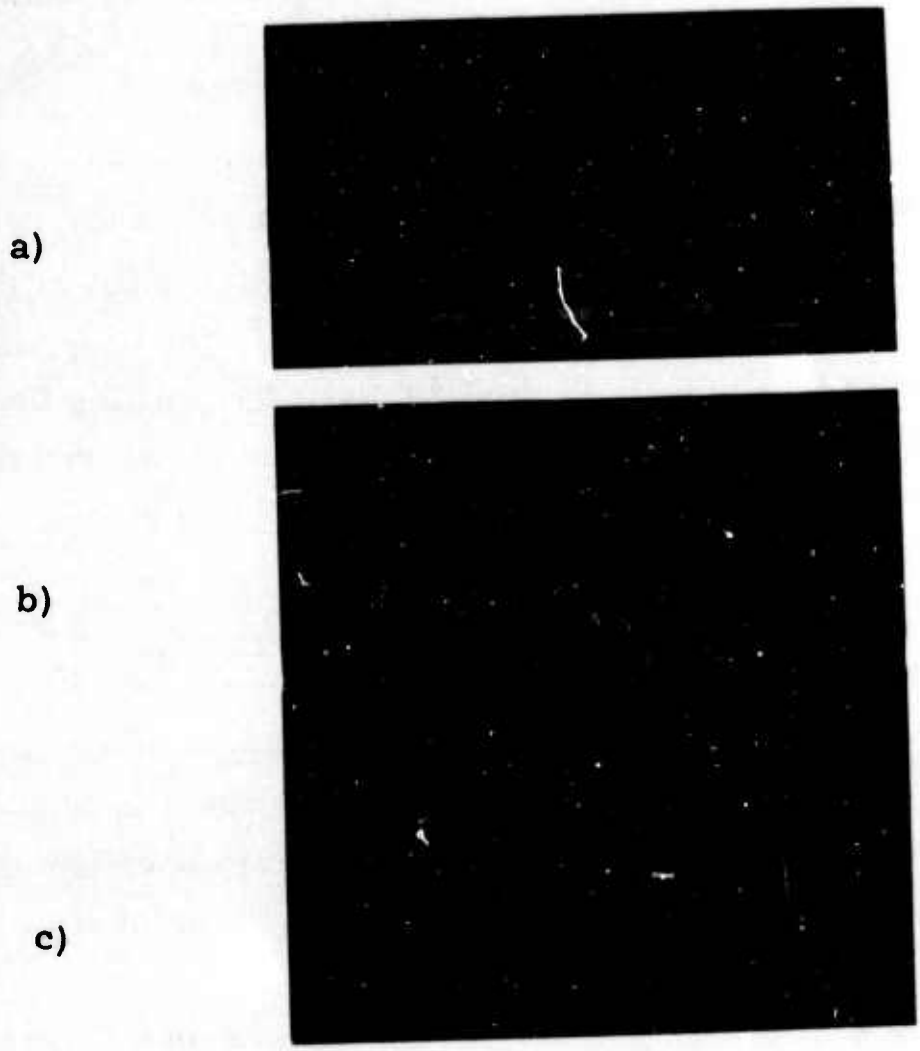
Fig. 37   Pulse Train Profiles and Spurious Oscillations in the Laser
Power Amplifier

Trace a - Normal operation at 7500 pps

Trace b - Spurious oscillation with second-stage
output blocked

Trace c - Normal operation at 7500 pps, but with
deliberate beam misalignment

B. Temporal Stability

In an earlier section, we pointed out that in experiments using resistive ballasts for the discharge tubes, a 20 percent peak-to-peak current ripple resulted in a 100 percent ripple of the output pulse train. The improvement produced by active current stabilization is shown in Fig. 38b. At an average power output of 130 W and a repetition rate of 7500 pps (17 mJ/pulse), the peak-to-peak ripple is 5 percent. At output levels between 500 and 1000 (65 to 130 mJ/pulse) the peak-to-peak ripple increases to 10 percent. The output power level is adjusted simply by varying the amount of nitrogen fed to the gas discharge. The pulse profile (Fig. 38a) shows the pulse shaping effect referred to previously. At full power output the leading edge rises to some three times the trailing edge.

C. Output Beam Profile

In order to obtain a maximum intensity of radiation incident on a target in the far field of a laser radar transmitter, it is necessary to have a beam of minimum divergence, derived from a simple uniform phase front. Our objective has been to produce 1 kW average power in such a uniform beam. With our present equipment, it has been possible to produce 100 W of signal power in a diffraction limited beam. At higher powers, the beam spreads and appears unstable.

Tests have been made on the transmitter output by focusing the beam with a spherical mirror used slightly off axis, and by probing the intensity distribution in the focal plane. The resultant pattern corresponds to the power field distribution of the beam. This was done by reflecting 5 percent of the converging beam at a NaCl-air interface and sweeping the focused profile across a pinhole backed up by a Au:Ge photodetector (Fig. 39). Typical traces at average cw power levels of 100, 200, and 500 W are shown in Fig. 40. After allowing for the finite size of the pinhole these observations give $1/e^2$ angles of less than 3×10^{-4}, 6×10^{-4}, and 10^{-3} rad, respectively. In addition to the increasing angular spread

75

a)

b)

Fig. 38   Pulse-to-Pulse Stability and Pulse Profile of the Transmitter
Operating at an Average Power Output of 130 W
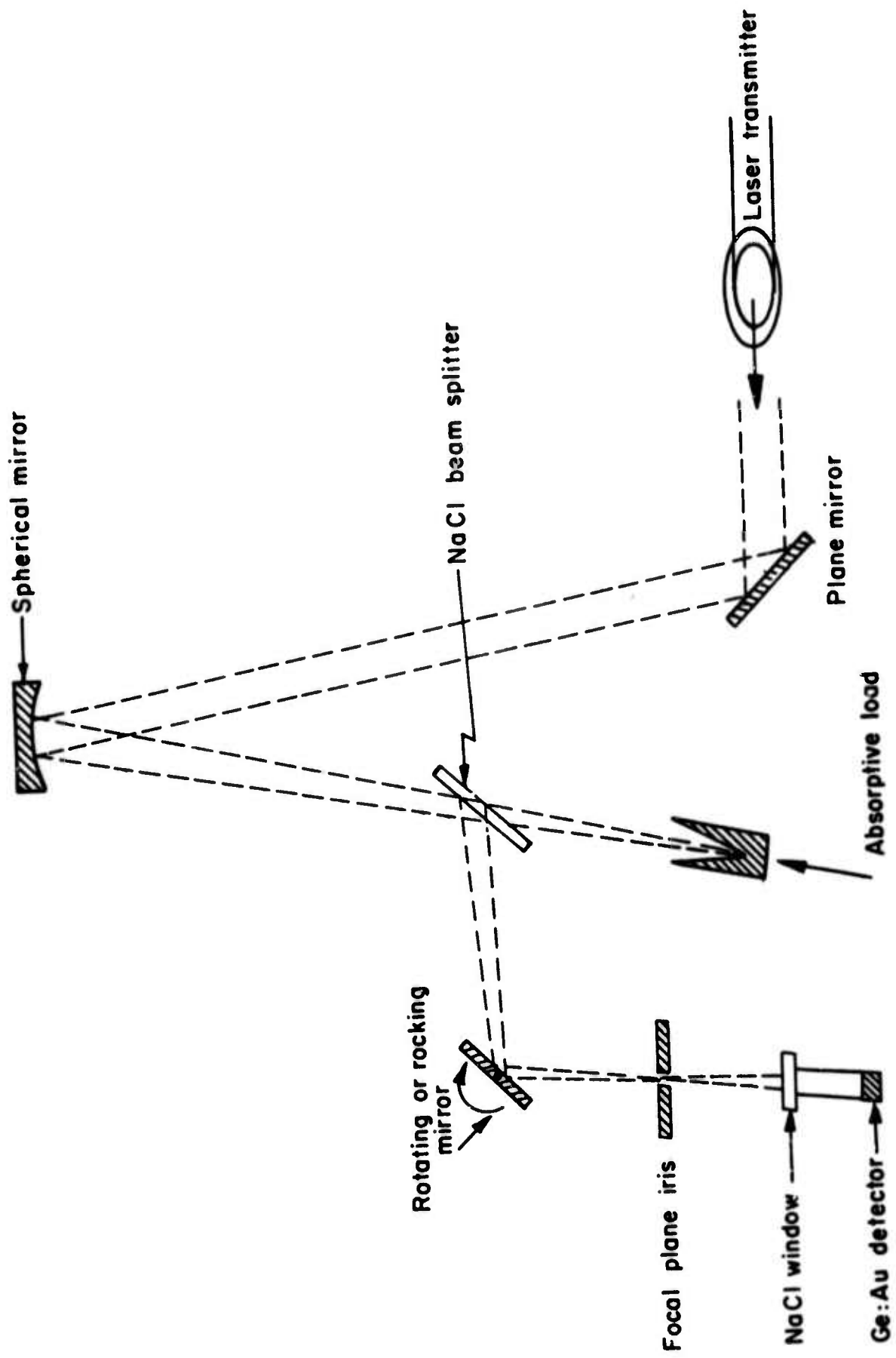
76

Fig. 39   Experimental Arrangement for Mapping the Far Field Pattern of the Laser Transmitter

77

Fig. 40   Equivalent Far Field Profiles for the Laser Transmitter Running
cw at Different Levels
a) 100 W
b) 200 W
c) 500 W

at high power levels, the wing structure fluctuates in time. The origin of the structure has not been established with certainty but it may be due to a reaction back onto the emission mode structure of the primary oscillator. A diffraction-limited gaussian beam from the transmitter should have an angular width of 2.5×10^{-4} rad.

Similar far field measurements were taken with the modulator in operation. By using a slow angular sweep of the output beam across the detector, we were able to record an "average" beam profile as a sequence of pulses. Thus each trace consisted of a measurement of the output of pulse 1 at angle θ_1, pulse 2 at θ_2, etc. In order to interpret the average profile as that appropriate to each individual pulse, it is necessary to assume little variation between pulses. A typical profile (Fig. 41) showed an asymmetrical side-lobe structure in addition to the central peak. We believe that this is due to diffraction effects taking place as the leading edge of the wheel perforation crosses the focussed beam profile. To check this interpretation, it would be necessary to observe the beam profile as a function of time for a specific output pulse. In addition to the fluctuating beam spreading, a slow expansion of the beam takes place after the equipment has been run at high power for a time longer than 15 minutes. We interpret this as due to a slow heating of the reflective optics in the optical modulator assembly. This effect should be controllable by air cooling of the various surfaces. To the eye, the output beam profile appears irregular when seen as a white light emission from a ceramic surface heated by the beam. In the absence of a signal beam injected from the modulator, the spurious oscillator output from the power amplifier shows a fine-grained pattern suggestive of multiple reflection from the edges and walls of cylinders. When the signal beam is turned on, this pattern changes to one of a central bright arc some 1 in. in diam surrounded by one or two arcs. Presumably these are produced by edge diffraction of the beam at one or another of the irises.

Fig. 41   Equivalent Far Field Profiles for the Laser Transmitter With
Pulsed Output

The presence of this near-field structure is a consequence of having a beam whose diameter is comparable with that of the amplifier tube. In order to eliminate the structure it would be necessary to use recollimating optics which continually restrict the beam to a small volume along the tube axis, or by using a spatial filter at the output. Neither of these possibilities is really practical, and considering that the observed patterns could be produced by diffracted waves carrying of the order of 1 percent of the output power into side lobes in the far field, it is doubtful whether they are worth eliminating.

The quality of the transmitter beam was degraded at various points in time by damage to the NaCl windows. The slow erosion of the external window surfaces due to moisture was inhibited by installing 10 W heater lamps in front of each window to raise its temperature above that of the surrounding surfaces. A hazy deposit built up on the internal surfaces after prolonged use. This may have been caused by dust carried to the windows when air leaks occurred in the amplifier and subsequently burnt by the irradiation. Together with these effects we observed the cross-hatched crystal-slip patterns which characteristically develop on NaCl windows subjected to high intensity 10.6μ radiation. The only way around the last problem seems to be to use a different window material. We have found that KCl windows show no such degradation even when subjected to $10^5 W/cm^2$ for many minutes. As a consequence, the NaCl optics have been replaced by KCl for the installation of the transmitter at the Millstone radar site. In future transmitters, however, it would seem desirable to use a window material more durable than the halides.

VII. EXPLORATORY PHASE

The final phase of this program was designed with two purposes in mind. The first was to use the 1 kW pulsed source to measure atmospheric backscatter; the second, to test the performance of the equipment when operated over extended periods. While the backscatter measurements were not successful, the attempt has exposed a number of problems in the use of high-gain amplifiers in heterodyne systems. Further, the correction of several deficiencies in the actual operation of the transmitter has resulted in an equipment which can be used continuously for many hours.

The original design for the backscatter experiment called for heterodyne detection of the return signal by combining it with a second signal taken directly from the primary oscillator. In attempting this experiment, we found that a catastrophic reaction on the primary oscillator occurred when the amplifiers were turned on. Figures 42 and 43 show typical signals from Au:Ge detector observing the output from the primary oscillator. The laser beam was reflected at 45° from a NaCl flat and its intensity was therefore strongly dependent on polarization. These signals indicated that complete switching of the polarization was taking place! The oscillator used in these first experiments maintained its polarization only because of a slight tilt deliberately applied to one of the end reflectors. It turned out that this asymmetry was so small that a polarization switch could be produced by the weak signal scattered back from the chopper blade in the modulator assembly.

Analysis of the detector signals indicated a spectrum limited to frequencies below 30 kc. This result suggests that gross changes in mode structure are involved which bring into play changes in the $N_2 - CO_2$ energy exchange. Only this latter exchange has an appropriate time constant. These effects are clearly analogous to the amplification effects observed by Doyle et al.[9] using He-Ne lasers.

Fig. 42   Mode Switching Induced by Modulator Backscatter
(Time scale: 1 div. = 1 msec)

Fig. 43   Mode Switching Induced by Modulator Backscatter
(Time scale: 1 div. = 2 msec)

It is obvious, after the fact, that backscatter from the chopper is particularly troublesome because of the effect of the parabolic focusing optics. The most effective backscatter is that which re-enters the oscillator at angles compared to the original output beam angle, that is, within a solid angle of 2×10^{-5} sterad. This isotropic backscatter from the first mirror of the collimator just in front of the oscillator and at a distance of some 1 1/2 meters from the output window will, for the most part, miss the oscillator. By contrast, radiation scattered to the same degree from the chopper blade will be collected by the first mirror over a solid angle of approximately 0.1 sterad and transmitted directly back into the oscillator.

The perturbation effects were greatly reduced, but by no means eliminated, when the primary oscillator was polarized in a more stable manner. A NaCl Brewster plate was placed inside the primary oscillator. This introduced a loss difference of approximately 15 percent between the two appropriate plane polarized modes. With this oscillator the perturbations due to backscatter were reduced to 5 percent of the full dc current measured in the Au:Ge photodetector. Spectral analysis of the signal shows frequencies predominantly below 2 Mc, consistent with the general appearance of the wave as being composed of spikes 1 - 2 μsec as base. The typical traces, shown in Fig. 44, are notable on two counts:

1. The apparent noisy output consists of a complex pattern which repeats itself with every revolution of the chopper blade.
2. The maximum effect occurs while the chopper edge is cutting across the focused beam.

When the power amplifier sections are turned on, the perturbation becomes even more pronounced at the beginning of the transmitted pulse. Apparently, we are observing an incipient instability as the high-gain amplifier begins to "see" the oscillator by diffraction around the edge of the hole in the chopper. This new perturbation, which persists for a period of 2 - 3 μsec, explains what we had observed many times during the earlier phases of the work, but had never entirely understood.

Fig. 44   Disturbance of the Primary Oscillator by Diffuse Backscatter
from the Modulator Chopper Blade.
(Full scale width = 500 μsec)

It appears that these perturbation effects can be eliminated only by introducing a nonreciprocal device between the oscillator and the amplifiers. On the other hand, a substantial reduction may be achieved by using a modulator different in form from the focal plane chopper. For example, electro-optic modulators capable of withstanding average power of 20 - 30 W could be placed both between the primary oscillator and first amplifier, and between the second-stage amplifier and power amplifier. These modulators could be synchronized so that the second one opened up only when radiation was already impinging on it. In this way spurious oscillation in the power amplifier could be avoided. Alternatively, a pair of Fabry-Perot etalons set at a small angle to the beam could be set in synchronized longitudinal oscillation at one-half the desired modulation frequency. These could be tuned to give a pulse-like transmission with a pulse width-to-spacing ratio of up to 20:1. In fact, we built such a modulator using germanium flats with dielectric coatings for 90 percent reflection and spaced out by 3 cm. This combination gave $\simeq 1$ percent transmission off-resonance, and in fact produced transmission pulses with a 10:1 spacing-to-half-width ratio. Unfortunately, the radial mechanical resonances of the Fabry-Perot assembly prevented its successful use at frequencies above 2 kc. Nevertheless, a properly designed device scaled to avoid the mechanical difficulties should produce an acceptable modulator.

The attenuation of a laser radar signal beam in passing through the atmosphere will be determined mainly by the presence of aerosol particles causing both scatter and absorption. Water droplets and ice crystals in particular will give very severe attenuation. In the absence of aerosols, the only significant attenuation would be that due to atmospheric CO_2 which should result in a power loss of some 10 percent per transit along a vertical path.

In addition to the over-all power loss incurred by aerosol scattering, the backscattered radiation from the near field of the transmitter optics could conceivably obscure the return signals from distant targets. At low

86

pulse repetition rates when there is no range ambiguity, this need not be considered a problem if we could install a simple transmit-receive switching device. A repetition rate of 10,000 pps, however, gives an unambiguous range of only 15 km, so for this and longer ranges we run the risk of backscatter interference. If we contemplate ranges up to 100 km, we could still obtain some 80 - 90 percent of the return signal information without interference by using a more elaborate transmit-receive switching code. There is a considerable technical advantage, however, for a first radar installation, in not having to introduce any switch in the first place.

We proposed to make a series of measurements of the actual backscatter intensity taken along vertical and near-vertical atmospheric paths, both to establish the severity of the clutter signal problem, and to get some idea of the penetration of clear, hazy, and thin cloud layers. In order to estimate the scatter to be seen in the absence of clouds, we made use of existing data on the size distribution of aerosol particles found in the atmosphere both near ground level and at 100 km above ground level, together with direct measurement of scatter at wavelengths in the visible spectral region.

From the size distribution, we can derive a curve of total scatter cross section versus wavelength by making an assumption of particle shape. In order to avoid unwarranted complication, we applied a smoothed spherical scatter function (Fig. 45) to a smoothed particle distribution derived from the data on number density[10] indicated in Fig. 46. The result (Fig. 47) shows that total scattering at 10.6μ should be about 1/20 of the value expected at 0.6μ. In fact, actual scatter data[11] at wavelengths below six microns suggest that our estimate at 10.6μ may be low. In addition, Mie scattering enhances the forward over the backward scattered intensity and may result in a backscatter an order of magnitude less than for uniform scattering. We may now use data gathered by Elterman[12], Krug-Pielsticker[13], and Newkirk and Eddy[14] on scattering and beam attenuation at visible wavelengths. These data show an attenuation coefficient of

Total cross-section in units of πa^2

10

1.0

0.1

0.01

0.001

0.1   0.2   0.3 0.4 0.5   0.8 10   2   3 4 5 6 8 10   20

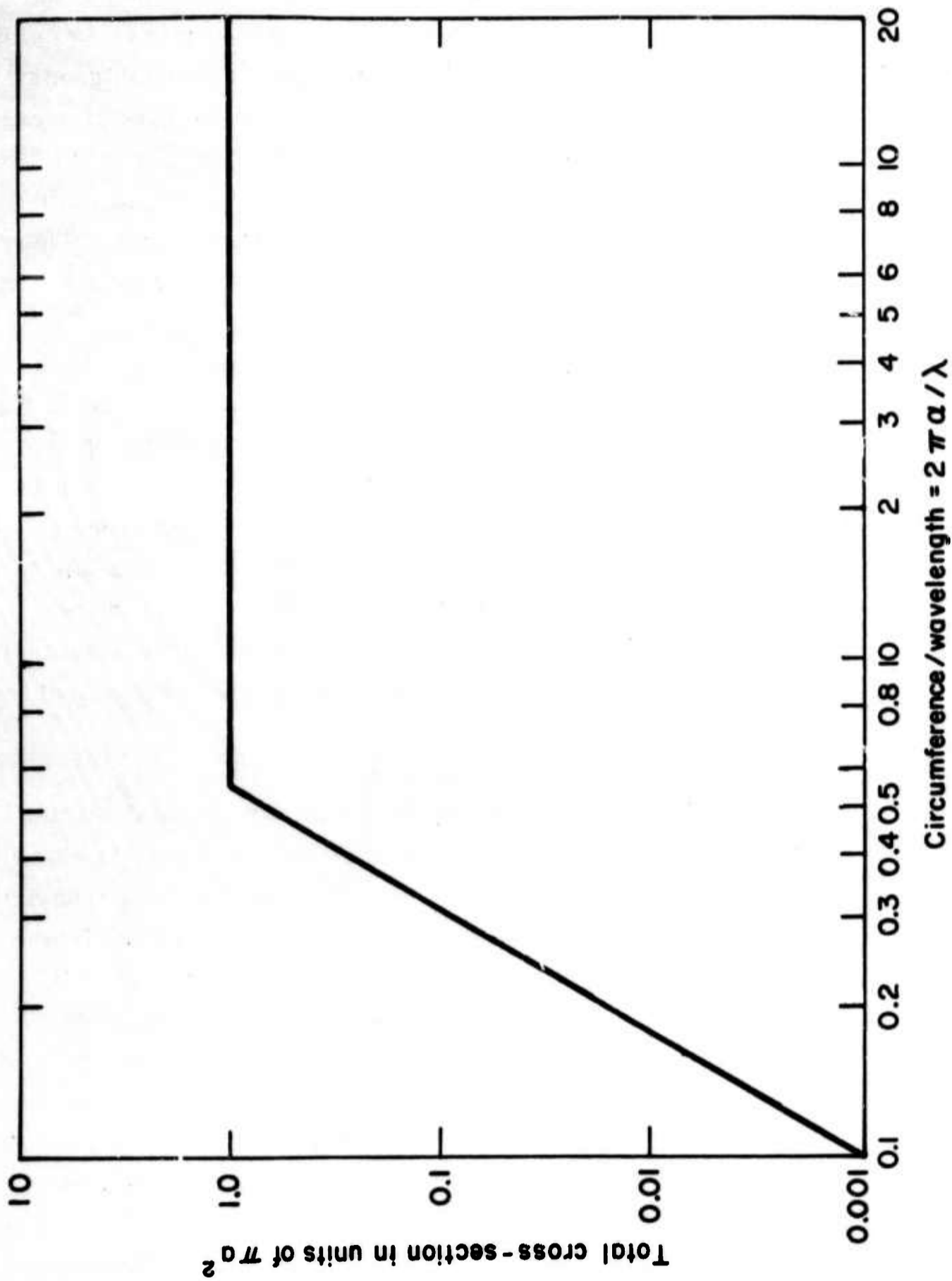Circumference/wavelength = $2\pi a/\lambda$

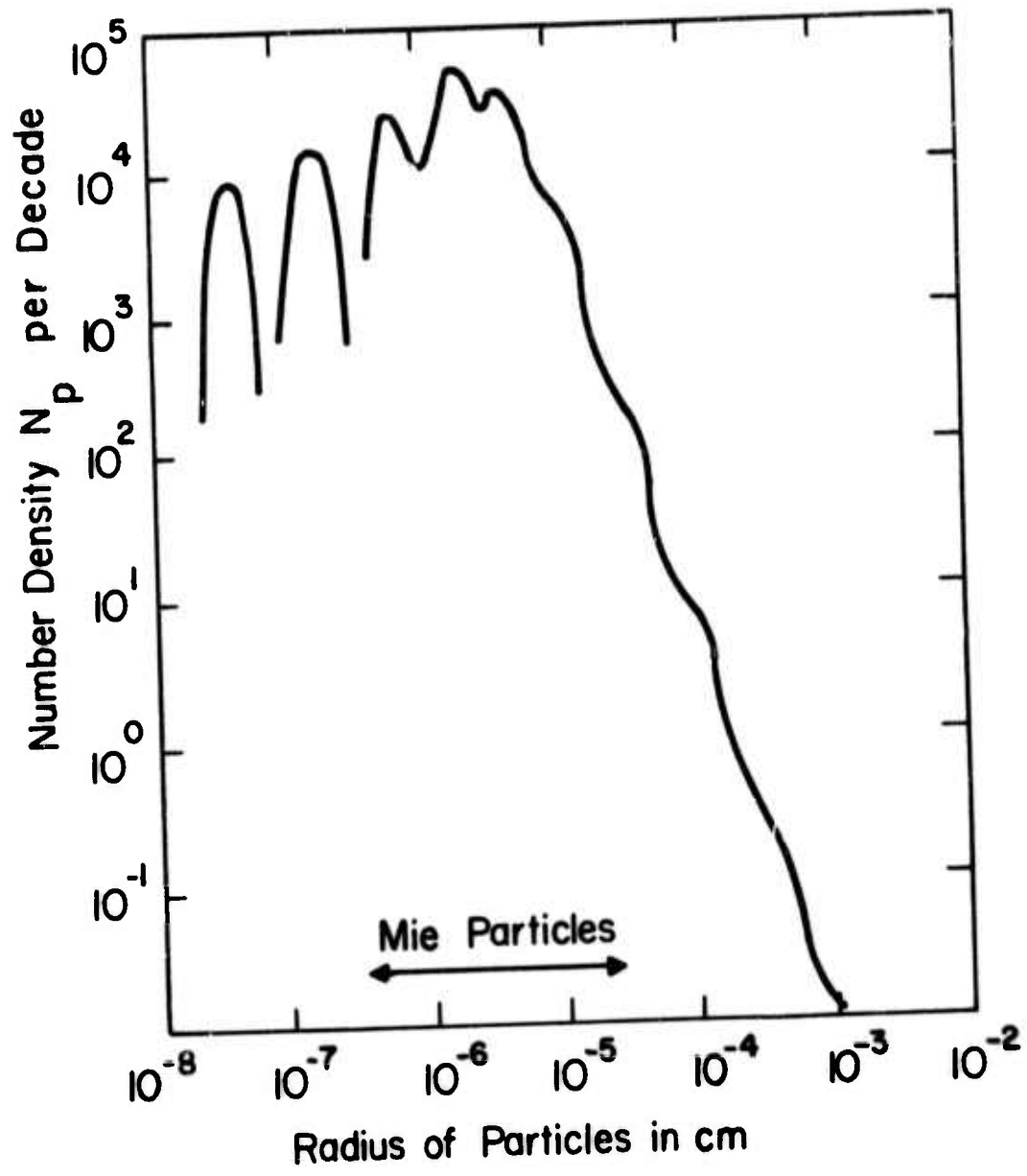Fig. 45   Simplified Function for the Total Scatter Cross Section of a Sphere

88

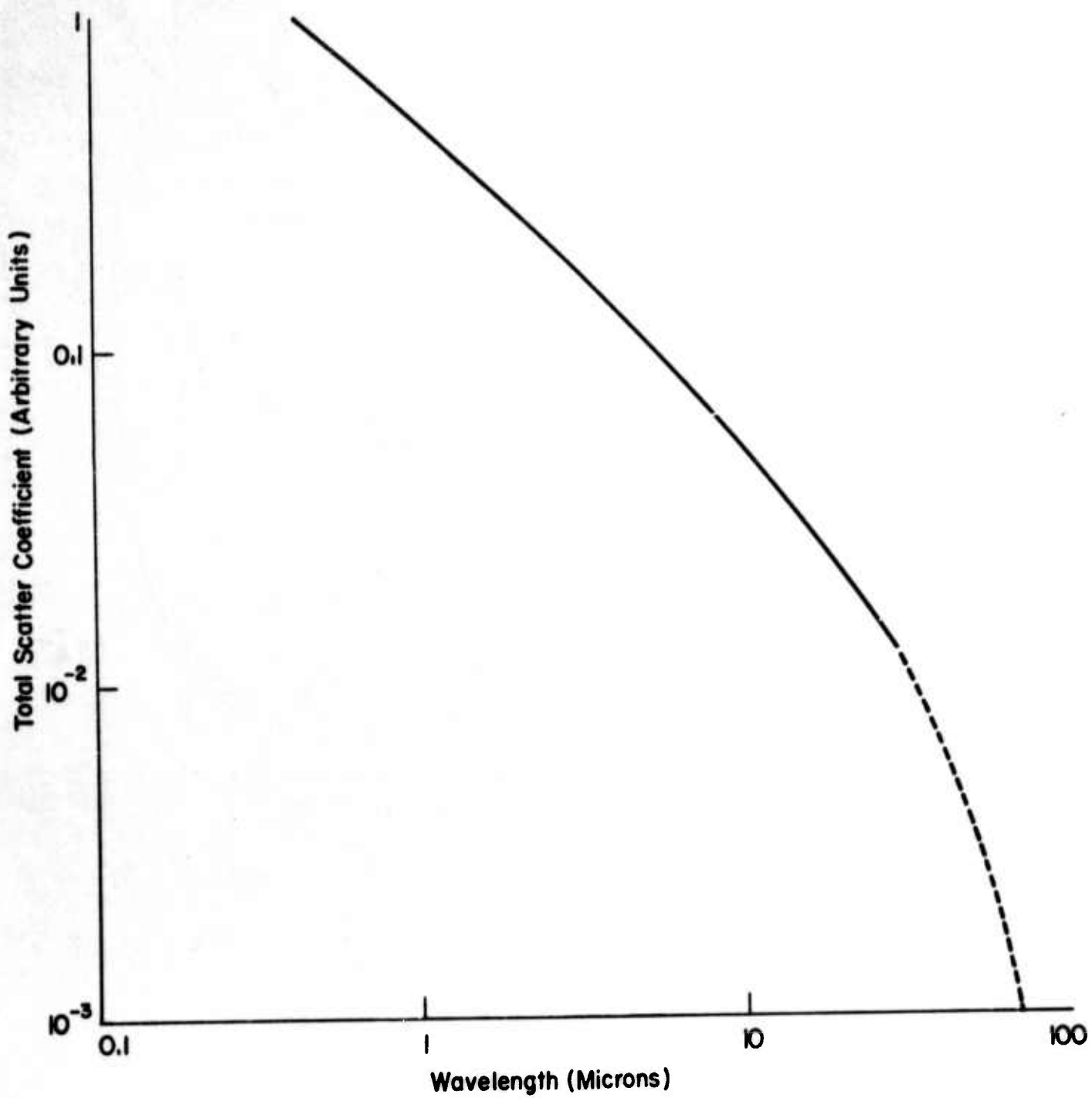Fig. 46   Particle Size Distribution for Atmospheric Aerosols

Fig. 47   Wavelength Dependence of Atmospheric Mie Scatter (Estimated)

90

approximately 0.6 km^{-1} at ground level, decreasing rapidly to about 0.01 at 5 km altitude and dropping more slowly to about 2×10^{-3} km^{-1} at 20 km. Beyond this altitude the scattering falls off rapidly and is down by an order of magnitude at 25 km. Above this latter altitude scattering should be very small except for possible layers near 80 - 100 km associated with meteoric dust.

Applying now our conversion factor of 5×10^{-2} to estimate the attenuation coefficient at 10.6μ wavelength, we get the result shown in Fig. 48. In order to proceed further, we assume that a 10-in. diameter beam is transmitted in a 10 μsec, 10 kW pulse, that the return is collected over the same aperture (0.03M^2) and that the instantaneous scatter signal comes from a 1.5 km segment of the path. The calculated return power level entering the aperture is shown in Fig. 49.

Bearing in mind that the detector noise level for heterodyne detection over a 10^6 cps bandwidth with a 10 percent quantum efficiency is 1.7×10^{-13} W, we see that a signal-to-noise ratio between 0.1 and 1 can be expected at a range of 24 - 25 km, the outer edge of the main aerosol layer. This ratio will increase rapidly with decreasing range, rising to something like 5×10^3 for a detector set to view only one resolution volume of the receiver optics. The actual power arriving at the detector, assuming that it is bigger than a single resolution element, would rise to the order of $10^{-7} \sim 10^{-6}$ W and could even be detected by an incoherent technique.

From this discussion it is clear that, for our contemplated experiments on atmospheric backscatter, the perturbation of the oscillator produced an intolerable background noise. While in principle such a repetitive interference signal can be removed by appropriate signal processing, here it is so large that the more satisfactory solution is to eliminate the interference. Assuming that a signal of 10 mW is required as a local oscillator reference signal, and that the intrinsic limiting sensitivity for the heterodyne detector of a return signal is 1.7×10^{-19} W/cycle bandwidth,
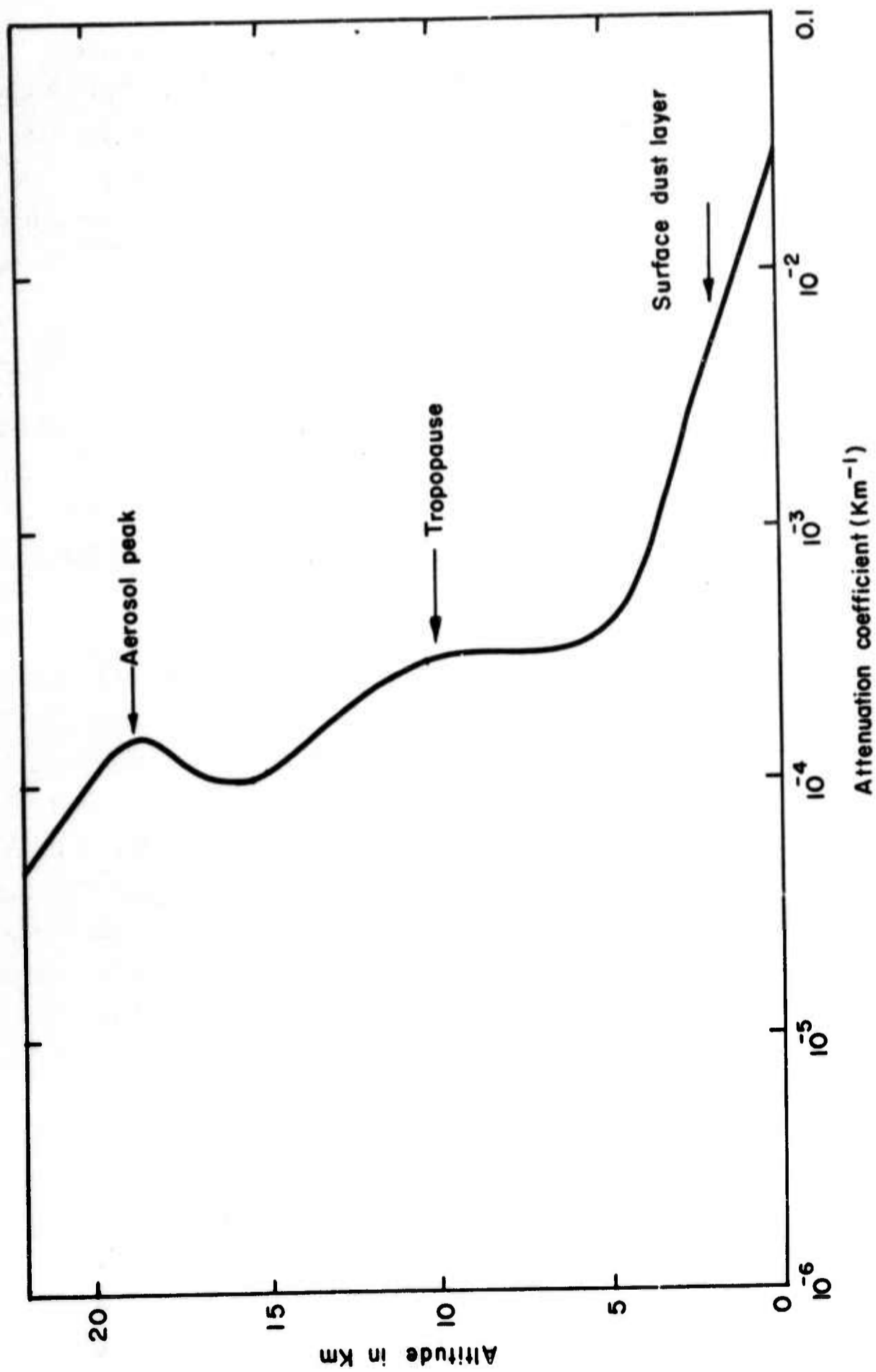
9.

Fig. 48   Estimated Scatter Losses at 10.6 μ

92
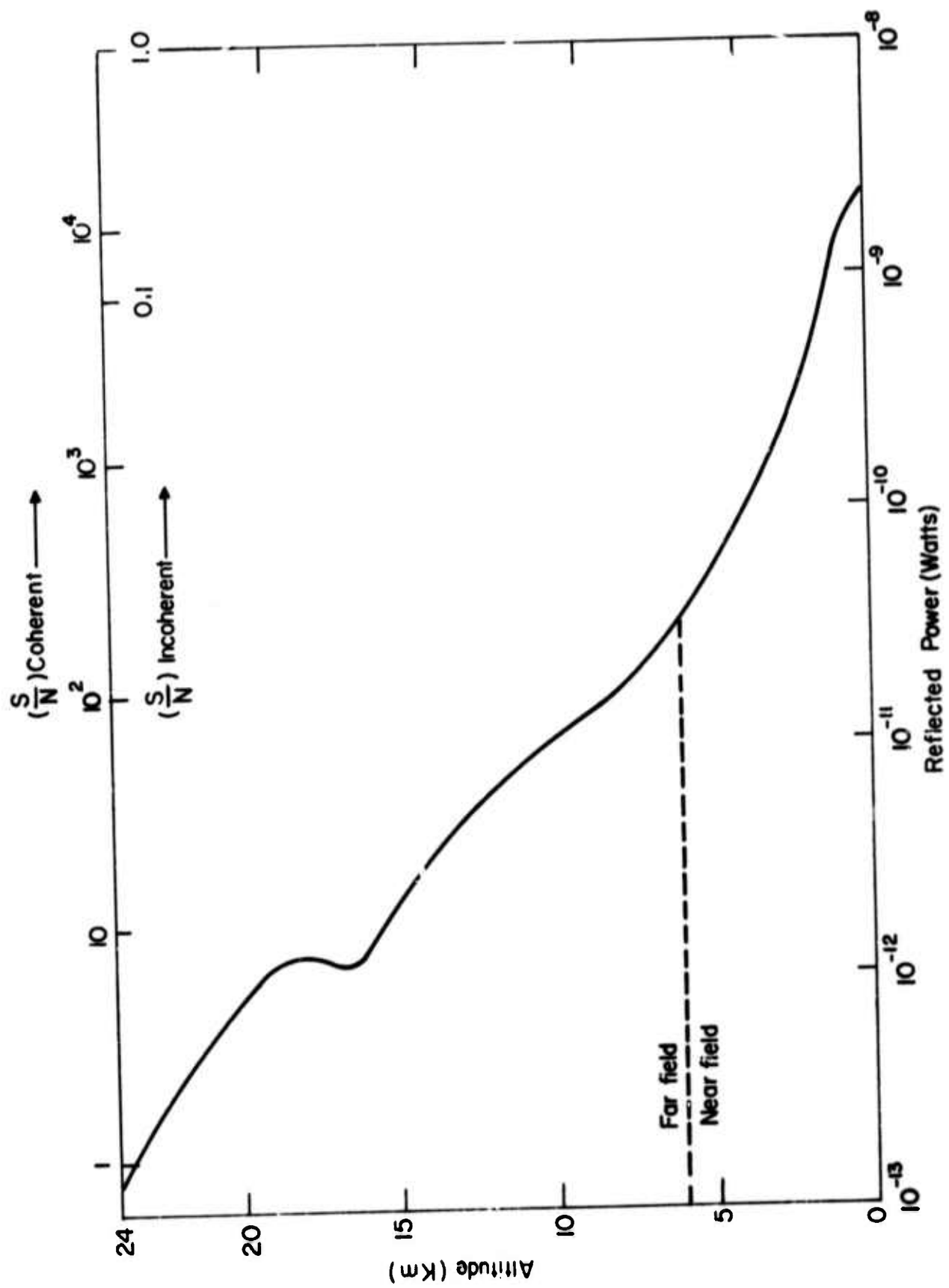
Fig. 49   Intensity of Scattered Radiation Incident on Detector vs Altitude
of Scatter (Estimated)

then for a bandwidth of 1 Mc the limiting signal is 1.7×10^{-13} W, while the 5 percent oscillator perturbation corresponds to a return signal of approximately $10^{-2} \times (0.05)^2$ or 2.5×10^{-6} W. Thus we see that the interference signal, while only one part in 10^8 of the signal incident on the chopper, is approximately 70 dB above the level of the expected limiting noise signal. Thus a technique had to be developed to reduce this background by 70 dB.

In the absence of a suitable isolator we decided that the most straight-forward approach to the problem was the use of twin oscillators, one to generate the primary signal, the other to provide the reference signal for heterodyne detection. These oscillators would have to be stable enough to have their beat signal remain within the bandwidth of the detection circuitry for a period long enough to make an observation. Two such oscillators were built using identical Invar frames, sealed-off discharge tubes, and internal optics with NaCl Brewster plate polarizers. These devices were firmly clamped together, allowed to come to thermal equilibrium, and tuned to produce a beat frequency below 2 Mc. In the normal laboratory environment, the beat frequency was found to drift at rates up to 500 kc/min, and to have a 1 sec bandwidth of between 100 and 200 kc. A typical set of beat signals taken at 4 sec intervals is shown in Fig. 50.

A number of attempts were made to observe scattering of the transmitter beam by particular matter in the atmosphere. The optical arrangement is shown in Fig. 51. The laser output was directed along a path through the roof of the building such that it spread over the field of view of a 10 in. diam reflecting telescope. A Cu-doped germanium detector at 4°K, with a bandwidth of 50 Mc, was placed at the focal plane of the telescope mirror. The remainder of the detector circuitry (Fig. 52) gave an impedance transformation from the $10^4 \Omega$ detector load resistor to a 75 Ω line by using a FET circuit operated at 77°K (Fig. 53). In order to improve the observed signal-to-noise ratio, the final pulse signal, after amplification and rectification, was integrated by a 100 channel device capable of resolving

94

Fig. 50   Heterodyne Signals Indicating Variation of Beat Frequency
Between Two Free-Running Laser Oscillators
(Time Scale: 1 div. = 10 μsec)

95
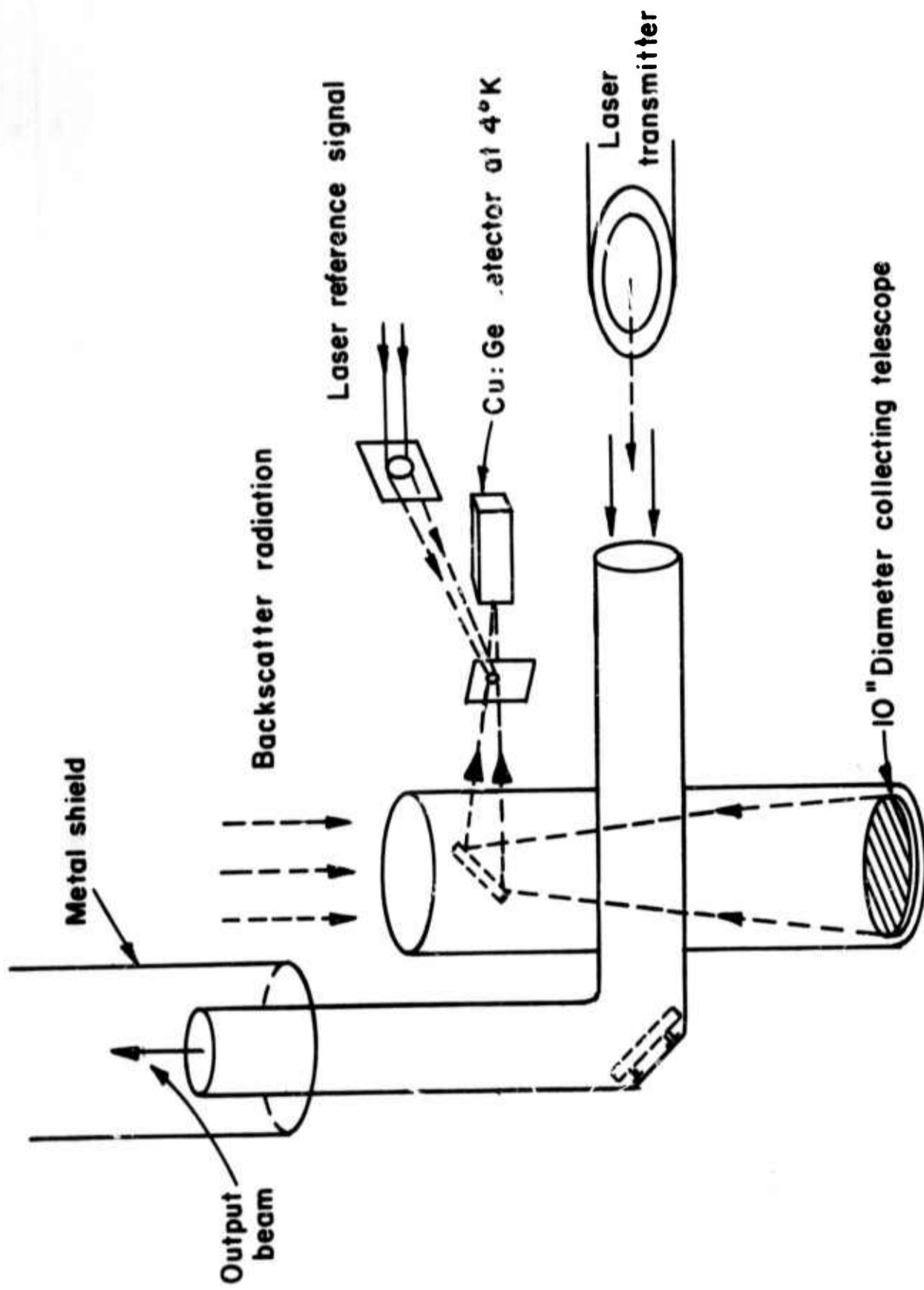
Fig. 51 Experimental Arrangement for Atmospheric Backscatter
Measurements
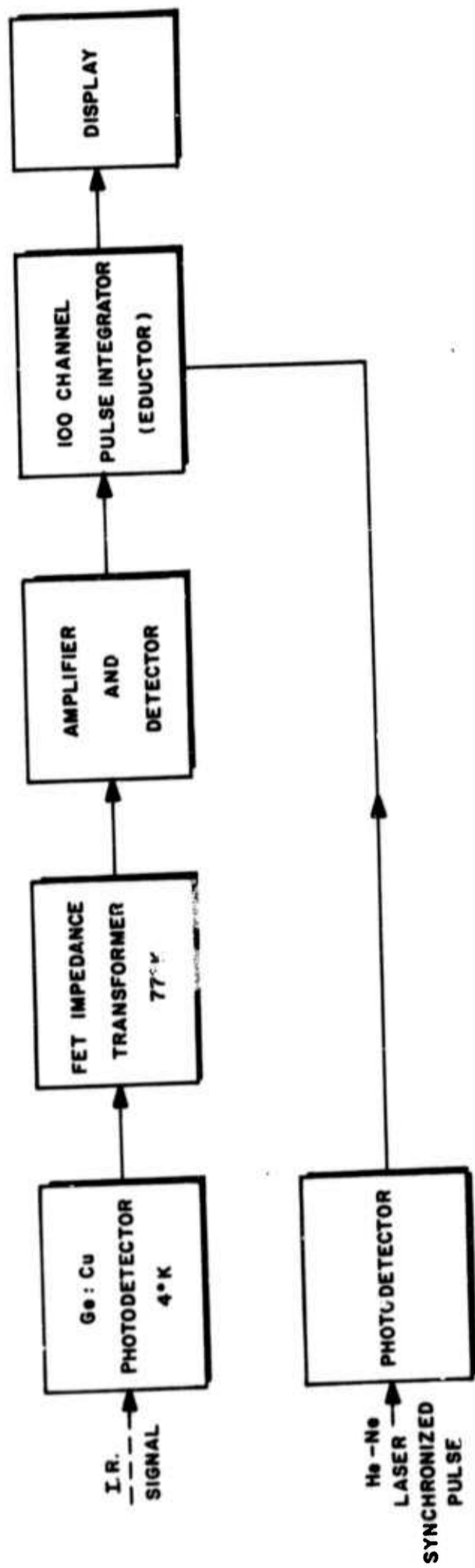
Fig. 52   Pulse Detection and Integration Circuitry (schematic)

97
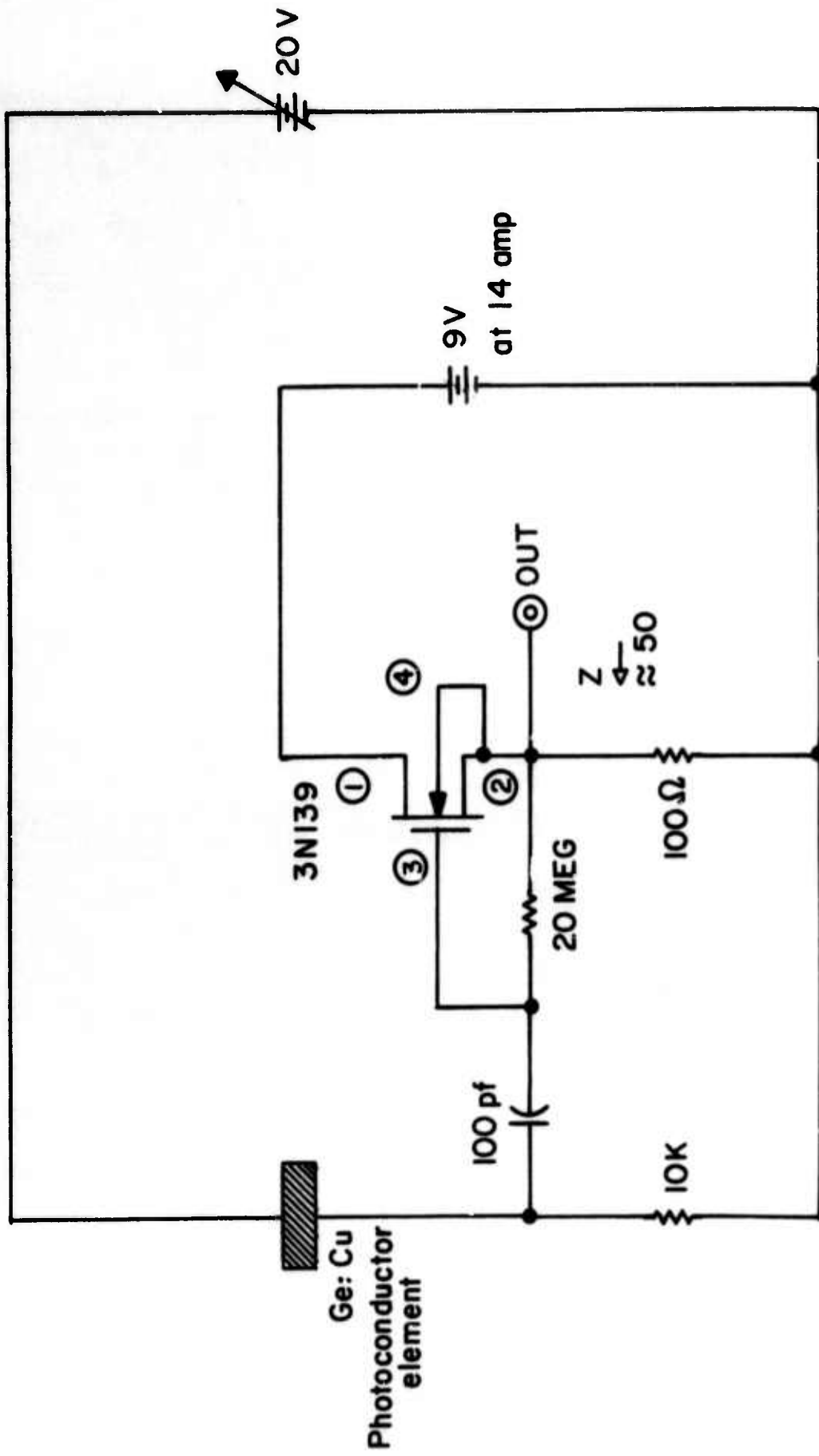
Fig. 53 FET Low Temperature Transformer Circuit

time intervals down to 10^{-6} sec and with an integration time constant of up to 30 sec. Thus, at a pulse repetition ratio of 10,000 pps, we could expect a signal-to-noise improvement of more than 500 times.

Signals were detected both with and without the use of a heterodyne reference signal from the laser. In all cases the signals were identified as reflections from the immediate vicinity of the laser despite repeated attempts to minimize reflections from the roof and radiation shield. No signal was detected later than 2 μsec beyond the trailing edge of the emitted pulse. Thus, if any atmospheric backscatter had been present, it would have been from points less than 1000 ft from the telescope exit.

VIII. CONCLUSIONS

In this program we set out to develop a pulsed laser source capable of use in a coherent Doppler laser radar system. To accomplish this task it was necessary both to enlarge our knowledge of pulse amplification in CO_2 lasers and to gain experience in handling both high-power and high-gain amplifiers.

While the work was successful in the sense that it produced a device suitable for radar field testing over the next two years, much remains to be done both in the improvement of the present transmitter and in the design of more practical field equipment and even higher power devices. As far as the present device is concerned, the replacement of the mechanical modulation system with electro-optic shutters could greatly improve its utility. Assuming that such devices, using for example gallium arsenide as the electro-optic elements, could be developed to handle average powers of up to 40 W without distorting the optical beam, their installation would give greater control on pulse shape and on the form of the pulse train. In addition, a greater system efficiency would be achieved both in the first- and second-stage amplifiers and in the power amplifier. At present, the only way to avoid the problem of reaction of the amplifier on the primary oscillator, and its consequent elimination as a stable reference signal, is to use two oscillators with either passive or severely filtered active stabilization. In order to use a single source for both output signal and heterodyne reference, it will be necessary to develop a nonreciprocal isolator to separate the oscillator from the first-stage amplifier. This device will have to handle some 20 W average power, and provide approximately 60 dB isolation.

Both these developments require advances in high power optical materials, rather than in device design. The same can be said for the windows used to separate the various amplifier stages and to transmit the

final beam into the laboratory. While the halide windows used in the present device are adequate for the moment, they should be replaced with gallium arsenide as soon as possible. Such windows will be more stable, less liable to damage by moisture, and will be able to be cleaned without damage to the optical surfaces. Unfortunately, a source of material suitable for large windows does not yet exist. This deficiency will become a major problem in ultrahigh power CO_2 lasers where diffraction limited performance is required.

A more significant aspect of the design of future transmitters has to do with their overall size. While it is true that present day high power ground-based radar devices are very large installations, and that by implication the construction of a laser radar of comparable power and size could be tolerated, it is clear that a major effort should be made to reduce the size of CO_2 laser sources by at least one order of magnitude. A 1 kW installation would then occupy about as much space as the optical equipment needed for beam control, while a more useful 10 - 100 kW source would then approximate the size of our present system.

Size reduction and increase of output efficiency are also required if airborne laser radar devices are ever to have wide acceptance. It is therefore most important to improve the power output per unit volume without degrading the beam profile. There is already the well-established fact that the power output per unit length in cylindrical oscillators decreases very slowly with tube diameter. This indicates a progressive increase in output per unit volume as the walls come closer to the most strongly excited region of the discharge. The difficulty in using small bore or thin slab amplifiers, of course, is that the natural spreading of the beam produces multiple wall reflections. The extensive use of refocusing optics would then be required. At the same time, the high small-signal gain in small-bore amplifiers would require the use of multiple isolators or optical switches (saturable

101

absorbers might be useful in this context) to a much greater extent than in the present 1 kW design. These difficulties were taken into consideration when we designed the prototype transmitter described in the earlier sections of this report, and were deliberately avoided for the sake of speed. In the future, however, they warrant greater attention.

We believe that future developments are likely to take a combination of two forms: 1) the use of multiple path periodically refocussed beams passing through amplifiers of constricted cross section, and 2) changes in the gas conditions and excitation techniques to improve the useful population per unit volume. In considering possible changes of gas and excitation conditions, the interesting results obtained by Hill[15] on pulse excitation of CO_2 - N_2 -He lasers suggests that a re-examination of our conclusion (see Sec. III) on the use of pulse excitation is in order. Hill's work has shown that in high voltage pulse discharges at gas pressures nearly ten times greater than our own, infrared pulse outputs of up to 10 J in less than 30 μsec can be obtained in a 2 1/2 meter section of 3 in. diam discharge, or can be repeated up to 40 times a second.

In comparison with our own work on pulse discharges, the increase of gas pressure produces a corresponding increase in the rates of energy transfer by collisions. The N_2 - CO_2 transfer time constant drops from 100 μsec to 10 μsec and explains the reduction of the length of the emitted pulse from our values of 300 - 500 μsec to less than 30 μsec. It is important to note that for the specific type of laser transmitter that we have developed, an output pulse wherein most of the energy is concentrated in the first 10 μsec would be quite as acceptable as our present pulse profile. Such pulses should be produced by a further increase in the partial pressures of N_2 and CO_2 gas in the discharge. Experiments along these lines should be carried out.

In considering the efficiency with which a given radar transmitter power and given pulse length can be used to detect and track a moving target,

it is soon clear that the more energy transmitted in each pulse the better. The degree of improvement of a system with a low pulse repetition rate as compared to our present 10,000 pps depends on the maximum time interval that can be allowed between pulses without either losing the target or reducing the accuracy of path prediction. For example, if a measurement is required every 0.01 second of time, a 10,000 pps system allows an integration of 100 pulses for each measurement whereas a 100 pps system relies on the single pulse return. A 1 kW source, in the first case, would give the return from 100 pulses each of 0.1 J integrated incoherently. The resultant signal-to-noise ratio would be the same as that from a single pulse $0.1 \times \sqrt{100}$ or 1 J. By contrast, the 100 pps system gives a single 10 J pulse for each measurement. In this example, then, a ten-fold improvement is obtained by using the low repetition rate system. Stated in another way, a 100 pps system with an average output of 100 W gives a performance equal to that of the 1 kW $\times$ 10,000 pps system. The high-pressure pulsed discharge work referred to previously suggests that a 100 W system may very well be achieved in an amplifier less than 5 m long, even allowing for the drop in output to be expected when the beam is reduced to a single transverse mode. This is clearly an important area for future development of laser radar sources.

REFERENCES

1. M. Weber and T. Deutsch, IEEE J. Quant. Elect. QE-2, 365 (1966).

2. D. R. Whitehouse, "High Power Gas Laser Research," Final Technical Report on Contract DA-01-021-AMC-12427(z), May, 1967.

3. C. K. Rhodes, M. J. Kelly, and A. Javan, J. Chem. Phys. 48, 5730 (1968).

4. N. Djeu, T. Kan and G. J. Wolga, IEEE J. Quant. Elect. QE-4, 256 (1968).

5. N. Djeu, T. Kan and G. J. Wolga, IEEE J. Quant. Elect. QE-4, 256 (1968).

6. H. Kogelnik and T. J. Bridges, IEEE J. Quant. Elect. QE-3, 95 (1967).

7. C. Frapard, M. Roulet and X. Ziegler, Phys. Letters 20, 384 (1966).

8. Van Lerberghe et al., C. R. Acad. Sc. Paris, t. 265, 359 (7 August 1967).

9. W. M. Doyle, W. D. Gerber and M. B. White, IEEE J. Quant. Elect. QE-3, 479-484 (1967).

10. See, for example, R. Penndorf, "The Vertical Distribution of Mie Particles in the Troposphere," Air Force Cambridge Research Center, Geophysical Research Papers No. 25 (March, 1954) and C. E. Junge, Air Chemistry and Radioactivity (New York, Academic Press) 1963, Chapter 2, "Aerosols".

11. See Handbook of Military Infrared Technology, W. L. Wolfe, ed., U. S. Government Printing Office (1965) p. 210.

12. L. Elterman, "An Atlas of Aerosol Attenuation and Extinction Profiles for the Troposphere and Stratosphere," Air Force Cambridge Research Laboratories, Report No. AFCRL-66-328 (Dec. 1966).

13. Ursel Krug-Pielsticker, "Messungen der Sonnenstrahlung bei Flugzeugaufstiegen bis 9 km Höhe," Berichte des Deutschen Wetterdienstes in der U.S. Zone, Nr. 8, Bad Kissingen, (1949).

14. G. Newkirk, Jr. and J. A. Eddy, "Light Scattering by Particles in the Upper Atmosphere," J. Atmospheric Sciences 21, 35-58 (Jan. 1964).

15. A. E. Hill, Appl. Phys. Letters 12, 324 (1968).

DOCUMENT CONTROL DATA - R & D

(Security classification of title, body of abstract and indexing annotation must be entered when the overall report is classified)

1. ORIGINATING ACTIVITY (Corporate author)	2a. REPORT SECURITY CLASSIFICATION
Raytheon Company Research Division Waltham, Massachusetts 02154	Unclassified
	2b. GROUP N/A

3. REPORT TITLE

Research Study of a CO_2 Laser Radar Transmitter

4. DESCRIPTIVE NOTES (Type of report and inclusive dates)

Final Technical Report   10/1/66 to 8/15/68

5. AUTHOR(S) (First name, middle initial, last name)

Perry A. Miles

6. REPORT DATE	7a. TOTAL NO. OF PAGES	7b. NO. OF REFS
December 1968	104	15

8a. CONTRACT OR GRANT NO. N00014-67-CO264	9a. ORIGINATOR'S REPORT NUMBER(S)
b. PROJECT NO. NR 015-714	S-1119
c. ARPA Order No. 306	9b. OTHER REPORT NO(S) (Any other numbers that may be assigned this report)
d.	

10. DISTRIBUTION STATEMENT

11. SUPPLEMENTARY NOTES	12. SPONSORING MILITARY ACTIVITY
N/A	Advanced Research Projects Agency Office of Naval Research Department of Defense

13. ABSTRACT

A prototype high power laser radar transmitter at 10.6μ wavelength has been developed for installation at Lincoln Laboratory's Millstone Hill radar site. This report summarizes the three phases of its development: 1) Exploratory work on the properties of dc- and pulse-excited CO_2 laser amplifiers and their use in producing trains of high power optical pulses, 2) Design of 1 kW average (10 kW peak) power transmitter, and 3) Operational tests of the transmitter. The signal for a stable oscillator is amplified to a level beyond 200 W, formed into a train of 10 μsec pulses by mechanical modulation before amplification to the 10 kW level. All amplifiers are dc-excited. Subjects treated include gain limitations set by spurious oscillation, pulse-to-pulse amplitude stability, oscillator-amplifier interaction, and output beam profile. Brief proposals are made for future development of the laser radar program.

14. KEY WORDS	LINK A		LINK B		LINK C	
	ROLE	WT	ROLE	WT	ROLE	WT
10μ Doppler Laser Radar						
CO_2 Laser Transmitter						
CO_2 Laser Pulse Amplification						
High Power Laser Amplifier						